2013

The characterization of dried aluminum hydroxide gel suspensions : particle size analysis and thermal analysis

Prathyusha Lella
The University of Toledo

A Thesis

entitled

The Characterization of Dried Aluminum Hydroxide Gel Suspensions:

Particle Size Analysis and Thermal Analysis

by

Prathyusha Lella

Submitted to the Graduate Faculty as partial fulfillment of the requirements for the Master of Science Degree in Pharmaceutical Sciences with Industrial Pharmacy option.

_____

Dr. Kenneth Alexander, Committee Chair

_____

Dr. Sai Hanuman Sagar Boddu, Committee Member

_____

Dr. Ming-Cheh Liu, Committee Member

_____

Dr. Patricia R. Komuniecki, Dean
College of Graduate Studies

The University Of Toledo

May 2013

An Abstract of

The Characterization of Dried Aluminum Hydroxide Gel Suspensions:
Particle Size Analysis and Thermal Analysis

by

Prathyusha Lella

Submitted to the Graduate Faculty as partial fulfillment of the requirements for the Master of Science Degree in Pharmaceutical Sciences with Industrial Pharmacy option.

The University of Toledo
May 2013

This study was performed to investigate the effect of flocculation on the sedimentation characteristics of dried aluminum hydroxide suspensions. Particle size analysis was performed using sieving, hindered settling theory and laser diffraction. Dried aluminum hydroxide suspensions were prepared in various dispersion media eg. Purified Water USP, 0.01%, 0.03% and 0.05% PEG 1000 solutions. The particle size of the suspensions was determined using settling behavior of the sediment. The rate of fall of the interface was plotted and the straight line portion of the graphs was used to obtain the values of the slope (Q). Further calculations were done and the Q-values were used to fit the Richardson and Zaki, Steinour and Dollimore and Mc Bride equations in order to obtain the particle size. The results from the hindered settling theory were found to be consistent with results from the Laser diffraction studies. However, it was found that sieve analysis was not the most appropriate technique to determine the particle size distribution since it could not measure the size of the individual particles. The particle size increased upon the incorporation of PEG 1000 and with increasing concentrations of PEG 1000 solution. This may be attributed to the floccule formation which was further

established by scanning electron microscopy. Thermal analysis was done to determine the amount of water associated with the suspensions. Differential Scanning Calorimetry was used to determine the amount of unbound water. The bound water could not be determined due to instrument limitations. However, TGA could not calculate the amount of bound water since the peak due to the water loss overlapped with the degradation peaks of aluminum hydroxide in the suspensions.

Dedicated to my parents Yugandhara Babu and Sujatha and my brother Bharat.

Acknowledgements

I would like to express my gratitude to my advisor Dr. Kenneth Alexander for his continual support and guidance over the past couple of years. I would like to thank him for his valuable suggestions and encouragement without which I would not have been able to complete my thesis. I am very thankful to him for taking time from his busy schedule to correct my thesis.

I would like to thank Dr. Sai Hanuman Sagar Boddu and Dr. Ming-Cheh Liu for being a part of my defense committee and for their valuable time and advice. I would like to thank Dr. Surya Nauli for being the Graduate Faculty Representative.

I would like to thank Dr. Pannee Burckle for training me and helping me use the Scanning Electron Microscope. I would also like to thank Dr. Timothy Fisher for allowing me to use the Laser Diffraction Instrument.

I would like to thank my labmates, Sriramya, Priti, Ishan, Meghavi, Sanjeev, Yingzhe, Vishak, Sharat, Ashsish and Heather for their friendship and making the time at University of Toledo, a wonderful experience.

I would like to extend my gratitude to all my friends who have been there for me through all the ups and downs and were supportive in every phase of my life.

I would like to thank my family members for their unconditional love and moral support in my life. Their prayers and encouragement are the reasons why I came this far in life. I will always have them in my heart, mind and spirit.

Table of Contents

List of Tables

List of Figures

Chapter-1

Introduction

A pharmaceutical suspension is a coarse dispersion in which the insoluble particles are dispersed in a liquid medium. The insoluble particles constitute the dispersed phase, which is maintained throughout the continuous phase. [1]

Application of Suspensions in Pharmacy: [2]

- They are easy to administer to patients who have a difficulty in swallowing solid dosage forms.
- It is an easy way to administer insoluble drugs. e.g. Prednisolone suspension.
- It can mask the bitter taste of unpleasant tasting drugs. e.g. The use of insoluble chloramphenicol palmitate in the form of a suspension instead of soluble chloramphenicol.
- Suspensions can be administered as parenterals in order to control the rate of drug absorption.
- Insoluble drugs can be formulated as suspensions that can be administered topically. e.g. Calamine lotion.

A formulator should keep the following in mind while formulating a suspension. [3]

- The suspended particles should not settle rapidly.

- The particles that reach the bottom of the container should not form a hard cake.
- The particles in a suspension should be easily redispersed by shaking to form a uniform dispersion.
- The viscosity should not be too high such that it interferes with the free flowing nature and pourability of the suspension.

In this project, the behavior of concentrated dried aluminum hydroxide gel suspensions has been studied. Suspensions tend to separate upon standing. Therefore, it is plausible to study the rate of settling. The primary objective of this study was to determine the particle size of the flocs in the suspension which helps in understanding its stability as well as to characterize the suspensions using thermal analysis. The effects of using PEG 1000 as a flocculating agent were studied.

Two theories are used to gain better insight into the particle size of suspensoid in a dispersion medium. Stoke's law is applied to dilute suspensions. This occurs when the suspended particles settle to the bottom of the container under the influence of the gravitational force. This implies that their fall is not affected by the surrounding particles. The density of the dispersed phase and the continuous phase are important parameters that influence the fall. [4] Stoke's law is given by the following equation.

$$Vs = \frac{[(\rho_s - \rho_l)]gD^2}{18\eta} \quad (1.1)$$

Whereas, in a concentrated suspension, the particles move en bloc or en mass, leading to the formation of an interface between the settling particles and the liquid above it. In such cases a modified Stoke's law is applied. These have been developed by Steinour, Richardson and Zaki and Dollimore and Mc. Bride. The equations that have

been used to determine the particle size of the concentrated suspensions are as follows. They are also discussed in detail in Chapter 3.

$$Q = V_s \varepsilon^2 10^{-A(1-\varepsilon)} \tag{1.2}$$

$$Q = V_s \varepsilon^n \tag{1.3}$$

$$Q = V_s 10^{-b\rho_m(1-\varepsilon)} \tag{1.4}$$

Sedimentation studies, laser diffraction and sieving are used to determine the particle size distribution of the particles in a suspension which are discussed in Chapters 5 and 7. Scanning electron microscopy was used to study the morphology of the particles.

Thermal analysis was performed to determine the water associated with the particles in the suspension. Differential Scanning Calorimtery (DSC) was used to determine the rate of heat flow through the heating and cooling cycles and to calculate the amount of unbound water present. Thermogravimetry was used to determine the change in the mass of a sample with respect to temperature and thereby calculate the amount of water associated with the suspensions.

Chapter-2

Theory of Dilute Suspensions

2.1 Introduction

A dilute suspension contains less than 2gm of the suspensoid in 100mL of the dispersion medium, in which the suspending particles are wide apart and settle freely. [1] These suspended particles settle to the bottom of the suspension under the influence of the force of gravity. If the density of the suspended particles is greater than that of the suspending liquid then they fall and if the reverse is true they rise. [2] The rate at which the particles settle increases until it reaches a constant rate, which it is called the terminal velocity. A number of factors such as the particle size, shape and density of the particles and the density of the suspending medium affect the terminal velocity. [3] In addition, it was found that Brownian movement also exerts a significant effect on the sedimentation of particles. [4]

2.2 Stoke's Law

Stoke's law describes the effect of certain factors on the rate of settling for the particles in a suspension. The behavior of particles in a dilute suspension was studied and a theoretical expression for the terminal velocity was obtained. The derivation of Stoke's

law is based upon balancing the forces acting in a viscous fluid continuum. [5] Figure 2-1 shows the various forces acting on a freely suspended particle.

2.2.1 Derivation of Stoke's law

Three forces affect the fall of particles under the influence of gravitational fields in a viscous liquid, which are: [6]

F_G: Gravitational force acting downwards

F_B: Buoyant force acting upwards

F_D: Drag force acting upwards.

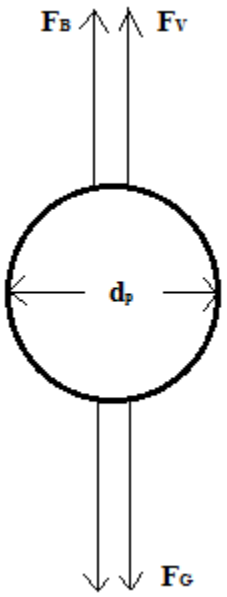

Figure 2-1: Depiction of various forces acting on the particle. [7]

The terms F_G, F_B, and F_D should be in equilibrium with the inertial forces (F_I). Therefore,

$$F_I = F_G - F_B - F_D \tag{2.1}$$

Newton's law of motion has been defined as: [8]

$$F = m\left(\frac{dv}{dt}\right) = m * a \tag{2.2}$$

Where,

dv: Change in the velocity

dt: Change in time

m: Mass of the body

a: Acceleration of the body

The gravitational settling force can be given by the following equation:

$$F_G = m * g \tag{2.3}$$

$$F_G = \rho_m \pi \frac{D^3}{6} * g \tag{2.4}$$

Where,

m: Mass of the particle

ρ_m: Density of the particle

D: Diameter of the sphere

g: Acceleration due to gravity

The force of buoyancy can be given by the following equations:

$$F_B = M * g \tag{2.5}$$

$$F_B = \rho_f \pi \frac{D^3}{6} * g \tag{2.6}$$

Where,

M: Mass of the same volume of the fluid

ρ_f: Density of the fluid

Upon reaching the terminal velocity, the equation for the motion of a sphere can be given by the following equations:

$$F_D = F_G - F_B \tag{2.7}$$

$$F_D = \left(\rho_m \pi \frac{D^3}{6} * g\right) - \left(\rho_f \pi \frac{D^3}{6} * g\right) \tag{2.8}$$

$$F_D = \left(\rho_m - \rho_f\right)\left(\frac{\pi}{6}\right)(g)(D^3) \tag{2.9}$$

The parameters controlling the behavior of particles are the Reynold's number [9] and the drag coefficient. [10] The Reynolds number determines whether the flow is laminar or turbulent. The Reynold's number describes the ratio of the velocity of the particle to the viscous forces resisting its motion and is given by:

$$R_e = \frac{\rho_f\, dv}{\eta} \tag{2.10}$$

The drag coefficient describes the ratio of the drag force to inertia of the particle and is given by:

$$C_D = \frac{F_D}{\left[\left(\frac{\pi}{4}\right)(D^2)(\rho_f)\left(\frac{v^2}{2}\right)\right]} \tag{2.11}$$

$$C_D = \frac{4gd(\rho_m - \rho_f)}{3\rho_m v^2} \tag{2.12}$$

The drag on the spherical particle falling in a fluid of infinite extent depends only on the viscous forces, upon reaching the terminal velocity. This can be given by the equation:

$$F_d = 3\pi D\ \eta V_s \tag{2.13}$$

Where (Vs) is the terminal velocity of the particle in the Stokes region and is given as:

$$V_s = \frac{(\rho_m - \rho_f)gD^2}{18\eta} \tag{2.14}$$

Substituting Equations 2.10 and 2.12 into Equation 2.14 we obtain:

$$C_D = 24/R_e \tag{2.15}$$

The drag coefficient and the Reynolds number are inversely proportional to each other. At low viscosities, the drag coefficient decreases as the particle velocity increases. This is called the laminar flow region. Stoke's law can be applied if the flow of the dispersion medium around the particles is laminar or streamlined. This means that the sedimentation

rate must not be so quick that it will set up turbulence, because this in turn will affect the sedimentation of the particle. [1] Stoke's law cannot be used if the Reynolds number is greater than 0.2, because at this value turbulence is set up. This transition is gradual and is preceded by a region of intermediate flow. [11]

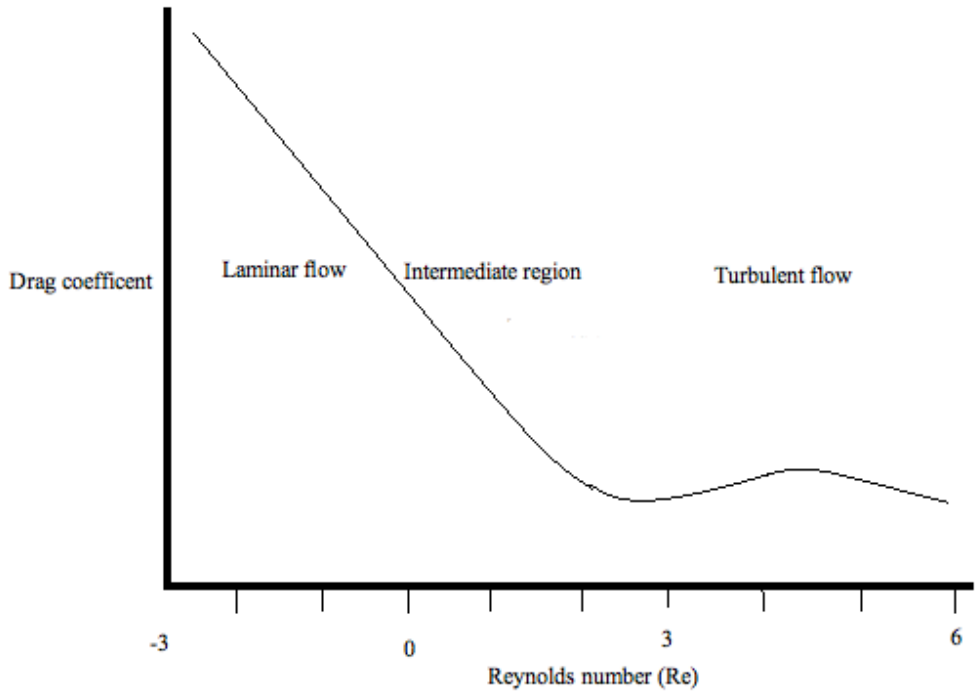

Figure 2-2: Relationship between the drag coefficient and Reynolds number for a sample settling in a liquid. [12]

2.2.2 Limitations of Stoke's law

Stokes law can be applied only to:

- Particles that are smooth and rigid and spherical in shape.

- Dilute suspensions.
- Particles which settle freely without any interference or collision with each other.
- Particles that have no physical or chemical interaction or affinity with the dispersion medium.

Chapter-3

Hindered Settling of Suspensions

3.1 Introduction

When we consider the kinetics of particles settling down under the force of gravity in a liquid medium, there are two different possibilities. [1] When the suspension is dilute, the fall of the particles is not affected by the surrounding particles. This means that the particles fall freely and unhindered. When the suspension is concentrated, the inter-spacings between the particles decrease and the fall of each particle is hindered by other particles in its path. The drag force created by the particle will affect the movement of the nearby particles. [2] The transition between these two possibilities is not sharp and is gradual. It increases with an increase in the concentration of the suspension. When the suspensoid concentration is too high (5%-10% or greater), the particles fall en bloc or en mass, leading to the formation of an interface between the settling particles and the liquid above it. [3]

The two important parameters that should be considered for hindered settling of suspensions are the rate of fall of the interface and the final volume of the sediment. [4] The factors that influence the settling of the particles include, but are not limited to: [5]

- The concentration of the suspension.

- The particle size distribution, to ascertain if the smaller particles fit in the spaces between the closely packed larger particles.
- The physical properties of the continuous phase.
- The chemical properties of the continuous phase.
- Flocculation of the particles.
- The time lapse since settling began.

The settling behavior of an insoluble particle under the force of gravity, as shown in Fig: 3-1 comprises a brief period of stability followed by rapid instability, where the particles fall freely under the force of gravity and finally a long period of decreased settling rate.[6]

The path followed by the insoluble solid particles in a suspension is as follows: [7]

- A Linear zone
- A Compressive zone
- A Stationary zone

The linear zone is affected by the eddy currents immediately after shaking and placing the apparatus on the bench. This is important because the calculation of the particle size using hindered settling is done using the slope of this zone. The compressive zone represents the compaction phase of the bed of settled particles under its own weight.

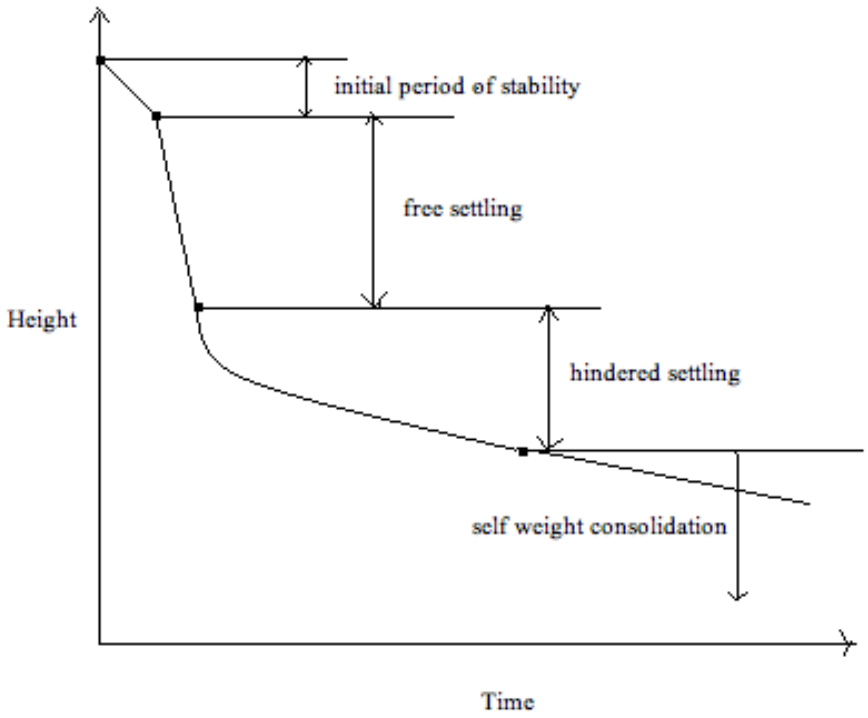

Figure 3-1: The settling behavior of insoluble particles in a dispersion medium. [6]

The settling rate decreases gradually. The stationary phase represents the phase where there is no more settling and the volume of the settled bed remains unaltered. The concentration of the solid in a suspension determines the rate of settling.

There are three types of plots for the settling of a suspension with an increase in the concentration of the solid. In suspensions having low concentration of solid particles, there is no compression zone. At higher concentrations, the compression zone merges into the linear zone. Figure 3-2 shows the behavior of the rate of settling for the interface or the sludge line plots for suspensions at different concentrations, where (3-2a)

represents low concentration of solids, (3-2b) represents medium concentration of solids and (3-2c) represents high solid concentration. [8]

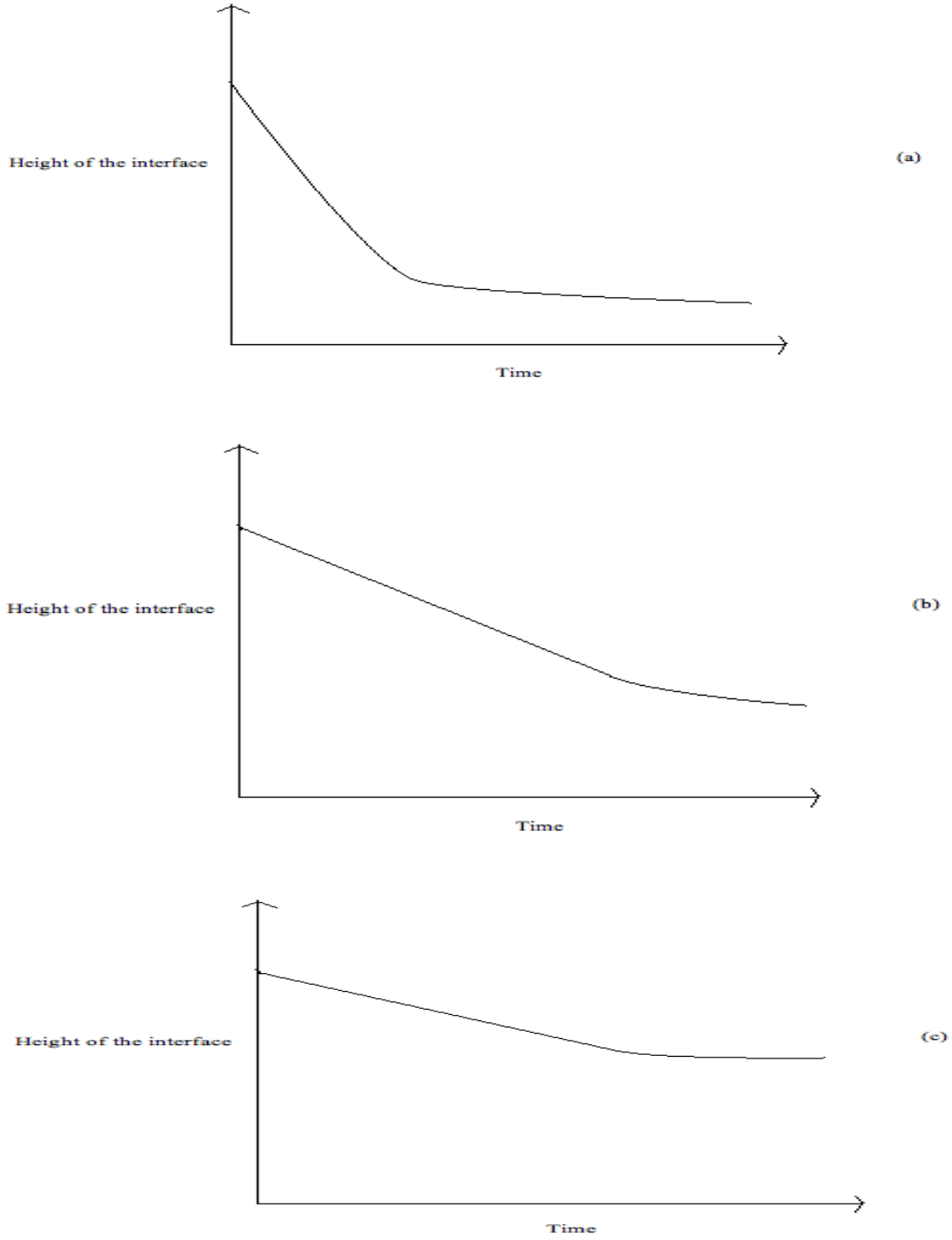

Figure 3-2 Types of hindered settling plots[8]

Two types of sedimentation methods are used to calculate the particle size [9], which includes:

- The calculation of the particle size directly from the Stoke's law. It involves the use of either pipette or hydrometer methods.
- The particle size measurement from hindered settling experiments by observing the change of the rate of fall of the interface with time.

3.2 Theory of Hindered Settling

Hindered settling provides a means for calculating the mean particle size economically. An equation to predict the velocities of the particles is necessary to account for the various sizes and densities of the particles, since hindered settling is based on the settling rates of particles. A large amount of research has been done in order to quantify hindered settling and calculate the settling rates of particles. [1, 10, 11] Stoke's law was expressed as a function of the concentration of the suspension, from which the mean particle size and the size of the aggregate could be determined. [12]

$$Q = V_s f(c) \tag{3.1}$$

Where,

f(c) is the function of concentration of the suspension

In most of the studies the concentration of the suspension was measured in terms of the initial liquid volume fraction or the initial porosity denoted by the term (ε). [11] (ε) is a ratio whose magnitude ranges between 0 and 1, whereas concentration can have varying magnitude. At a pure solid condition, ($\varepsilon = 0$) and at infinite dilution. ($\varepsilon = 1$).

$$\varepsilon = 1 - \frac{volume\ of\ the\ solid}{volume\ of\ the\ suspension} = 1 - \frac{m}{\rho_m V} \tag{3.2}$$

Where,

m: the mass of the solid

ρ_m: density of the solid particle

V: total volume of the suspension

We know that:

$$C = \frac{m}{V} \tag{3.3}$$

Where C is the concentration of the suspension

Therefore,

$$(1 - \varepsilon) = \frac{C}{\rho_m} \tag{3.6}$$

Equation 3.1 can also be written as:

$$Q = Vf(1 - \varepsilon) \tag{3.5}$$

The above relationships can be used to calculate the average particle size and also the size of the flocs in the case of flocculation.

Extensive research has been done by Steinour, [13-15] and Richardson and Zaki. [10] Steinour studied the theory of hindered settling and proposed the replacement of fluid density and viscosity with effective density and viscosity. He modified the Stoke's equation by introducing a single function (Φ) and (ε) for porosity. His equation fits only within his range of experimental study and is limited to particles having Reynolds numbers less than 0.0025. Richardson and Zaki proposed an empirical formula which extended the range of the Reynolds number to between 0.2 and 489. [2]

3.3 Modification of Stoke's Law

As discussed previously in Chapter 2, Stoke proposed an equation for the various factors affecting the rate of settling for particles in a suspension, which he presented as:

$$V_s = \frac{(\rho_m - \rho_f) g D^2}{18\eta} \tag{3.6}$$

3.3.1 Steinour's equation

Steinour modified the Stoke's law by introducing a new single function [Φ(ε)] and a new term, (ε) which denotes porosity. [5, 14-17] Therefore Equation 3.6 was transformed to:

$$V_s = \frac{(\rho_m - \rho_f) g D^2 \varepsilon}{18\eta} \Phi(\varepsilon) \tag{3.7}$$

Where,

ε :the initial porosity of the suspension or the liquid volume fraction of the uniformly mixed suspension.

V_s: Average relative velocity between the spherical particles and the liquid.

$$(1 - \varepsilon) Q = \varepsilon (V_s - Q) \tag{3.8}$$

Where,

Q: The measured velocity of the particle relative to a fixed horizontal plane.

The volumes for the solid and fluid that move in opposite directions past a unit of horizontal cross section in unit time were equated to give Equation 3.8.

Equation 3.8 can also be written as:

$$Q = \varepsilon V_s \tag{3.9}$$

Substituting Equation 3.6 into Equation 3.9 gives:

$$Q = \frac{(\rho_m - \rho_f) g D^2 \varepsilon^2}{18\eta} \Phi(\varepsilon)$$

(3.10)

Steinour considered the hydraulic radius of the suspension and derived an equation for [Φ(ε)] such that:

$$\Phi(\varepsilon) = \frac{\varepsilon}{1-\varepsilon} \theta(\varepsilon) \tag{3.11}$$

When the suspension is diluted to infinity, ($\varepsilon \longrightarrow 1$) and [Φ(ε)] becomes unity. Therefore Equation 3.7 becomes Equation 3.6.

Where,

$[\theta(\varepsilon)]$: the effects of shape that are not evaluated by considering the hydraulic radius.

Upon substitution of Equation 3.11 into Equation 3.10, we get

$$Q = \frac{2gr^2(\rho_m - \rho_f)\varepsilon^3 \theta(\varepsilon)}{9\eta(1-\varepsilon)} \tag{3.12}$$

Equation 3.12 can also be written as:

$$Q = V_s \frac{\varepsilon^3 \theta(\varepsilon)}{1-\varepsilon} \tag{3.13}$$

To calculate the radius, Equation 3.12 can be rearranged as:

$$r = \left\{ \frac{9Q\eta(1-\varepsilon)}{2g(\rho_m - \rho_f)\varepsilon^3 \theta(\varepsilon)} \right\}^{\frac{1}{2}} \tag{3.14}$$

In order to account for the settling of a spherical particle in the presence of a bound stagnant layer of immobile liquid, Steinour made modifications to the equation and proposed the following equation.

$$Q = V_s \frac{(\varepsilon - W_1)^3 \theta(\varepsilon)}{(1-W_1)^2(1-\varepsilon)} \tag{3.15}$$

Where,

W_1 : The ratio of volume of the immobile liquid to the total volume of solid including the pores along with immobile liquid.

W_1 can also be written as,

$$W_1 = \frac{\alpha}{\alpha+1} \tag{3.16}$$

Where,

α: The quantity of liquid in millimeters per unit bulk volume of the solid.

Steinour proposed an empirical equation which fit his experimental data, which is

$$Q = V_s \varepsilon^2 10^{-A(1-\varepsilon)} \tag{3.17}$$

Where, the value of A is 1.82.

Taking the logarithm of the above equation, we obtain:

$$Log\left(\frac{Q}{\varepsilon^2}\right) = A\varepsilon + (LogV_s - A) \tag{3.18}$$

3.3.2 Richardson and Zaki's equation

An empirical equation for Q was proposed by Richardson and Zaki [5,10,11] which is:

$$Q = V_s \varepsilon^n \tag{3.19}$$

Where,

n: dimensionless term.

The term (n) is important since it gives the equation for the maximum initial porosity where the solid flux, which is $Q(1-\varepsilon)\rho_S]$, would give the maximum value. The term solid flux represents the mass transfer per unit area of cross section per unit time down the sedimentation column. Equation 3.19 is simple and yields results more easily than Steinour's equation. As the value of (ε) increases, the value of $(1-\varepsilon)$ reaches zero. A

graph plotted with $[Q(1-\varepsilon)]$ on the Y axis and (ε) on the X axis reaches a maximum at some point,(ε_1). In many experimental interface settling rates, it is often observed that only the increasing slope is produced and the maximum value of (ε) is not observed. The slope can be given as

$$\frac{d\{Q(1-\varepsilon)\}}{d\varepsilon} = \frac{d\{V_s\varepsilon^n(1-\varepsilon)\}}{d\varepsilon} = -V_s\varepsilon^n + nV_s\varepsilon^{n-1}(1-\varepsilon) \tag{3.20}$$

Where $Q(1-\varepsilon)$ reaches its maximum value when $d\{Q(1-\varepsilon)\}/d\varepsilon = 0$ at the point (ε_1). Therefore,

$$V_s\varepsilon_1^n = V_s\varepsilon_1^n n\varepsilon_1^{-1}(1-\varepsilon_1) \tag{3.21}$$

The value of (n) and (ε_1) can be calculated from Equation 3.21 as:

$$n = \frac{\varepsilon_1}{(1-\varepsilon_1)} \tag{3.22}$$

$$\varepsilon_1 = \frac{n}{(n+1)} \tag{3.23}$$

Therefore the Richardson and Zaki Equation 3.23 can be rewritten as:

$$Q = V_s\varepsilon^{\varepsilon_1/(1-\varepsilon_1)} \tag{3.24}$$

Taking the logarithm of both sides of Equation 3.23 gives:

$$LogQ = LogV_s + nLog\varepsilon \tag{3.25}$$

The plot of $LogQ$ vs $Log\varepsilon$ should ideally give a straight line.

3.3.3 Dollimore and McBride's equation

Dollimore and McBride [6, 10, 11] proposed an empirical equation based on their observations. The logarithm of the rate of fall of the interface against the suspension concentration gave a linear plot.

$$LogQ = a - bC \tag{3.26}$$

Equation 3.25 can be written as

$$Q = (10^{a})(10^{-bC}) \tag{3.27}$$

Where,

C: concentration of the suspension and a, b are constants.

The concentration (C) can be replaced with the initial porosity (ε) by substituting Equation 3.6 into Equation 3.26 to give:

$$Q = V_s 10^{-b\rho_m(1-\varepsilon)} \tag{3.28}$$

The Dollimore and McBride equation can be analyzed as follows:

$$B = b\rho_m = \frac{1}{(1-\varepsilon_1)} \tag{3.29}$$

Where,

B: constant for porosity value.

$$\varepsilon_1 = \frac{1}{(1-B)} \text{ , when B<1} \tag{3.30}$$

This gives the following equation:

$$Q_{max} = V_s(10^{-1}) = \frac{V_s}{10} \tag{3.31}$$

Taking the log on both sides, we arrive at the following equation:

$$LnQ = LnV_s - b\rho_m(1-\varepsilon) \tag{3.32}$$

Using Equation 3.28, the above equation can be written as:

$$LnQ = (LnV_s - B) + B\varepsilon \tag{3.33}$$

A plot of (Q) against (ε) will ideally give a slope of (B) and an intercept of $(LnV_s - B)$. Dollimore and McBride also gave a method to calculate the porosity corresponding to the maximum sedimentation mass transfer (ε_1). For this, Equation 3.27 should be multiplied on both sides by the term (1-ε) to obtain the following equation:

$$Q(1-\varepsilon) = V_s 10^{-b\rho_m(1-\varepsilon)}(1-\varepsilon) \tag{3.34}$$

Upon differentiation of the above equation we get:

$$\frac{d\{Q(1-\varepsilon)\}}{d\varepsilon} = 2.303\, b\rho_m(V_s)\left[10^{-b\rho_m(1-\varepsilon)}\right]\left(1-\varepsilon-\frac{1}{2.303 b\rho_m}\right) \tag{3.35}$$

The above value becomes zero when the term $\left(1-\varepsilon-\frac{1}{2.303 b\rho_m}\right)$ is zero, and this occurs at $\frac{d\{Q(1-\varepsilon)\}}{d\varepsilon} = 0$ such that:

$$\varepsilon_1 = 1-\left(\frac{1}{2.303 b\rho_m}\right) \tag{3.36}$$

3.4 Summary of the various equations used in the hindered settling of suspensions

Steinour's Equation:

$$Q = V_s \varepsilon^2 10^{-A(1-\varepsilon)} \tag{3.37}$$

$$Log\left(\frac{Q}{\varepsilon^2}\right) = A\varepsilon + (LogV_s - A) \tag{3.38}$$

Richardson and Zaki's Equation:

$$Q = V_s \varepsilon^n \tag{3.39}$$

$$LogQ = LogV_s + nLog\varepsilon \tag{3.40}$$

Dollimore and McBride's Equation:

$$Q = V_s 10^{-b\rho_m(1-\varepsilon)} \tag{3.41}$$

$$LnQ = LnV_s - b\rho_m(1-\varepsilon) \tag{3.42}$$

Chapter-4

Flocculation of Suspensions

4.1 Introduction

The process of forming loose aggregates is called flocculation and the aggregates are called flocs. Usually in a flocculated system, a clear distinct interface is seen separating the sediment from the clear supernatant liquid since particles tend to fall together. This is seen because even the small particles present in the suspension become a part of the floc. [1] The flocs tend to preserve their structure in the sediment and contain entrapped liquid. The final sediment volume is therefore large and there is ease of redispersion of the suspension upon shaking. In a deflocculated system, there is no clear interface observed and the supernatant is usually turbid. This is because the larger particles tend to settle more rapidly leaving behind the small particles which is based on Stoke's law. [2] The disadvantage associated with a deflocculated system is that a compact cake is formed as the particles settle down to the bottom of the container. Therefore, a flocculated system is recommended where the final product should be free flowing and should consist of a uniform distribution of dose. [3, 4]

The major differences between a flocculated and deflocculated system are that in

a deflocculated system the particles exist as separate entities whereas in a flocculated system they exist as loose aggregates or flocs. The rate of sedimentation is higher in a flocculated system when compared to a deflocculated one. It is easier to redisperse a flocculated system than a deflocculated system since in the former the sediment is loosely packed whereas in the latter a hard cake is formed. A clear boundary is present between the sediment and supernatant in a flocculated system whereas a cloudy interface is present in a deflocculated system.[5]

Thermodynamic considerations are important during the formulation of suspensions. For any pharmaceutical system to be stable, the free energy should be kept as low as possible. Free energy is defined as the difference between the enthalpy and the product of the temperature and entropy. Equation 3.1 gives the relationship between the free energy, interfacial tension and the change in the total surface area of a system.[6]

$$\Delta G = \gamma_{SL} \Delta A \tag{3.1}$$

Where,

ΔG: Free energy of the system

γ: Interfacial tension between the solid and liquid

ΔA: Change in the total surface area

For the preparation of suspensions, the solid is broken down into smaller particles and dispersed in the continuous phase. As the particle size decreases, the surface area increases and subsequently the surface free energy also increases. This makes the system thermodynamically unstable. In order to stabilize the system, the free energy should be as low as possible. This can be achieved either by decreasing the interfacial tension or by decreasing the surface area. In order to decrease the interfacial tension, surfactants can be

used in the formulation. A decrease in the total surface area occurs when the particles tend to form groups held together by weak Van der waals forces. This grouping of particles to form loose and fluffy agglomerates is called flocculation. [7]

4.2 Zeta potential

Zeta potential is an electro-kinetic property that is exhibited by any particle in a suspension. Electrical charges develop at the solid -liquid interface in a suspension. This occurs due to the ionization of the functional groups present at the surface or due to the surface adsorption of ions. The stability of a suspension is determined by these electrical charges. These charges are responsible for the development of an electrical potential between the surface and the electrically neutral bulk solution, due to their uneven distribution around the particles. A double layer is formed due to the surface charge and the counter ions present next to it.[8, 9]

The inner most layer, where the ions are strongly bound is called the Stern layer. The outer layer where the ions are less firmly associated is called the diffuse layer. The particle is surrounded by a layer of liquid, which consists of two parts. There is a notional boundary within the diffuse layer where the ions and particles form a stable entity. When a particle moves due to some reason, then the ions which are inside the boundary also move along with it. Those ions lying outside the boundary are present in the bulk of the dispersant. The potential difference at this boundary or the surface of the hydrodynamic shear is called the zeta potential. It gives a measure of the net surface charge on the particle and potential distribution at the interface. It is an important parameter in the characterization of the electrostatic interaction between particles in dispersed systems and the properties of the dispersion as affected by this electrical phenomenon. [11]

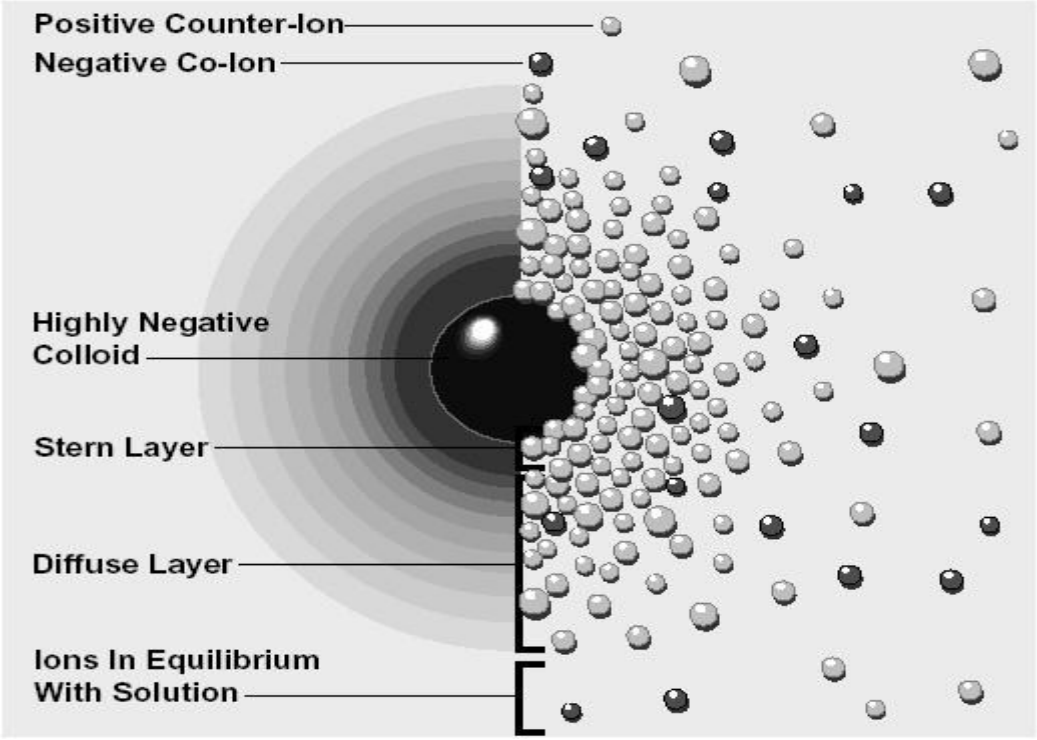

Figure 4-1: Zeta potential [10]

4.3 Controlled flocculation

Controlled flocculation refers to the intentional conversion of a deflocculated suspension to a flocculated suspension. A combination of control of the particle size and the use of appropriate flocculants gives rise to this phenomenon. Electrolytes, polymers and surfactants are used as flocculating agents. [12]

4.3.1 Electrolytes

They act by decreasing the zeta potential and reduce the electrical barrier between particles. They allow the formation of loose aggregates by a process of bridging between adjacent particles. As the valency of the ions increases, there is an increase in flocculating

power of the electrolytes. [3] For example the flocculating efficiency of calcium ions is greater than sodium ions ($Ca^{+2} > Na^{+1}$). Zeta potential decreases gradually when electrolytes are added to a positively charged deflocculated system. At some point the zeta potential reaches zero. Upon further addition of the electrolyte, the zeta potential drops and becomes negative. [12] Electrolytes were also found to increase the adsorption of the polymers onto the particles in the suspension. An example of this is alum which was found to improve the adsorption of anionic copolymers of acrylamide in a wood pulp and anatase suspension. [14]

4.3.2 Surfactants

These include ionic and non-ionic surfactants. The non-ionic surfactants act in a similar way like the polymers. They get adsorbed onto the surface of the particles, thereby forming loose aggregates. The ionic surfactants neutralize the charge on the particle, thereby yielding a flocculated system. An example of a surfactant is sodium dodecyl sulfate used to stabilize a suspension of alumina in water. [15]

4.3.3 Polymers

Polymers have been widely used in various industries to bring about the flocculation of suspensions. Examples of polymeric flocculants include the following. [16]

- Non-ionic flocculants: Polyvinyl pyrrolidone, polyethylene oxide, polyvinyl alcohol, polyethylene oxide
- Cationic flocculants: poly(dimethyl ammonium chloride), cationic polyacrylamide, polyethylene imine, polyvinyl pyridine, diallyl dimethyl ammonium chloride,

- Anionic flocculants: polyacrylic acid, polyvinyl sulfate, hydrolyzed polyacrylamide.

The process of flocculation by a polymer is affected by the following factors. [17]

- Mixing of the polymer molecules with particles in the suspension.
- Adsorption of the polymer chains on the particles in suspension.
- The change in the arrangement or the confirmation of the polymer molecules from an initial state to an equilibrium state.
- Collisions between the particles containing the adsorbed polymer, thereby forming aggregates.
- Breaking of the flocs

The mechanisms of polymer flocculation include charge neutralization, bridging and depletion flocculation. [18]

When polymers are present in solution, they either accumulate at the surface of the interface or tend to avoid the surface region. The former phenomenon happens when the segments of the polymers have a higher affinity for the surface sites than the solvent. This is called as adsorption. The latter happens when the solvent adsorbs preferentially. This is called as depletion. Both adsorption and depletion polymers affect the stability of suspensions.

The adsorption phenomenon occurs due to electrostatic interaction, hydrogen bonding, hydrophobic interaction or ion binding. Flocculants having a high charge density bring about flocculation through a process of charge neutralization. When a polymer of opposite charge gets adsorbed, there is a reduction in the net surface charge. Maximum flocculation occurs when the zeta potential value is close to zero. [19]

Adsorption polymers, when present in low concentration lead to the formation of large flocs through the process of polymer bridging. [21] Polymers have loops and chains extending into the surrounding dispersion medium which are long enough to encounter another particle. The segment of the polymer attached to the surface of the particles is called train. Trains are separated by segments that extend into the surrounding liquid by loops. The end of each polymeric chain has longer segments called tails that extend out into the solution. Figure 4-2 shows a polymer chain with trains, loops and tails. [22]

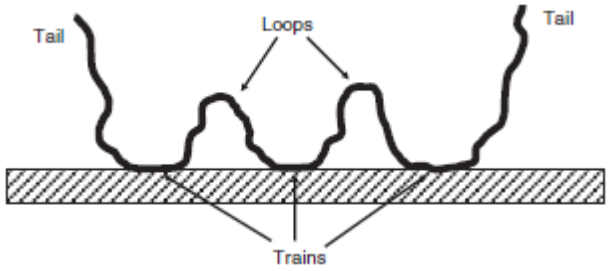

Figure 4-2: Polymer chain showing trains, loops and tails**.** [20]

Figure 4-3 shows a polymer in water that is positively charged. It gets adsorbed onto the surface of negatively charged particles. It brings the particles together to form floccules.

The flocculation efficiency of a polymer is affected by the molecular weight of the polymer and also the concentration of particles in the suspension. High molecular weight polymers readily form bridges between particles and at long inter-particle distances. Low molecular weight polymers are less effective. This is because bridging

requires the particles to be in closer proximity.

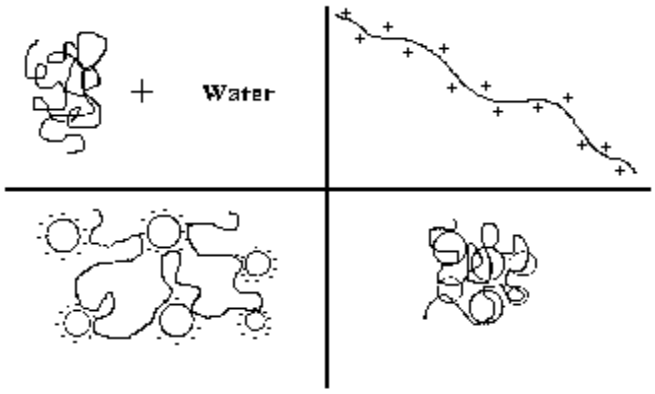

Figure 4-3: Adsorption polymer in low concentration [20]

When the particle concentration is high, then the bridging process is more effective because the particles are closer to each other. [21] When the polymer is present in higher concentration it coats the surface of the particles. This prevents the particles to get close in the range of attractive forces, leading to steric stabilization. [21, 23]

Depletion flocculation occurs due to polymers that are present in the dispersion medium but are not adsorbed onto the particles. When this type of polymer is present the dispersion medium, it is depleted from a layer of dispersion medium surrounding the particles compared to its concentration in the bulk of the solution. This leads to an increase in the osmotic pressure outside the particles which leads to attraction between the particles and thereby flocculation. [24, 25]

Dual polymer systems can also be used to bring about flocculation. They have a synergistic effect. The polymer with lower molecular weight gets adsorbed onto the particle surface while the higher molecular weight polymer aids in the bridging process

of several particles. An example of this is the flocculation of alumina suspensions by the addition of a low molecular weight polystyrene sulfonate to act as an anionic anchor for the high molecular weight, cationic polyacrylamide. [23]

Chapter-5

Instrumentation

5.1 Scanning Electron Microscopy

5.1.1 Introduction

Scanning Electron Microscopy (SEM) was developed in the late 1960's in order to study the morphology and surface characteristics of the sample in the natural state. [1] The texture, crystalline nature of the specimen, chemical composition, orientation of the sample can be determined using this technique. SEM can be used to measure very small samples in the size range of 0.01 to 10 μm. [2] It is widely used in the pharmaceutical industry for the analysis of raw materials as well as finished products. It is commonly used for qualitative analysis. It can also be quantitative, where the size of the material can be determined using image analysis. [3] Usually SEM does not show surface structures at the level of a monolayer. This can be overcome by decreasing the energy of the incident electrons to less than 1000 eV. It is at this point that the electrons do not penetrate beyond 50 angstroms beyond the surface of the specimen. [4]

The advantages of SEM over the conventional microscopy are: [5]

- Higher magnification, which reveals more details.

- Greater depth, which makes the examination of specimens simpler and a three dimensional image can be obtained.

The disadvantage associated with SEM is that its use is limited to solids that are stable in vacuum. [6]

5.1.2 Principle

A beam of electrons are emitted by a source which can be a tungsten filament, tungsten field emission tip or Schottky emitter upon heating to a temperature of 2700 K. This process is called a thermionic emission. The voltage difference between the cathode and the anode accelerates the electrons. The voltage difference can be as low as 0.1 keV or as high as 50 ke. [7] The interactions between the electrons and sample can be elastic or inelastic in nature. The atomic nucleus or the valence electrons deflect the incident electrons giving rise to elastic scattering. In this type of scattering there is negligible energy loss and there is a wide-angle directional change of the scattered electrons. When these elastically scattered electrons are captured for imaging, they are called 'back scattered electrons' (bse) or reflected primary electrons. Back scattered electrons have the same energy as that of the incident electrons. They are high energy electrons that are elastically scattered through an angle of 90^0 or more. [8]

The electrons and atoms of the sample interact with the incident electrons in different ways and give rise to inelastic collisions. This leads to the transfer of energy from the primary beam of electrons to the atom of that sample. The factors that determine the amount of loss in energy, are the binding energy of the electron to the atom and also if the electrons are excited singly or collectively. The excitation of electrons of the specimen during the ionization of the specimen atoms leads to the production of

secondary electrons. The excited atoms will decay into the ground state, producing X-ray photons, Auger electrons or both. The excess energy of the excited atoms, when transferred to the second outer shell electron emits the electron and yields Auger electrons. When the excess energy of the excited atom is released in the form of photon, the energy released can be high. In this case the photon will be the X-ray part of the electromagnetic spectrum and thereby yield X-rays. In some cases, electrons having sufficient energy to pass right through the sample without any interaction. Such electrons are called unscattered electrons and provide no information about the specimen.[8-10]. The various signals are analyzed in order to obtain details about the specimen being analyzed.

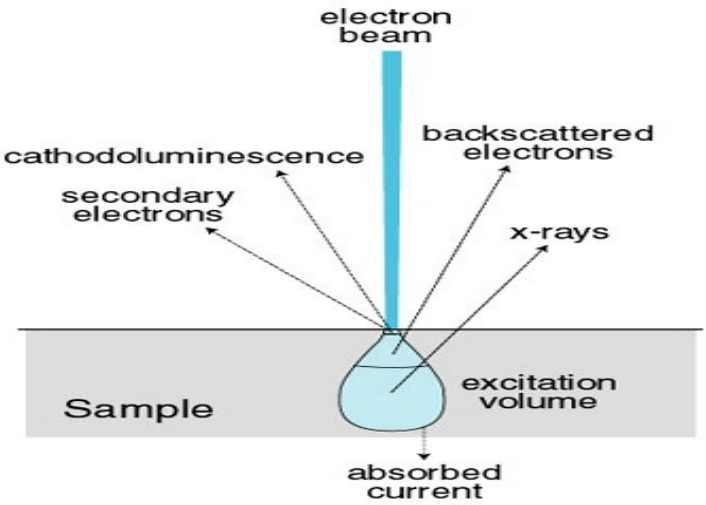

Figure 5-1: Types of signals [11]

5.1.3 Instrumentation

A SEM instrument is comprised of the following parts:

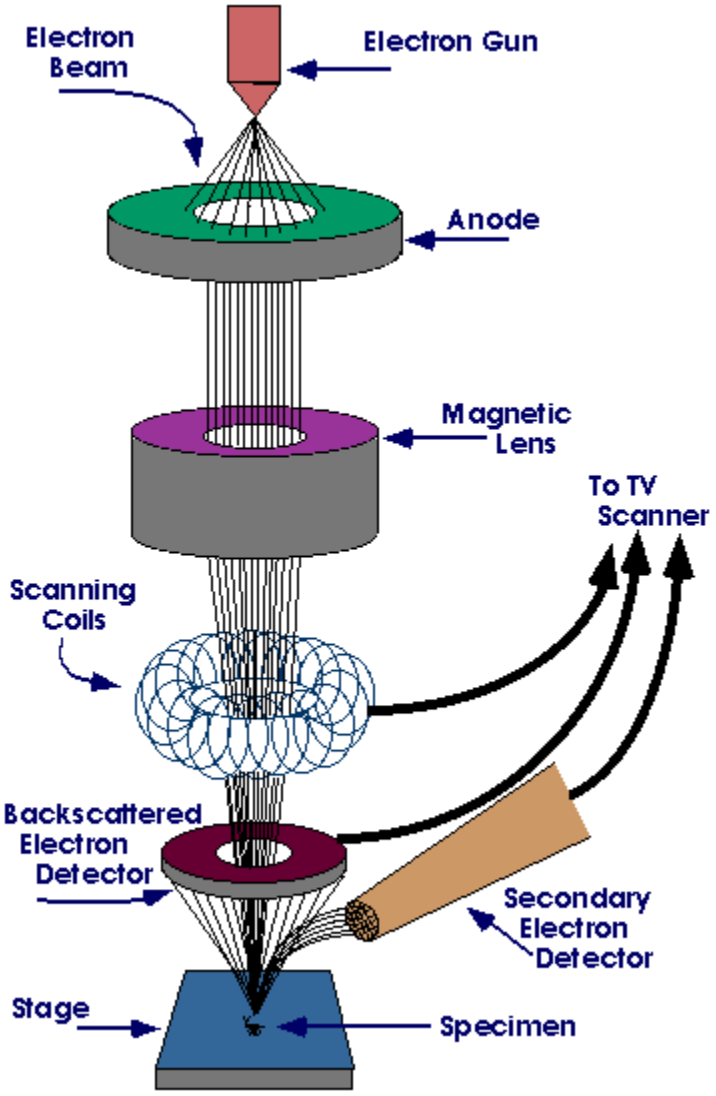

Figure 5-2: Schematic of SEM [11]

a) Source: The electron gun is the source of electrons and it is very crucial with respect to the performance of the SEM. The quality of the final image depends on the amount of current the gun provides. Three types of electron guns are used in SEM. They include:

- The Thermionic tungsten gun
- The Lanthanum Hexaboride (LaB_6) gun
- Field Emission gun

In the thermionic tungsten gun and the Lanthanum Hexaboride gun, current is passed through the cathode thereby heating it and leading to the production of electrons from its surface. The electrons form a real crossover, which is achieved by placing a Wehnelt electrode in front of the cathode. The Wehnelt electrode is negatively biased with respect to the cathode and focuses the emitted electrons. [12]

Field emission is a process where electron emission occurs from a cold metal surface when subjected to an electron accelerating field ($108V/cm^2$) in the presence of a vacuum. Field emission guns are comprised of a negatively biased suppressor electrode which is present behind a finely pointed cathode. The suppressor electrode pushes the emitted electrons forward, thereby creating high electric field strength at the cathode surface. The cathode tip is 15 nm in diameter. The electrons leaving the cathode do not cross over and seem to emanate from a virtual source, which is found by projecting the emitted rays backward from the anode plane. [12, 13]

The advantages of a field emission gun are: [13]

- No energy is required for the cold cathode.
- A large number of electrons emitted.

- There minimum chromatic aberration since the all the electrons leaving the cathode have the same energy.

b) Lenses: Two types of lenses are used in SEM. They are the condenser lens and objective lenses. The condenser lenses converge and collimate the diverging beam into parallel beams. About 3 magnetic lenses are used in SEM. They regulate the amount of demagnification while the objective lenses focus the electron beam on the specimen. They contribute more towards regulating the magnification. There are three types of objective lenses including a pinhole lens, immersion lens and snorkel lens. These lenses are usually water-cooled since a large amount of current flows through their windings. [9, 14]

c) Detector: Detectors receive the signals from the specimen and convert them into electric signals followed by amplification. Various types of detectors are used in scanning electron microscopy. The commonly used detector is the scintillator photomultiplier type which has the advantage of high signal to noise ratio when compared to most other detectors. However, it is very expensive and too bulky. Among the other detectors are the solid state detector, specimen current detector and cathodoluminiscence detector. [15, 16]

d) Output: Once the required information about the specimen is obtained, the output image is recorded either by using optical photographic methods or electrical analog methods or digital methods. [13]

5.1.4 Applications of SEM

SEM has been used to determine the surface characteristics and morphology of a wide variety of materials. The disadvantage associated with it is that its use is limited to solids that are stable in a vacuum.

5.2 Laser Diffraction

5.2.1 Introduction

Laser diffraction is an unparalleled technique of measurement capacity. This technique is used for the characterization of industrial sprays, powders, suspensions and emulsions.[17, 18] It can be used for particles having a size range of 0.1-1000 μm. It is known for providing accurate and precise measurements. [19] It is used to determine the size distribution for a collection of particles. [20]

5.2.2 Principle

Laser diffraction instruments use the principle that particles in a laser beam scatter the laser light. The angle of scattering in the forward direction is small for large particles whereas smaller particles scatter light at wider angles. The angle of scattering of the laser beam is inversely proportional to the particle size. The scattering of light by particles produces signals that are measured by a series of detectors that are placed at different positions. These signals are then converted to particle size distribution with the help of a model based matrix. For each set of size classes, the matrix contains the calculated signals at all detector elements per unit volume of spherical particles. [21, 22] This technique combines two different physical techniques which are the Mie scattering and Fraunhofer diffraction.

The theory behind Mie scattering is very complex. The conclusion of Mie's theory is the appearance of many maxima in the intensity of scattered light as a function of the scattering angle. The difference in the refractive index and the size of the particles determine the number and the position of the maxima. When the particle size increases from 1/10 to 10 times of that of the incident light's wavelength, there is a reduction in the intensity and the interference due to scattering of the particle is out of phase.[22]

Figure 5-3 (a) Diffraction pattern of a large particle

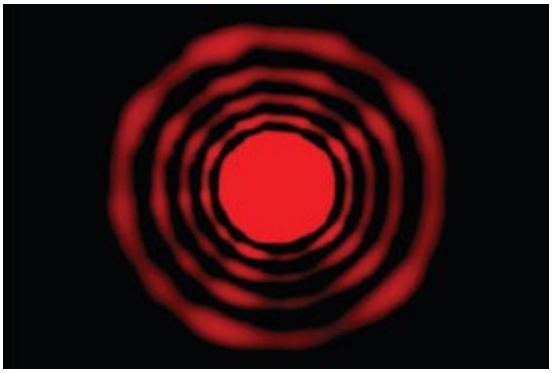

Figure 5-3 (b) Diffraction pattern a small particle[23]

When the particle size approaches the wavelength of the incident light, rigorous Mie theory computations are employed. The Mie theory is used to obtain an optimal analysis of the distribution of light energy in order to determine the particle size distribution. This theory can be treated as a computational box where the scattering angle values can be fed in order to arrive at the size of the particles. It holds good for all particulate matter in all transparent media. The media can be liquids, gases or transparent solids. Therefore, the particle size of suspensions, emulsions, spray droplets and vapors can be analyzed with this technique. [24]

The Fraunhofer diffraction was used previously in older instruments. The theory behind this process is that the particles being measured are opaque and light is scattered at narrow angles. Hence, this can be applied to only large particles. [24]

The advantage of this technique is the speed and its reproducibility.[25] Also, the amount of sample required is from a few milligrams to grams and both dry and wet samples can be used. [26] The instrument does not require any external calibration. [27]

However the disadvantages include the following: [28]

- When the scattering is very small, any small change will affect the results. This can occur when there is a temperature difference in the liquids in the cell or when the sample is not uniformly mixed or if the flow rate of the sample is very high.

- There could be multiple scattering. Ideally, it is assumed that each photon encounters one particle. If a single photon is scattered by a series of particles, then

it is difficult to analyze the pattern of scattering. Dilution of the sample can be done to overcome this problem.

- The particle shape also affects the scattering pattern. Spherical, rod shaped, ellipsoid particles can be analyzed but it cannot be used for particles with an irregular shape.

5.2.3 Instrumentation

The set-up of a laser diffraction particle size analyzer is shown in Figure 5-4.

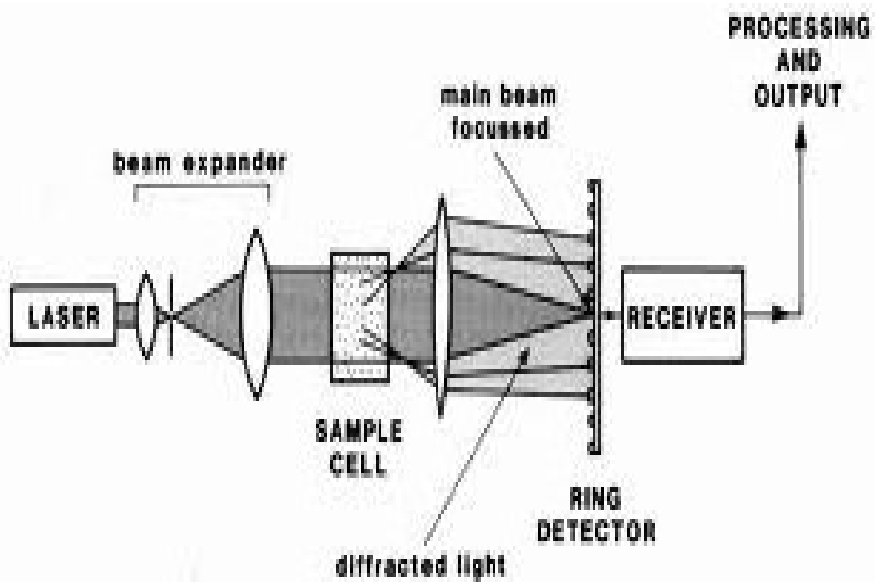

Figure 5-4 Schematic of Laser diffraction particle size analyzer[29]

A helium-neon laser is usually used as the source of a coherent, intense laser beam. The wavelength of the beam produced is fixed. It is around 632.8 nm and the power is usually 2-10 mW. A beam expander is used to produce a uniform parallel beam of 5-10 mm in diameter which is used to illuminate the sample sufficiently. [30] A zone plate is

used to allow only the central intensity maximum of the laser beam and cut off the unwanted scattering and diffraction. The beam thus produced is directed to the sample being analyzed, which is present in a sample cell. The light from the sample passes through a transform lens. This transforms the light that has been scattered at a wide range of angles, into an output image where the scattering angle corresponds to an annular ring in the detector. The detector is a diode array that measures the intensity distribution of the scattering pattern. The particle size distribution is obtained corresponding to the scattering patterns using Mie's calculations. [28, 31]

5.2.4 Applications

A laser diffraction technique is used to accurately measure the particle size distribution of a wide variety of substances. It is used to analyze suspensions, emulsions, dry powders inhalers and also used in aerosol studies to measure the size of the droplets. [28, 32] It can also measure transient changes such as dissolution and particle agglomeration. [18]

5.3 Thermal Analysis

5.3.1 Introduction

The International Confederation for Thermal analysis and Calorimetry (ICTAC) defined "Thermal analysis as a group of techniques in which a property of a sample is monitored against time or temperature while the temperature of the sample remains in a specified atmosphere is programmed".[33] Hemminger and Sarge modified the above definition as "Thermal Analysis means a generic term for a group of techniques in which the temperature of matter is varied according to a specified program and the matter's

properties are measured as a function of temperature". [34] A generalized flow diagram for designing a Thermal Analysis instrument is given in Figure 5-5.

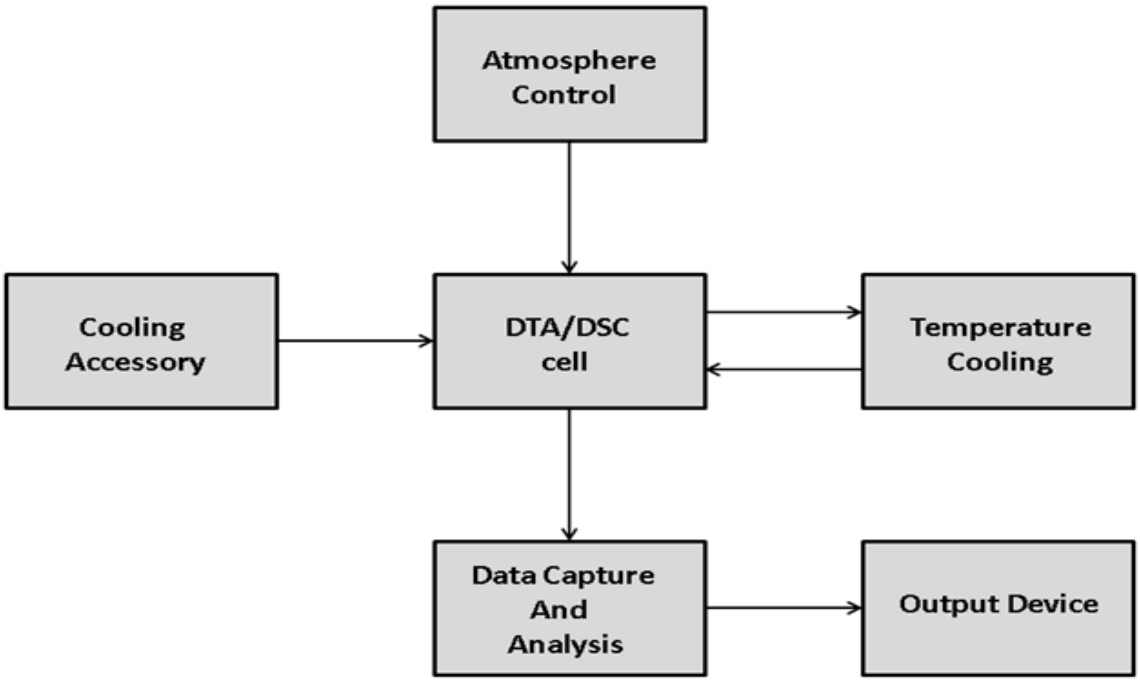

Figure 5-5 Flow diagram for designing a Thermal Analysis instrument

A technique can be classified as a thermal analytical technique, if the following criteria are satisfied. [35]

1) A physical property must be measured.

2) The measurement should be expressed directly or indirectly as a function of temperature.

3) The measurement should be made with a temperature controlled program.

A number of properties of the sample can be measured using thermal analysis which are listed in Table 5.1. [36]

Table 5.1: Property measured and technique used in Thermal Analysis

Property	Technique
Temperature	Thermometry
Temperature difference	Differential Thermometry
Heat flow difference	Differential Scanning Calorimetry
Mass	Thermogravimetry
Dimensions or mechanical properties	Thermomechanometry
Pressure	Thermomanometry
Electrical properties	Thermoelectrometry
Magnetic properties	Themomagnetometry
Optical properties	Thermoptometry

The samples used for thermal analysis are usually limited, but not necessarily, to solid substances. Liquids can also be analyzed but provide less information compared to solids. Gases are not usually analyzed using thermal analysis. The samples are analyzed in an inert atmosphere with a temperature controlled program. A combination of the above techniques is usually used in order to obtain better understanding and interpretation of the results.

5.3.2 Differential Scanning Calorimetry

Differential Scanning Calorimetry obtains thermal information of a sample by heating or cooling it alongside an inert reference. It is defined as "A technique in which a difference in the heat flow (power) to the sample (pan) and reference (pan) is monitored against time or temperature while the temperature of the sample, in a specified atmosphere, is programmed".

The differences in heat flow occur due to:

- The heat capacity of the sample which increases with temperature (baseline).

- Transitions that occur in the sample (events superimposed on the heat capacity baseline). [37]

5.3.2.1 Instrumentation

The major components of the system include:

- Sensors and an amplifier
- Furnace and a temperature sensor
- The programmer and computer
- The recorder and plotter

Sensors are usually thermocouples. Copper- Constantan or chromel- alumel thermocouples are used for low temperatures and Pt-Pt/13%Rh is used for higher temperatures. A few instruments also make use of multiple thermocouples or thermopiles to increase the signal. The sample pans used are made out of aluminum, silver, steel, gold or platinum. The pan can be sealed or left open depending on the sample being analyzed. The purge gases used are usually inert and nitrogen or argon. Oxygen or air can also be used depending on the sample and the desired effect. [38]

5.3.2.2 Types of DSC

There are two types of DSC instruments which are Power Compensated DSC and Heat Flux DSC.

a) Power compensated DSC

In power compensated DSC, the heat flow is measured directly to or from the sample. [39] The sample and reference are heated using two separate heaters and the temperature difference is kept close to zero. The difference in the electrical power needed

to maintain equal temperatures is measured. [40] The heat to be measured is completely compensated by electrical energy. [41]

$$\Delta P = D(\Delta Q)/dt \quad (5.1)$$

The sample is placed into in a sample pan and inserted onto one end of the sample holder and the empty reference pan made out of the same inert material is placed on the other end of the holder. The holder is then placed at the center of the furnace.

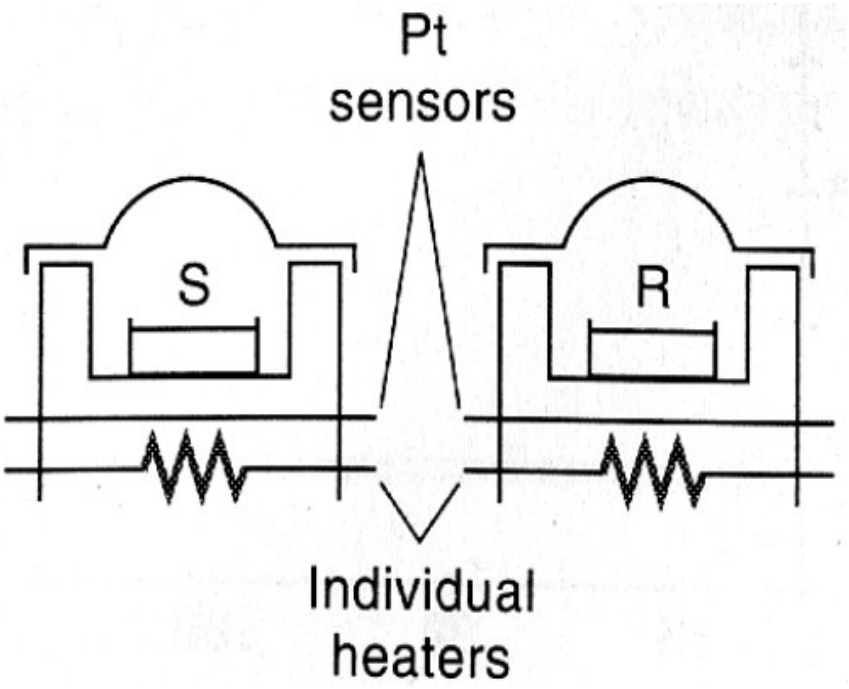

Figure 5-6 Schematic for a Power compensated DSC [40]

b) Heat Flux DSC

In a heat flux DSC the change in temperature between sample and empty reference pan is measured. [39] The sample and reference are heated from the same source. The difference in temperature is measured, and the signal is converted to a power

difference using calorimetric sensitivity. [40] The sample containers are placed on the disc, symmetrical to the center. The arrangement of the temperature sensors and the sample containers must always be the same in order to avoid measurement discrepancies. The temperature sensors used are usually thermocouples or resistance thermometers. This category of Heat flux DSC belongs to a heat exchange calorimeter. [41]

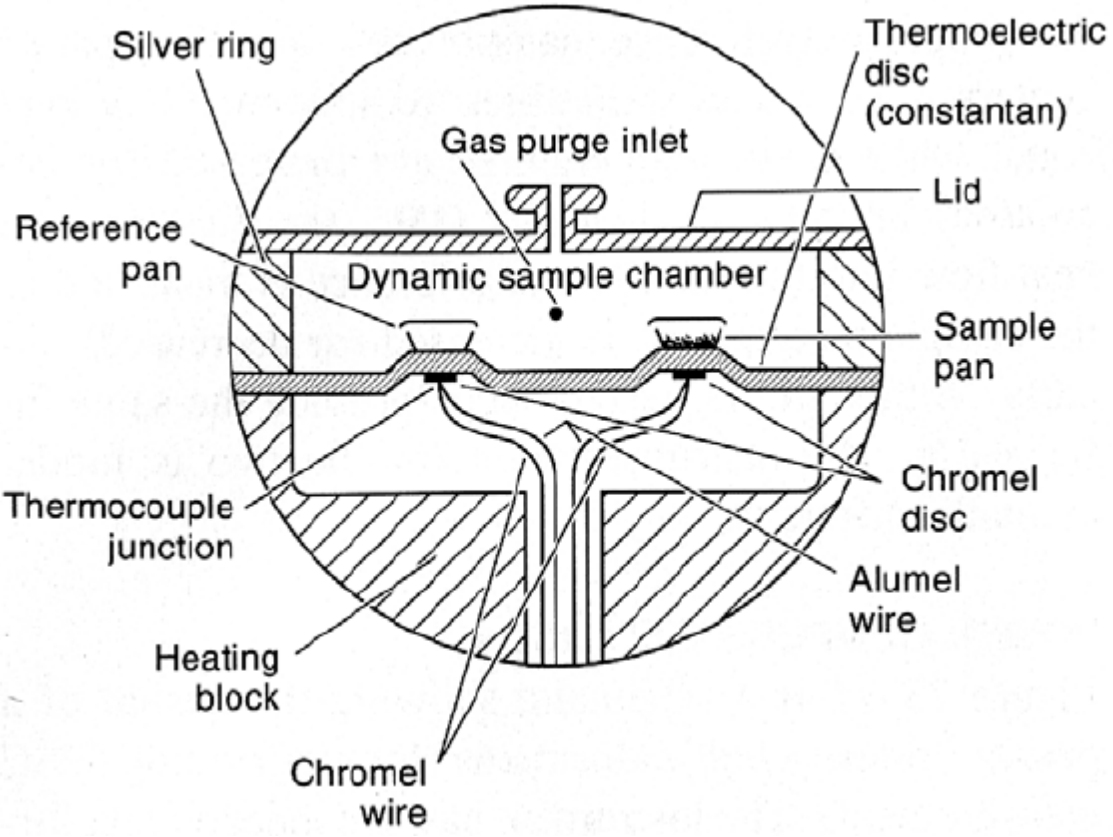

Figure 5-7 Schematic for a Heat Flux DSC [40]

5.3.2.3 Applications of DSC [42]

DSC is used in the following areas:

- Easy and fast determination of the glass transition temperature, melting and crystallization temperatures, heats of fusion and reaction.
- Determination of purity of compounds.
- Measurement of liquid crystal transitions.
- Evaluation of the kinetics of polymer crystallization.
- Evaluation of the kinetics of chemical reactions.

5.3.3 Thermogravimetry

Thermogravimetric analysis is based on the change in the mass of the material with an increase in the temperature. ICTAC defined TG as a technique whereby the mass change of a substance in an environment heated or cooled at controlled rate is recorded as a function of time (t) or temperature (T). [43] The apparatus used to obtain a thermogravimetric curve is called a thermobalance. It is a very sensitive balance that accurately measures the change in the mass of the material upon heating. [44] The data obtained from this technique is called a thermal curve with temperature on the X-axis and mass on the Y-axis. When time is used on the X coordinate, then a second curve of temperature versus time is necessary to indicate the temperature program that has been used. [45]

5.3.3.1 Instrumentation [46] [47]

Typically, the instrument consists of the following parts:

1) A sensitive balance;
2) A furnace, a temperature measuring device, usually a thermocouple;

3) Programmer or computer; and a

4) Recorder, Plotter, Data acquisition system.

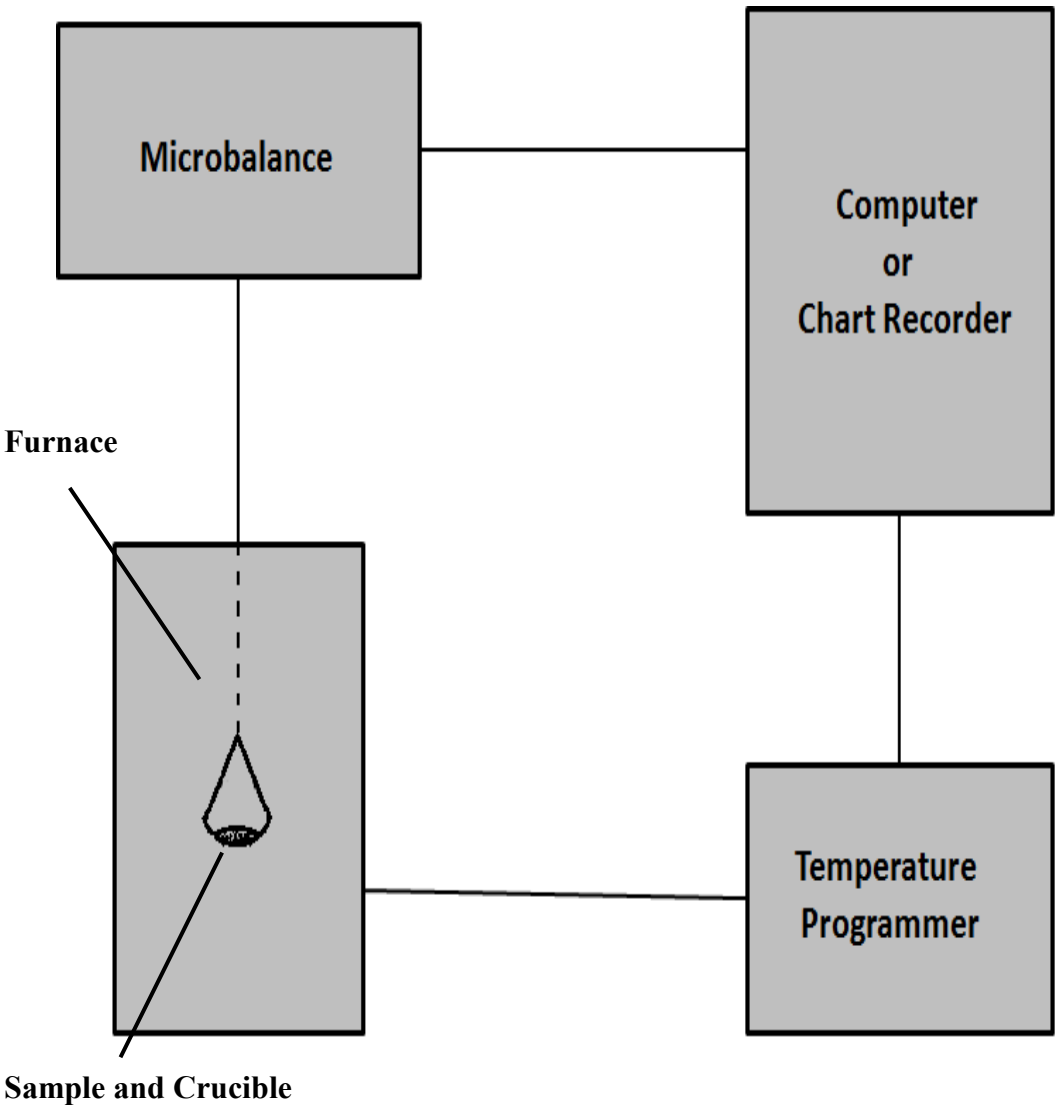

Figure 5-8 Schematic for TGA data acquisition

The crucible is placed on the balance and the former is suspended into the furnace. This set up will prevent the direct contact of the temperature sensor with the crucible which otherwise would hinder the readings of the balance. . The temperature is hence in the vicinity of the crucible. The temperature responses for each specimen under analysis and the sensor are different since both are of different materials, have different heat capacities and mass. The balance assembly records the initial weight of the compound and monitors the change in weight with an increase in temperature. [48]

Various types of balances have been used for thermogravimetric analysis, which include pivoted, cantilever and torsion beam. A rotating pivot is present in the modern microbalance. It is controlled by a zero detection device, which is generally a light coupled to a photo cell and a magnet and a moving coil system to restore balance. [49] The resolution of these balances is usually around 1μg or better. The sample size ranges from a few milligrams to 30 grams. In order to avoid any corrosion of the balance due to the presence of reactive gases, inert gases are often purged.

The choice of the atmosphere plays an important role in TGA results. Usually nitrogen at room temperature is used as the purge gas. It delays the onset of decomposition. [50] Oxygen can also be used as the purge gas where oxidation or burn off is required. Helium is usually used when the instrument is attached to a mass spectrometer to avoid confusion between nitrogen ion whose mass is 28 and carbon monoxide. The advantages of using helium are that the resolution is better and the cooling time is comparatively less. [51] This technique is performed in the presence of static or dynamic atmospheric conditions. A static condition is one in which the composition of gases remains unchanged when gases are evolved in the reactions. A

dynamic atmospheric condition is one which the composition of the gases changes when gases are evolved in the reaction. [47]

The furnace is a non-inductively wound electrical resistance heater. It should be such that the heat from it does not affect the balance mechanism. It should be capable of a rapid response and a range of heating and cooling rates. [52]

The pans that are used for the analysis are usually made of aluminum or platinum. However, aluminum pans cannot be used above 600^0C since the melt is above 650^oC-700^oC. Open aluminum pans are less expensive than platinum, carbon or ceramic pans.. Pans can be sealed or open. Small holes can be punched through the lids of the sealed pans to control the heat and loss of decomposition products. Pan liners are also available, if required. [51]

The output generated by the computer carries out all the required calculations and manipulations and plots for the TG curve.

The most common use of TGA is in the determination of the composition of a chemical through the examination of the various steps in the weight loss process. The TGA curves are of various types as seen in Figure 5-9. [53, 54] An explanation for each curve is as follows:

Type I: No changes are seen from this type of curve. The sample does not undergo any decomposition and there is no loss of volatile compounds.

Type II: There is an initial sudden loss in the mass of the material. Care should be taken to make sure that the curve is not because of the moisture present in the carrier gas or moisture adsorbed onto the sample. The samples should be run again in order to confirm the weight loss.

Type III: This curve shows that there is a one-step decomposition of the sample being analyzed. The stoichiometry and the kinetics of the reaction can be determined from it.

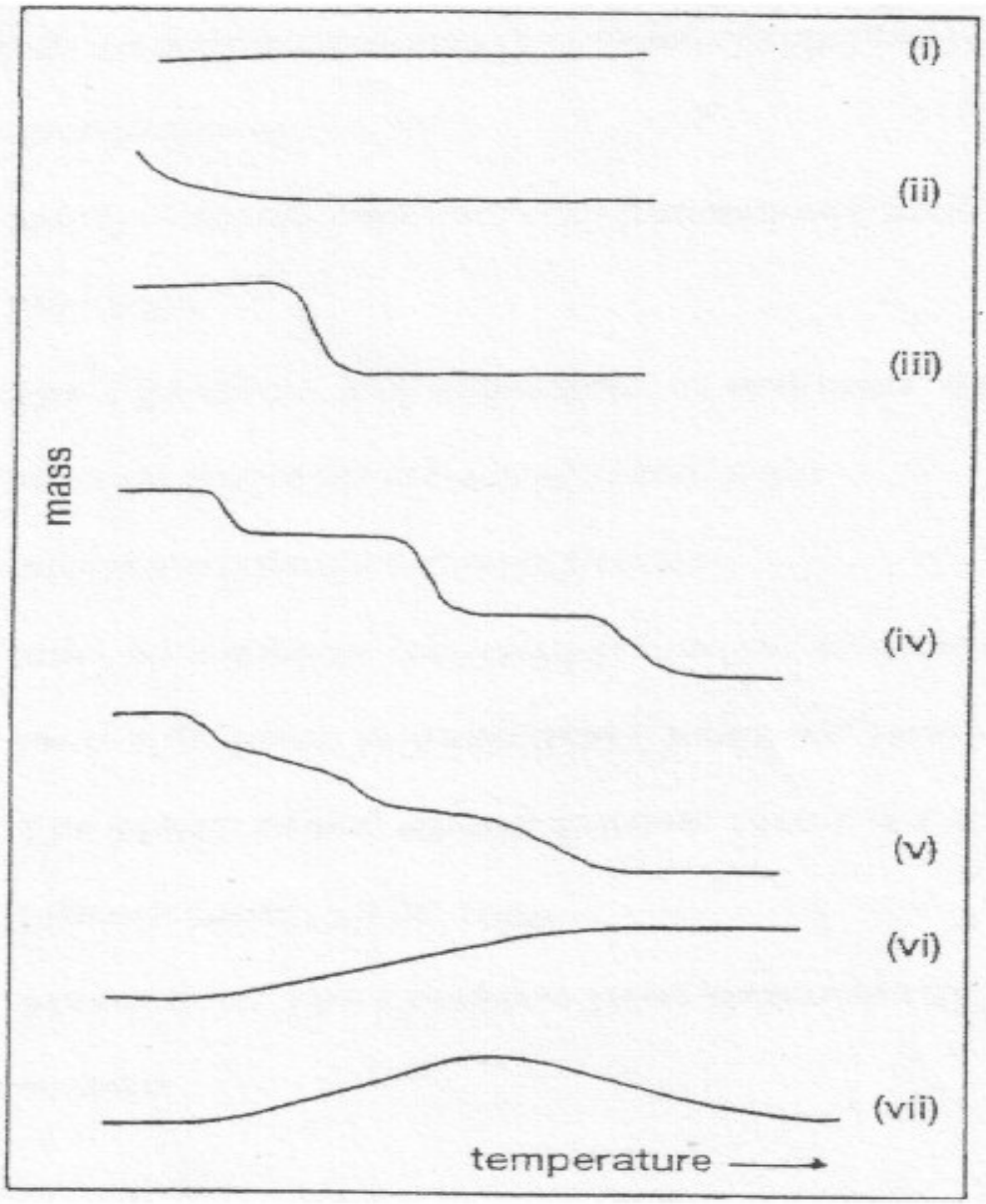

Figure 5-9 Types of TGA curves seen with various chemicals [53]

Type IV: This curve shows that there is a multiple step decomposition of the sample with stable intermediates. The stoichiometry of the reaction can be determined from this along with the temperature limit of stability of both the reactant and the intermediate.

Type V: This curve represents also represents multiple step decomposition of the sample but with the formation of less stable intermediates. Very less information is obtained from these graphs. However, the overall stoichiometry of the reaction can be obtained.

Type VI: This curve shows that there is an increase in the mass of the material which can happen in case of oxidation of the sample.

Type VII: Usually, we do not come across these kind of curves. It could be because of oxidation of the sample which later decomposes at higher temperature.

5.3.3.2 Applications [5]

Thermogravimetry can be used in the following situations:

- To understand the decomposition mechanism and thermal stability of various materials.
- TG curves can be used to identify compounds and get information about their purity since they provide fingerprints of compounds.
- Corrosion studies can be performed
- Polymorphism studies can be done
- Drugs can be characterized during processing or during accelerated stability studies.

- Composition analysis of complex materials can be done since their components can be sequentially removed.

Chapter-6

Methods and Materials

6.1 Materials

6.1.1 Dried Aluminum Hydroxide Gel U.S.P

Dried aluminum hydroxide gel is a white amorphous powder that is obtained by subjecting aluminum hydroxide to drying at low temperature until it has the required amount of Aluminum oxide. [1] It should contain an equivalent not less than 76.5% of aluminum hydroxide. It may also contain varying amounts of basic aluminum carbonate and bicarbonate. [2] The structure of aluminum hydroxide is given in Figure 6-1.

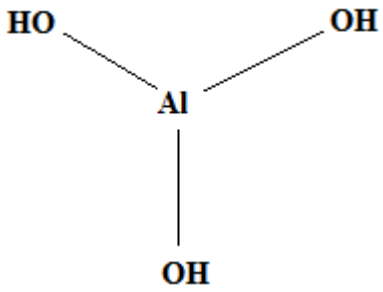

Figure 6-1: Structure of aluminum hydroxide

6.1.1.1 Properties of dried aluminum hydroxide gel U.S.P

Dried aluminum hydroxide powder was obtained from Spectrum Chemical Manufacture Corporation. Its CAS number is 21645-51-2 and its Lot number is YG0190. A 4% suspension of aluminum hydroxide in water has pH of not more than 10. [3,4]

Table 6.1: Properties of dried aluminum hydroxide gel USP.

Property	Description
Formula weight	78.00 g/mol
Appearance	White amorphous powder
Density	2.42 g/cm³
Solubility	In water: 0.0001 g/100 mL (20 °C); Soluble in acids, alkalis

6.1.1.2 Occurrence

Aluminum hydroxide is found naturally in the form of three polymorphs namely Gibbsite (α-$Al(OH)_3$), Bayerite (β- $Al(OH)_3$) and Nordstrandite (γ- $Al(OH)_3$). The formation of these polymorphs depends on the pH, the ratio of the aluminum ions to hydroxyl ions, the presence of other organic and inorganic ligands and the presence of clay minerals. [5]

6.1.1.3 Uses

- Dried aluminum hydroxide gel may be suspended in distilled water to make the official Aluminum Hydroxide Gel USP.

- It is primarily used as an antacid in the management of peptic ulcer, gastritis, peptic esophagitis, gastric hyperacidity and hiatal hernia. The major advantage of aluminum hydroxide is that no systemic alkalosis is produced.
- It is externally used as a mild astringent and desiccant. It is a constituent of some foot powders. In silicosis therapy, inhalation of powdered aluminum hydroxide for a few minutes per day over a period of several weeks has been shown to give improvement in the condition. [1]
- It is used in the purification of water. It adsorbs bacteria and other impurities present in water. [6]
- It is used as a mordant in the dye industry. It is precipitated out of a solution onto fibres to be dyed and immersed in a dye bath. The resultant color depends upon the combination of the dye and the mordant. [7]
- It is used in the manufacture of aluminum silicate glass, which is used is a high melting point glass used in cooking utensils. [2]
- It is used in waterproofing fabrics, production of fire clay, paper and pottery. [2]

6.1.1.4 Incompatibilities

Aluminum hydroxide for gastrointestinal problems accompanying the use of tetracycline antibiotics has resulted in complexation and decreased absorption of the antibiotic. [3]

6.1.1.5 Handling and Storage

It may cause eye irritation and may also affect behavior, metabolism, blood, liver, gastrointestinal and musculoskeletal systems. Avoid contact with eyes, skin and clothing and breathing dust. Hands must be washed thoroughly after handling.

It is kept in a tightly closed container and stored in a cool, dry, ventilated area. It should be protected against physical damage. It is kept it isolated from incompatible substances. The containers of this material may be hazardous when empty since they retain product residues. [3]

6.1.2 Polyethylene Glycol 1000

PEG is the abbreviation for polyethylene glycols. As the name suggests, it refers to a chemical compound composed of repeating ethylene glycol subunits. It is commercially available as mixtures of different oligomer sizes in broadly or narrowly defined molecular weight ranges. Various grades are commercially available such as 200, 300, 400, 600, 1000, 4500 etc. They do not hydrolyze or deteriorate at typical conditions.[8] PEG 1000 was chosen for the current study. It is also known as Carbowax 1000 or Macrogol 1000. [1]

PEG 1000 was procured from Spectrum Chemical Manufacture Corporation. The CAS number is 25322-68-3 and the Lot number is WR 3123. Chemically it is α-hydro-ω-hydroxy poly(oxy-1,2-ethanediyl). The molecular structure of PEG is represented in Figure 6-2. The properties are given in Table 6.2. [9]

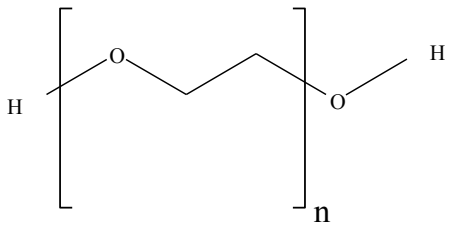

Figure 6-2: Structure of PEG 1000

Table 6.2: Properties of PEG 1000 [9]

Property	Description
Average molecular Weight	1000g/mole
Appearance	Solid(Waxy)
Solubility	Soluble in cold water, hot water. Soluble in many organic solvents. Readily soluble in aromatic hydrocarbons.

6.1.2.1 Uses

- Its blandness renders it acceptable for hair dressing creams, skin creams, shaving creams, lotions and a wide variety of cosmetic preparations.
- It is used as anti-dusting agent in agricultural formulations.
- It is used in electroplating process.
- It is an important ingredient in cleaners, detergents and soaps with low volatility and low toxicity solvent properties.
- It is applicable in wood working operations as a dimensional stabilizer.
- It is used as a plasticizer and a humectant in ceramic mass, adhesives and binders.
- It is used as a fabric softener and antistatic agent in textile industry.
- In the present study it has been used as flocculating agent to improve the stability of the Aluminum hydroxide suspensions. A 0.01%, 0.03%, 0.05% concentration of PEG 1000 were used in the study. [2]

6.1.2.2 Incompatibilities

Polyethylene glycol 1000 has been found to be incompatible with strong acids, strong bases, strong oxidizing agents and polymerization catalysts. [9]

6.1.2.3 Safety and Storage

Inhalation of PEG 1000 in large quantities may cause irritation of the upper respiratory tract. One must avoid contact with eyes and skin. In the case of contact, wash with plenty of water for at least 15 minutes. The containers of this material should be kept tightly closed. It should be stored in a cool, well-ventilated area. [9]

6.2 Methods

6.2.1 Preparation of Aluminum hydroxide suspension

A 15, 20, 25, 30, 35 gm portion of dried aluminum hydroxide gel was weighed accurately and transferred into a 200 mL measuring cylinder and the volume was made up to 150 mL with RO water. The suspension was dispersed by inverting the cylinder 20 times after which it was left undisturbed for 24 hours. The volume was then made up to the 200 mL mark using distilled water and the suspension was dispersed by inverting the measuring cylinder 20 times. The time taken for the height of the interface to drop was noted until the there was no further change in the interface height. This procedure was done in triplicate. The height of the interface versus time was plotted and the Q-value (slope) was obtained for the linear zone as shown in Figure 6-3.

6.2.2 Preparation of various concentrations Polyethylene glycol solutions

Varying concentrations, namely 0.01%, 0.03%, and 0.05% of Polyethylene glycol 1000 solutions were prepared to determine the effects of the polymer solution on the hindered settling of aluminum hydroxide suspensions. An accurately weighed 0.1 gm, 0.3 gm, 0.5 gm of Polyethylene glycol 1000 were dissolved in approximately 900 mL of water using a magnetic stirrer. The final volume was made up to 1000 mL with RO water. The solutions were covered and left overnight so that the polymer swells and gets

dispersed in the dispersed medium. The solutions were stirred to ensure uniform dispersion before use.

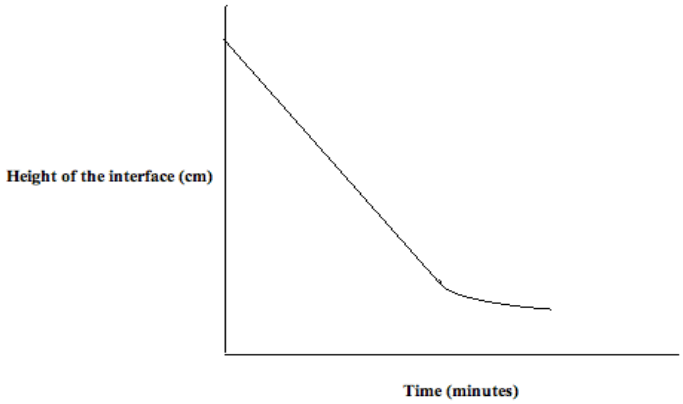

Figure 6-3: Plot of Height of interface versus time

6.2.3 Determination of Density

A pycnometer was used to determine the density of the liquids .The pycnometer is a glass flask with a close-fitting glass stopper with a capillary hole through it. The fine hole releases a top-filled pycnometer and allows for obtaining a given volume of measured and working liquid with accuracy.

The weight of the empty pycnometer was noted. The pyconometer was then filled with the liquid until it overflowed. The outside of the bottle was cleaned until dry and the weight was recorded again. The difference in the weights was used for further calculations. This procedure was repeated to calculate the density of the polymeric solutions and the difference was recorded relative to the weight of the dispersion medium. The specific gravity could be determined relative to water.

The density was calculated using the following formula.

Density= weight (g)/volume(mL) (6.1)

6.2.4 Determination of Viscosity

The viscosity of the liquid media was measured using the Ostwald viscometer. The Ostwald viscometer was placed in a constant temperature bath at $20^0 \pm 0.5\ ^0$C. The required amount of the sample was added. It was then drawn up to the mark above the upper mark. The time taken for the liquid to fall from the upper to the lower marks was recorded and used for further calculations. Water was used as the standard and the viscosity of the water and the other solutions was determined, from which the relative viscosity of the sample was calculated.

$$(\eta_l / \eta_w) = (\rho_l t_l / \rho_w t_w) \quad (6.2)$$

Where,

(η_l) is the viscosity of the sample liquid and (η_w) is the viscosity of water.

(ρ_l) is the density of the sample liquid and (ρ_w) is the viscosity of water.

(t_l) is time taken by the sample liquid to fall from the upper mark to the lower mark

(t_w) is the time taken by water to fall from the upper mark to the lower mark. The density of water at 20^0 C is 0.98g/cm^3 and the viscosity of water is 0.01poise (g.cm^{-1}sec^{-1}).

6.2.5 Sieving

Sieving is one of the oldest techniques used for classifying powders and granules by particle size distribution. An analytical testing sieve is constructed from a woven wire mesh, which is of simple weave that is assumed to give nearly square apertures. It is woven into the base of an open round cylinder. A series of screens were used to perform

the sieve analysis with a mesh number of 170, 200, 230, 250, 300, and 325. The sieves were arranged in a descending order of mesh number. The screen with a mesh number 170 was placed on the top and covered with a lid followed by the others sieves and a pan at the bottom. This arrangement of sieves was shaken for 20 minutes manually in circular motions. The amount of powder left on each of the sieves including the powder left in the bottom most pan, was weighed. The weights obtained were further used to obtain a particle size distribution curve. Table 6.3 shows the dimensions and variations for U.S. standard sieves.

Table 6.3: Dimensions and variations for U.S. standard Sieves. [10]

Mesh No	Sieve opening (μm)	Average particle size (μm)	Permissible variation in average opening from the standard sieve designation (μm)	Maximum opening size for not more than 5% of openings (μm)	Maximum individual opening (μm)
20	850	≥850	±35	925	970
40	425	637.5	±19	471	502
60	250	337.5	±12	283	306
80	180	215	±9	207	227
100	150	165	±8	174	192
120	125	137.5	±7	147	163
140	106	115.5	±6	126	141
170	90	98	±5	108	122
200	75	82.5	±5	91	103
230	63	69	±4	77	89
250	58	60.5	±4	72	83
300	48	53	±4	60	70
325	45	46.5	±3	57	66

6.2.6 Laser Diffraction

The particle size distribution and the mean particle size were determined using a Malvern Metasizer 2000[e] and the data was recorded and analyzed using Malvern[e] software. A 25gm/200mL concentration of aluminum hydroxide suspension in Purified Water USP and in various concentrations of PEG 1000 solutions were chosen and analyzed using this instrument. About 5 drops of the suspension were poured into flow system and the data was collected.

6.2.7 Scanning electron microscopy

Scanning electron microscopy images were taken using a JSM 5200 Scanning Electron Microscope (Tokyo, Japan). It was operated at 1.00 kV. The samples were prepared by taking a few drops of the suspension and spreading them on clean glass slides. The slides were placed in the oven and dried at low temperature. A double sided piece of tape was used to fix the sample to the stub. A low vacuum sputter coating machine was used to deposit a thin coat of gold atoms to make the sample conductive. The stub was inserted in a sample insertion slot and images were taken.

6.2.8 Differential Scanning Calorimetry experiment

The instrument used for DSC experiments was DSC 822[e] Mettler Toledo with TS0800GCI gas controller. The data was evaluated using STARe software. A 25gm/200mL concentration of aluminum hydroxide suspension in Purified Water USP and various concentrations of PEG 1000 solutions were chosen and analyzed using this instrument. About 20 mg of the sample was weighed into 100 µL Aluminum pans. aluminum lids with a piercing hole were used to cover the pans and were sealed. The purge gas used was Nitrogen at a flow rate of 20mL/ minute.

The temperature program used was as follows:

- Cooling cycle from 25^{o}C to -30^{o}C at 10^{o}C/min
- Held at -30^{o}C for 5 minutes
- Heating cycle from -30^{o}C to 150^{o}C at 10^{o}C/min
- Heating cycle from 150^{o}C to 500 ^{o}C at 50 ^{o}C/min

6.2.9 Thermogravimetric analysis

The instrument used for the TGA experiments was a TGA/SDTA 851^{e} Mettler Toledo with TS0800 GCI gas controller. The data was evaluated using STARe software. Aluminum hydroxide suspension in Purified Water USP and various concentrations of PEG 1000 solutions were chosen and analyzed using this instrument. About 20 mg of the sample was weighed into 100 µL Aluminum pans. Aluminum lids with a piercing hole were used to cover the pans and were sealed. The temperature program involved the heating of the samples from 25^{o}C to 100^{o}C at 10^{o}C/min. The purge gas used was Nitrogen at a flow rate of 20mL/min.

Chapter-7

Results and Discussion

7.1 Sieve Analysis

Sieving was performed thrice for dried aluminum hydroxide gel using the same sample size (60 gm), and the results were averaged and are given in Table 7.1.

Table 7.1: Particle size data obtained by sieving for Dried Aluminum Hydroxide Gel

US sieve No.	Standard size opening	Average particle size	Mass left on each sieve	% left on each sieve	Cumulative % left on each sieve	% cumulative passing
170	90	90	7.940	13.490	13.480	86.520
200	75	82.5	9.570	16.259	29.749	70.251
230	63	69	27.540	46.789	76.538	23.462
250	59	61	7.540	12.810	89.348	10.652
300	49	54	3.850	6.541	95.889	4.111
325	45	47	1.620	2.752	98.641	1.359
pan	-	35	0.800	1.359	100.000	0.000
Total	-	-	58.860	100	-	-

Mesh size 140 did not retain any particles implying that the batch of dried aluminum hydroxide gel had all its particles in a size range less than 106 μm. Dried

aluminum hydroxide gel was retained on sieves with mesh sizes ranging from 170 to 325. This implies that the particles have a size range of 25 to 90 µm. The minor loss in the cumulative mass left on the sieves could have occurred during the shaking and transferring processes. The results of the experiments were not exactly reproducible. This could probably due to the mechanical motion produced during sieving.

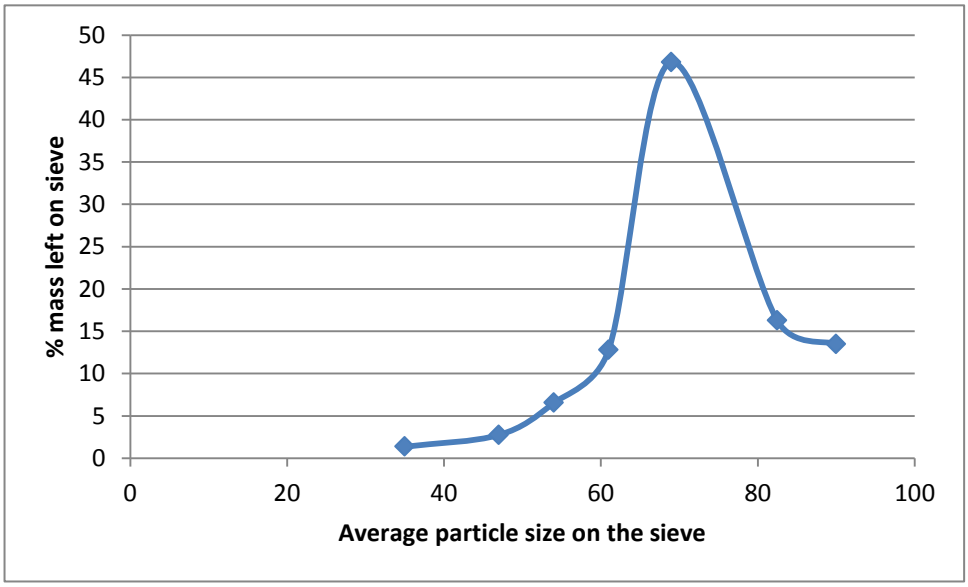

Figure 7-1: Frequency Distribution obtained from sieving

The frequency distribution in Figure 7-1 should ideally be a bell shaped curve which is usually seen for free flowing powders. Dried Aluminum hydroxide powder did not show the ideal bell shape which suggests that the powder may not free flowing.

When cumulative frequency is plotted against the average particle size, the graph should ideally be a sigmoid curve. From Figure 7-2, it can be seen the data obtained is very close to a sigmoid curve, although it is not very smooth. This could be due to the non-free flowing property of the powder as previously discussed. Both graphs are used to

represent the particle size distribution for a given population. The mean for the population was calculated and was found to be 76 μm. The median and mode were found to be 61 and 69 μm, respectively. The mean and mode values are close to each other indicating that the choice of sieves for the experiment were appropriate. The particle size obtained from this experiment was compared with the particle size obtained using other techniques given in the following sections.

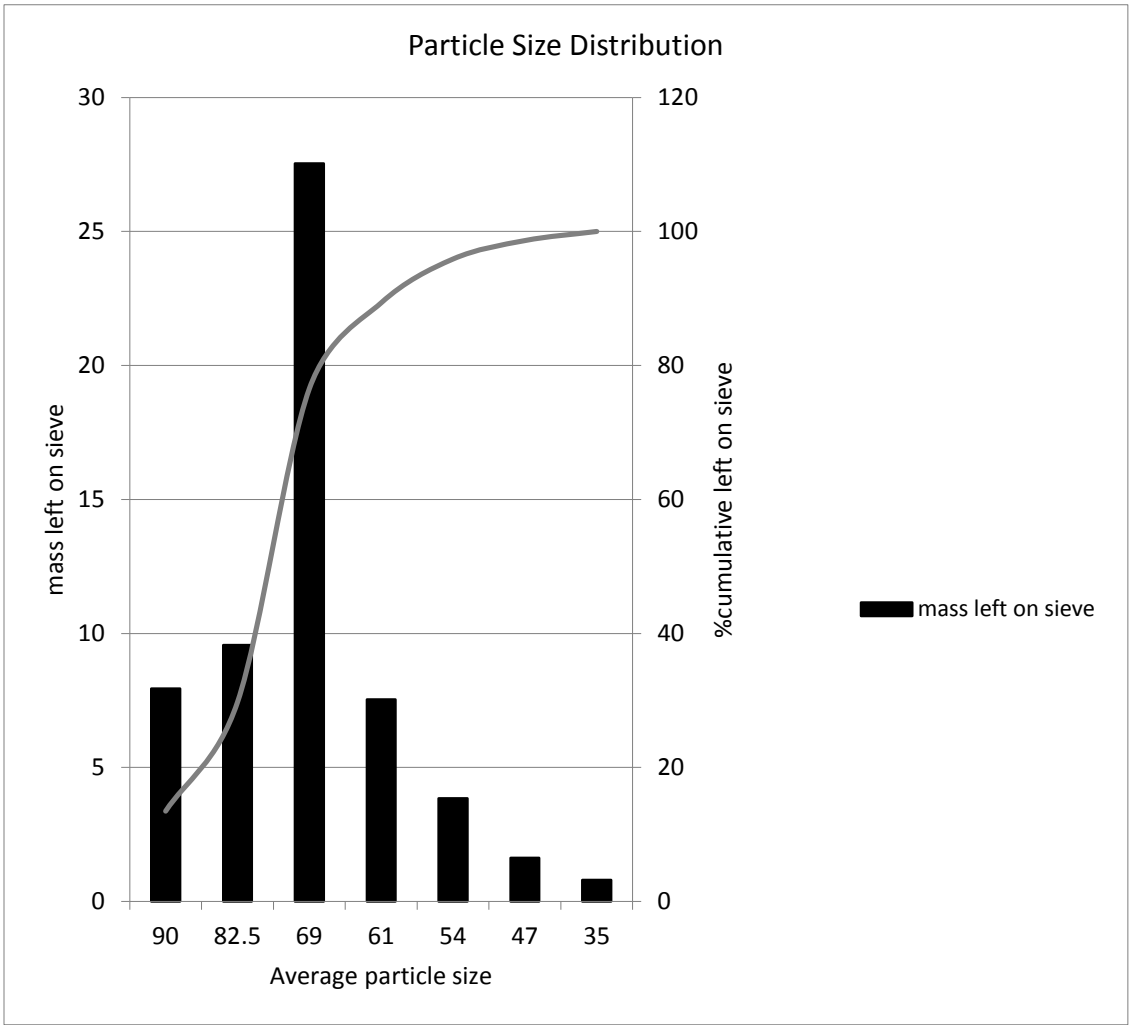

Figure 7-2: Particle size distribution obtained from sieving

7.2 Determination of density and viscosity

The density and viscosity of the various concentrations of the polymeric solutions were calculated as discussed in Section 6.2.3 and 6.2.4. The results are given in Table: 7.2. The density for the dried aluminum hydroxide gel which was obtained from the literature and used in the calculations is 2.42 g/mL. The viscosity was increased by 50% and 168.1% for 0.01% PEG and 0.05% PEG 1000 respectively, when compared to purified water USP. This increase was sufficient to study the effect of the polymeric solution on the particle size of the suspension.

Table 7.2: Density and Viscosity Results

Dispersion medium	Density (g/mL)	Viscosity (centipoise)
Purified water USP	0.98758	0.01
0.01% PEG 1000	0.98801	0.015
0.03% PEG 1000	0.99224	0.02006
0.05% PEG 1000	0.99615	0.02681

7.3 Hindered Settling

Hindered settling studies were performed using PEG 1000 as the flocculating agent. An optimum concentration range exists for every polymer, within which it can effectively form bridges. [1] Various concentrations of the polymeric solution were used to flocculate the suspensions. 25gm of dried aluminum hydroxide gel was suspended in 200 mL of various concentrations of PEG 1000 as the dispersion media, in order to pick the suitable concentrations of PEG 1000. It was found that concentrations higher than 0.05% PEG1000 deflocculated the system and a distinct interface was not visible. Hence,

the limit for the maximum concentration of the polymeric solution to be used was established as 0.05%. Walles et al suggested that when a high concentration of polymers are used the flocculation decreases due to steric stabilization of the flocs, thereby leading to a stoppage of the bridging process. [2, 3] The lower limit was chosen based on the minimum concentration that could bring about an increase in the particle size. Suspensions having a concentration less than 0.01% were prepared to determine their settling behavior. However, the interface was cloudy. This could be due to the fact that the number of particles required to bring about flocculation was not sufficient.

Figures 7-3 to 7-6 show the rate of fall of the interface for 15gm/200mL, 20gm/200mL, 25gm/200mL, 30gm/200mL, 35gm/200mL aluminum hydroxide suspensions in purified water USP, 0.01% PEG, 0.03% PEG, 0.05% PEG 1000 as the dispersion media. The rate of fall was done in triplicate for each suspension concentration. The straight line portion of the graphs obtained was taken and the values were plotted and the slope values (Q) were recorded. The average of the Q values for each set of data was calculated and these values were used in further calculations. The (ε) values were then calculated, and both (ε) and Q values were fit into the Richardson and Zaki, Steinour, and Dollimore and Mc Bride equations to obtain the particle size.

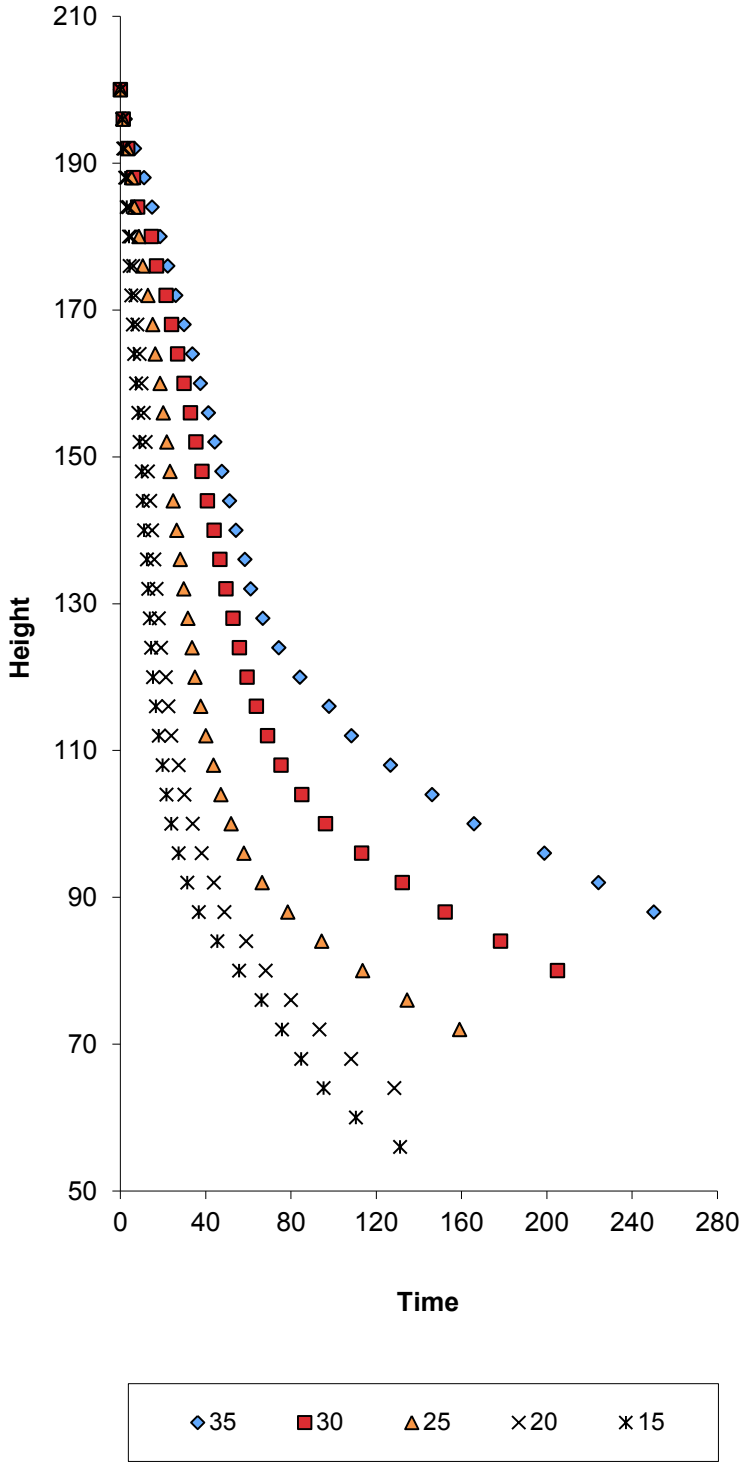

Figure 7-3: Rate of fall of dried aluminum hydroxide gel in Purified Water USP

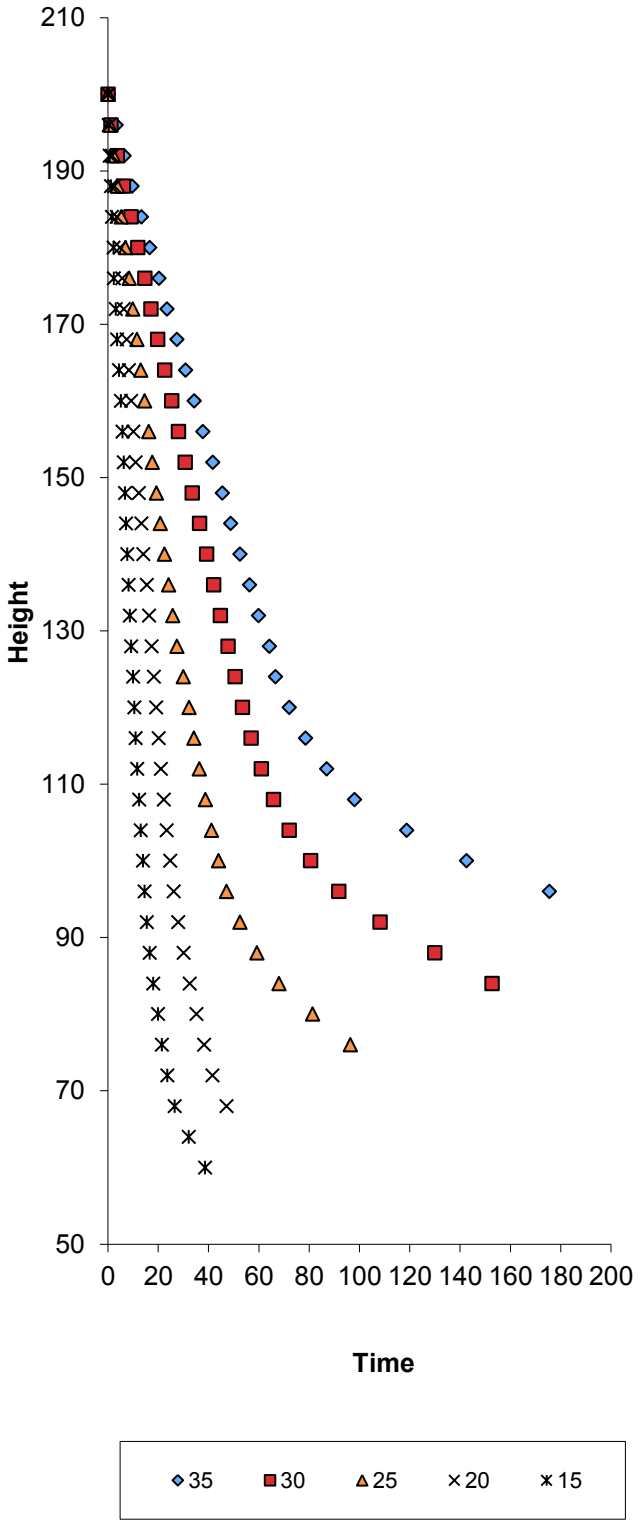

Figure 7-4: Rate of fall of dried aluminum hydroxide gel in 0.01% PEG 1000

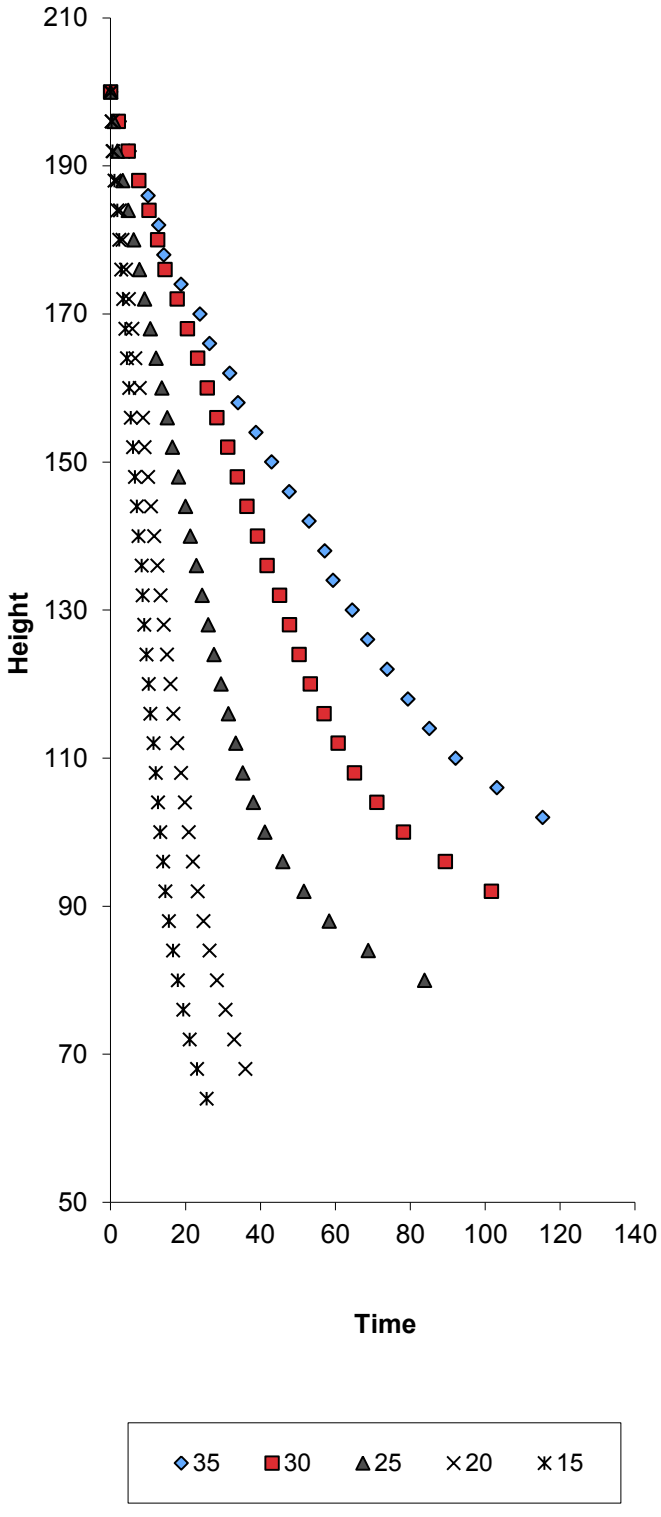

Figure 7-5: Rate of fall dried aluminum hydroxide gel in 0.03% PEG 1000

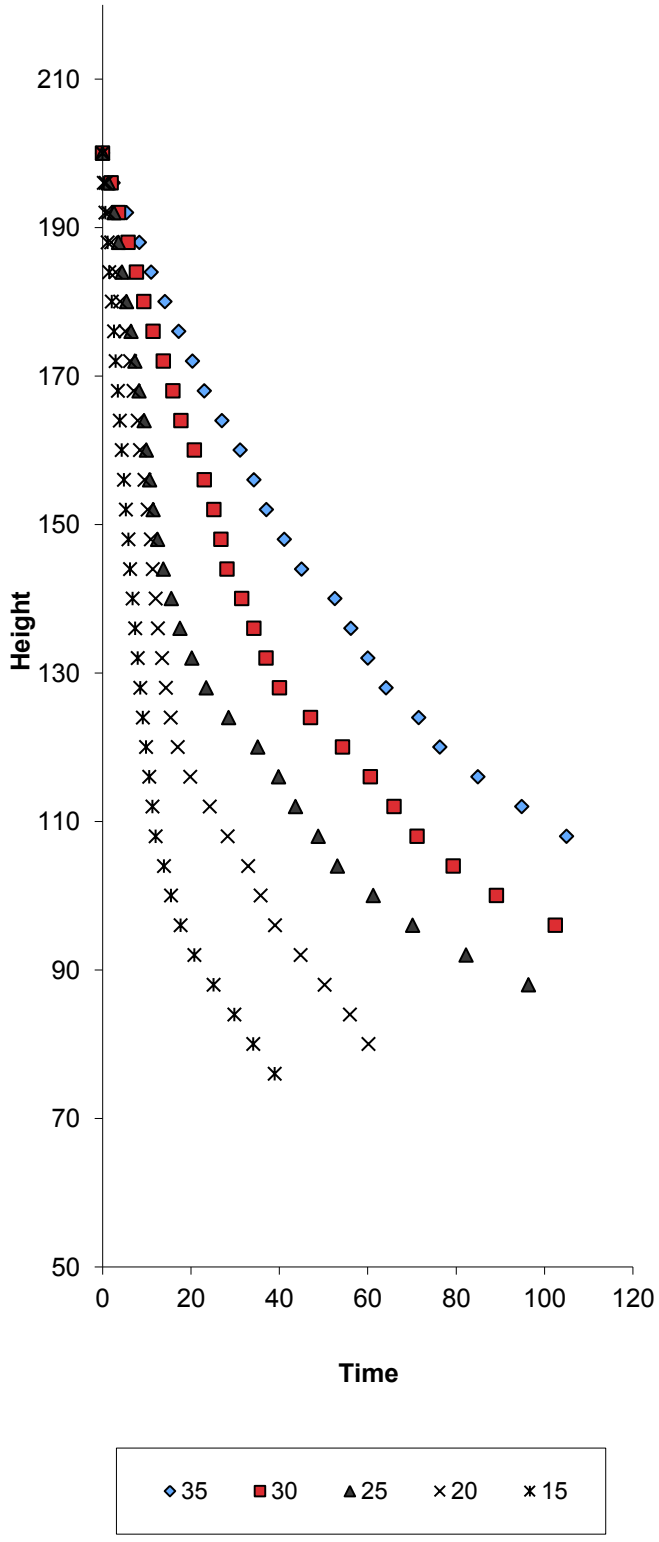

Figure 7-6: Rate of fall of dried aluminum hydroxide gel in 0.05% PEG 1000

As discussed previously, the straight line portions of the above graphs were plotted and the Q values were determined from the slopes as given in Tables 7.3 to 7.6. (ε) values and further calculations are shown in Tables 7.7 to 7.10.

Table 7.3: Q values obtained for $Al(OH)_3$ suspensions in Purified Water USP

Wt	Conc (g/mL)	Q1	Q2	Q3	Qavg	SD
15	0.075	5.3869	5.2924	5.3238	5.3344	0.0393
20	0.1	4.0142	4.0149	3.9847	4.0046	0.0141
25	0.125	2.1274	2.1213	2.1324	2.1270	0.0045
30	0.15	1.2511	1.239	1.2532	1.2478	0.0063
35	0.175	1.054	1.0548	1.0504	1.0531	0.0019

Table 7.4: Q values obtained for $Al(OH)_3$ suspensions in 0.01% PEG 1000

Wt	Conc (g/mL)	Q1	Q2	Q3	Qavg	SD
15	0.075	7.3963	7.5075	6.8139	7.2392	0.3042
20	0.1	4.259	4.1276	4.1099	4.1655	0.0665
25	0.125	2.6414	2.6231	2.6277	2.6307	0.0078
30	0.15	1.5132	1.5104	1.504	1.5092	0.0039
35	0.175	1.1519	1.1319	1.1425	1.1421	0.0082

Table 7.5: Q values obtained for $Al(OH)_3$ suspensions in 0.03% PEG 1000

Wt	Conc (g/mL)	Q1	Q2	Q3	Qavg	SD
15	0.075	7.6449	7.7896	7.3279	7.5875	0.1928
20	0.1	4.8907	4.9084	4.7022	4.8338	0.0933
25	0.125	2.8012	2.7401	2.7958	2.7790	0.0276
30	0.15	1.526	1.5262	1.4988	1.517	0.0129
35	0.175	1.0888	1.0995	1.0864	1.0916	0.0057

Table 7.6: Q values obtained for $Al(OH)_3$ suspensions in 0.05% PEG 1000

Wt	Conc (g/mL)	Q1	Q2	Q3	Qavg	SD
15	0.075	8.8125	8.8229	8.8021	8.8125	0.0085
20	0.1	4.4984	4.481	4.491	4.4901	0.0071
25	0.125	4.2287	4.2367	4.2052	4.2235	0.0134
30	0.15	1.9007	1.897	1.8868	1.8948	0.0059
35	0.175	1.2714	1.2707	1.2656	1.2692	0.0026

Table 7.7: Calculation of ε and other parameters for $Al(OH)_3$ suspensions in Purified Water USP

$\varepsilon=1-(C/\rho_m)$	logε	logQ	1- ε	$Log(Q/\varepsilon^2)$
0.9690	-0.0137	0.7271	0.0310	0.7544
0.9587	-0.0183	0.6026	0.0413	0.6392
0.9483	-0.0230	0.3278	0.0517	0.3738
0.9380	-0.0278	0.0961	0.0620	0.1517
0.9277	-0.0326	0.0225	0.0723	0.0877

Table 7.8: Calculation of ε and other parameters for $Al(OH)_3$ suspensions in 0.01% PEG 1000

$\varepsilon=1-(C/\rho_m)$	logε	logQ	1- ε	$Log(Q/\varepsilon^2)$
0.9690	-0.0137	0.8597	0.0310	0.8870
0.9587	-0.0183	0.6197	0.0413	0.6563
0.9483	-0.0230	0.4201	0.0517	0.4661
0.9380	-0.0278	0.1787	0.0620	0.2343
0.9277	-0.0326	0.0577	0.0723	0.1229

Table 7.9: Calculation of ε and other parameters for $Al(OH)_3$ suspensions in 0.03% PEG 1000

$\varepsilon=1-(C/\rho_m)$	logε	logQ	1- ε	$Log(Q/\varepsilon^2)$
0.9690	-0.0137	0.8801	0.0310	0.9074
0.9587	-0.0183	0.6843	0.0413	0.7209
0.9483	-0.0230	0.4439	0.0517	0.4900
0.9380	-0.0278	0.1810	0.0620	0.2366
0.9277	-0.0326	0.0381	0.0723	0.1032

Table 7.10: Calculation of ε and other parameters for $Al(OH)_3$ suspensions in 0.05% PEG 1000

$\varepsilon=1-C/\rho_m$	logε	logQ	1- ε	$Log(Q/\varepsilon^2)$
0.9690	-0.0137	0.9451	0.0310	0.9724
0.9587	-0.0183	0.6523	0.0413	0.6889
0.9483	-0.0230	0.6257	0.0517	0.6717
0.9380	-0.0278	0.2776	0.0620	0.3332
0.9277	-0.0326	0.1035	0.0723	0.1687

The values listed in Tables 7.3 to 7.10 are used to fit into Richardson and Zaki, Steinour, and Dollimore and Mc Bride equations and the graphs thereby obtained are given in Figures 7-7 to 7-18. The equations used are summarized below:

Richardson and Zaki's Equation:

$$Q = V_s \varepsilon^n \tag{7.1}$$

$$LogQ = LogV_s + nLog\varepsilon \tag{7.2}$$

Steinour's Equation:

$$Q = V_s \varepsilon^2 10^{-A(1-\varepsilon)} \tag{7.3}$$

$$Log\left(\frac{Q}{\varepsilon^2}\right) = A\varepsilon + (LogV_s - A) \tag{7.4}$$

Dollimore and McBride's Equation:

$$Q = V_s 10^{-b\rho_m(1-\varepsilon)} \tag{7.5}$$

$$LnQ = LnV_s - b\rho_m(1-\varepsilon) \tag{7.6}$$

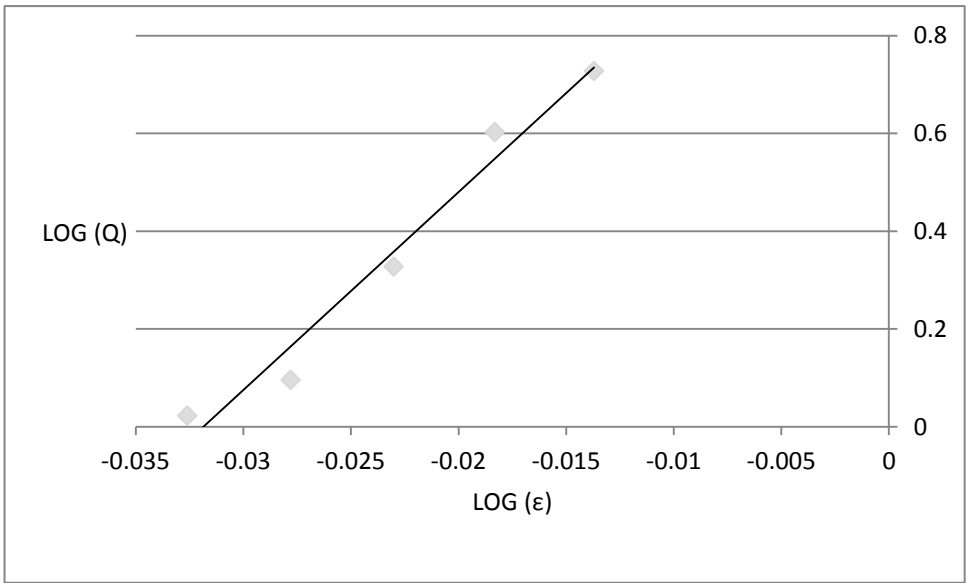

Figure 7-7: Richarson and Zaki equation plot for $Al(OH)_3$ suspensions in Purified Water USP where the slope = 40.488, intercept = 1.2897, R^2=0.9701

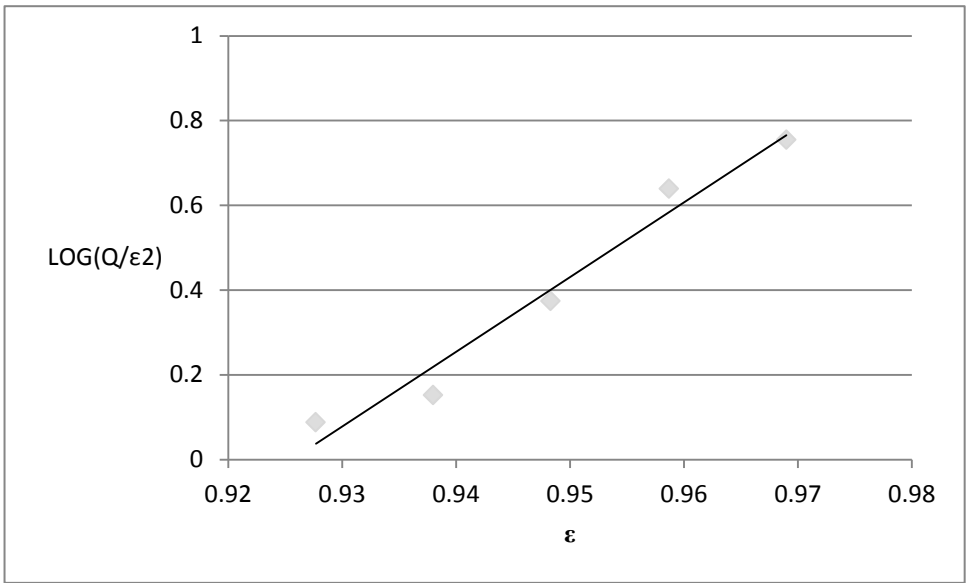

Figure 7-8: Steinour equation plot for $Al(OH)_3$ suspensions in Purified Water USP where the slope = 17.631, intercept = -16.319, R^2=0.968

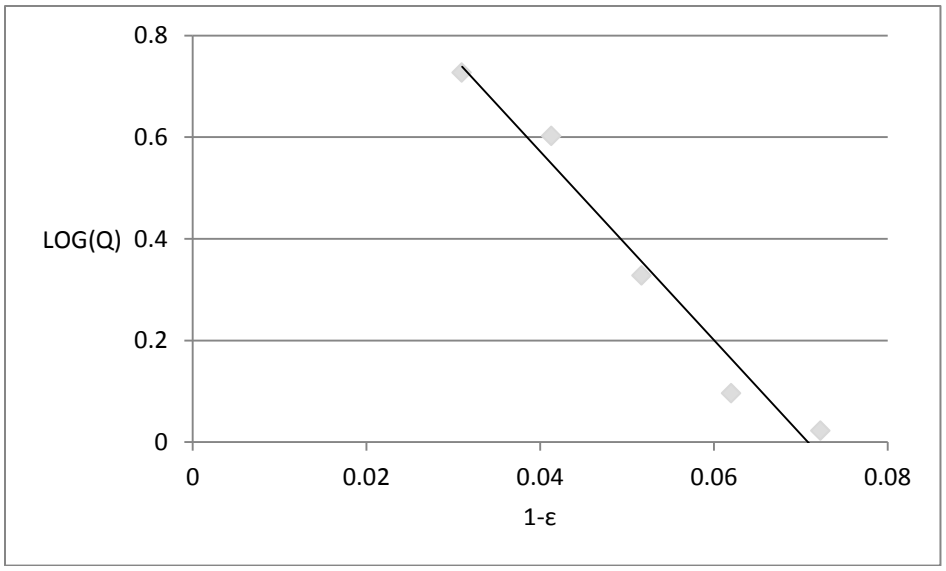

Figure 7-9: Dollimore and Mc Bride equation plot for $Al(OH)_3$ suspensions in Purified Water USP where the slope = -18.549, intercept = 1.3135, R^2=0.9711

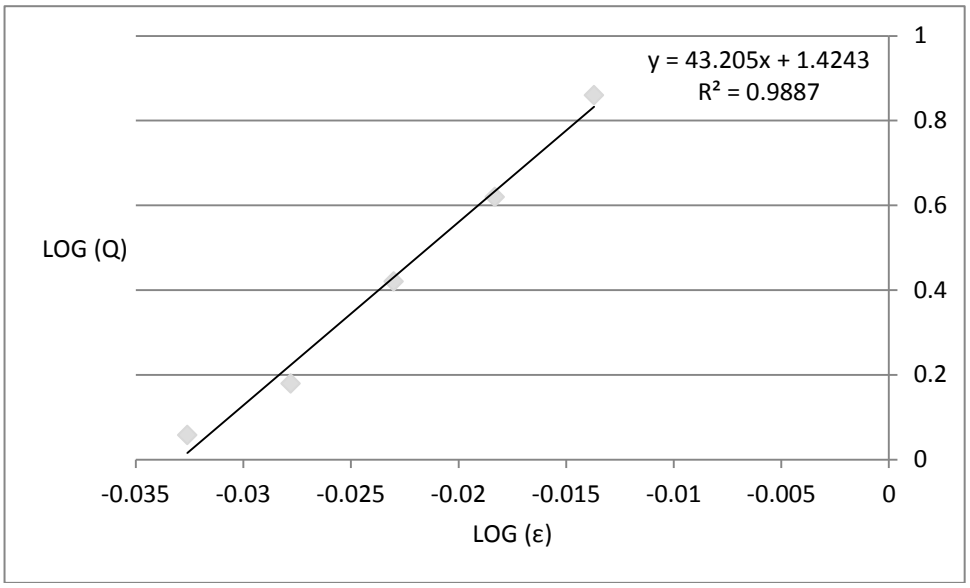

Figure 7-10: Richarson and Zaki equation plot for $Al(OH)_3$ suspensions in 0.01% PEG 1000 where the slope = 43.205, intercept = 1.4243, R^2=0.9887

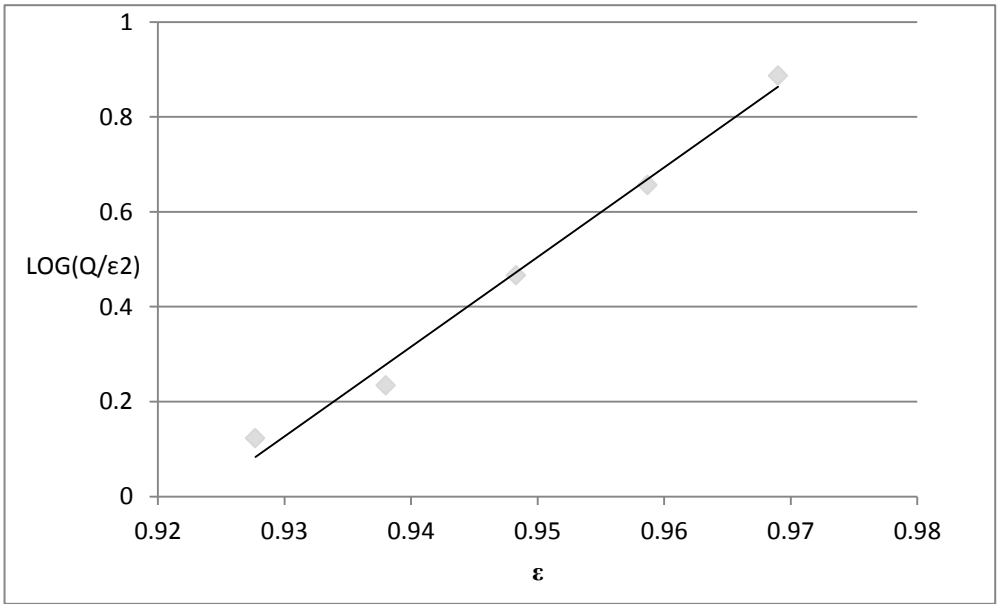

Figure 7-11: Steinour equation plot for $Al(OH)_3$ suspensions in 0.01% PEG 1000 where the slope = 18.88, intercept = -17.431, R^2=0.989

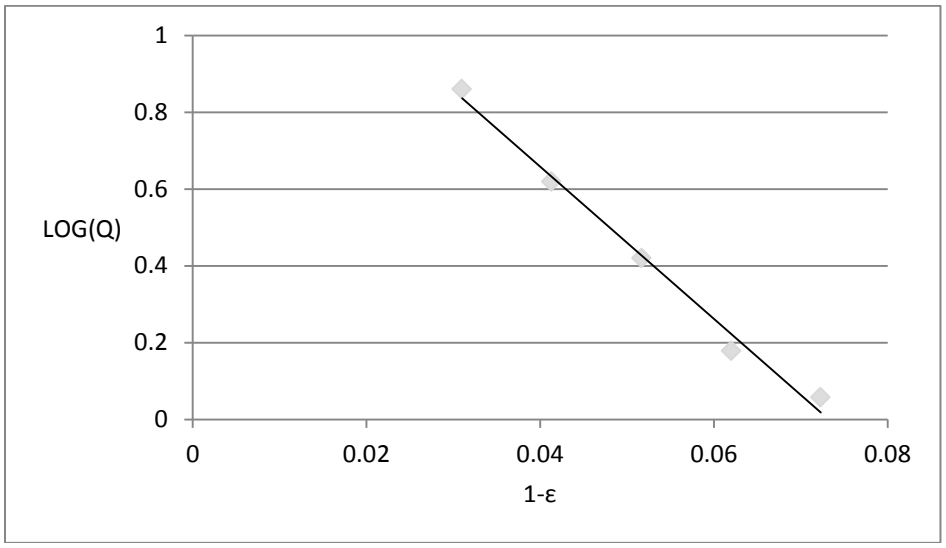

Figure 7-12: Dollimore and Mc Bride equation plot for $Al(OH)_3$ suspensions in 0.01% PEG 1000 where the slope = -19.798, intercept = 1.4499, R^2=0.9901

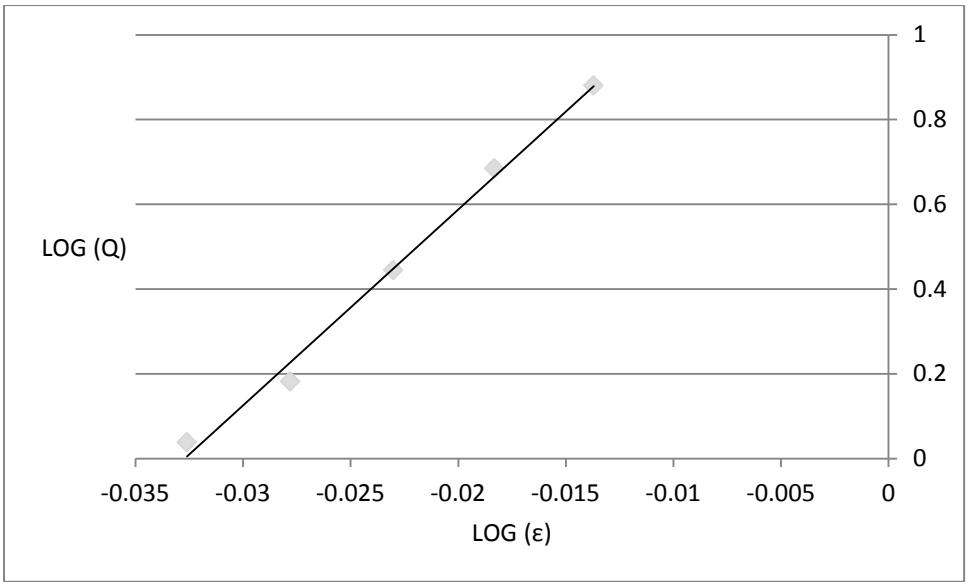

Figure 7-13: Richarson and Zaki equation plot for $Al(OH)_3$ suspensions in 0.03% PEG 1000 where the slope = 46.234, intercept = 1.5126, R^2=0.9926

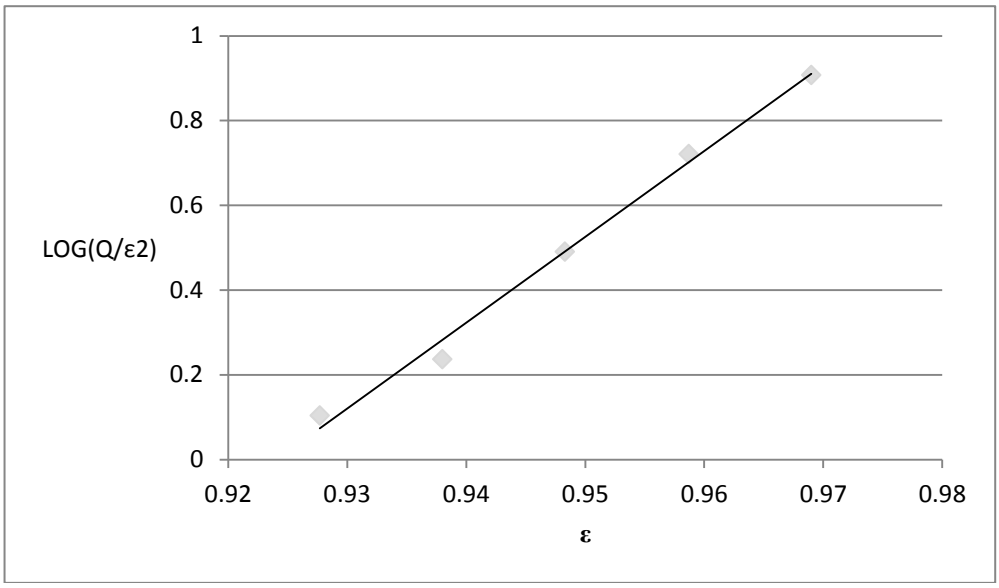

Figure 7-14: Steinour equation plot for $Al(OH)_3$ suspensions in 0.03% PEG 1000 where the slope = 20.26, intercept = -18.722, R^2=0.9924

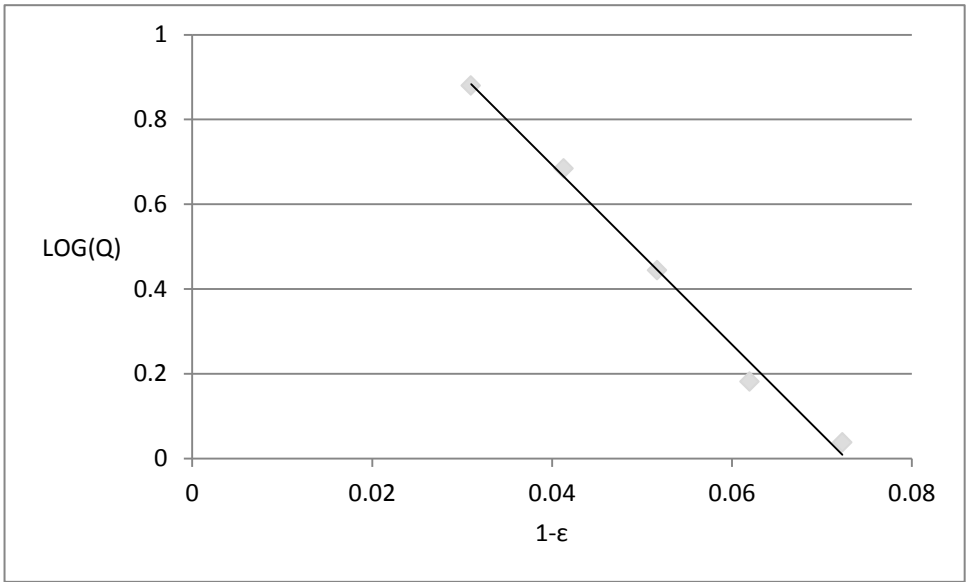

Figure 7-15: Dollimore and Mc Bride equation plot for $Al(OH)_3$ suspensions in 0.03% PEG 1000 where the slope = -21.176, intercept = 1.5394, R^2=0.9931

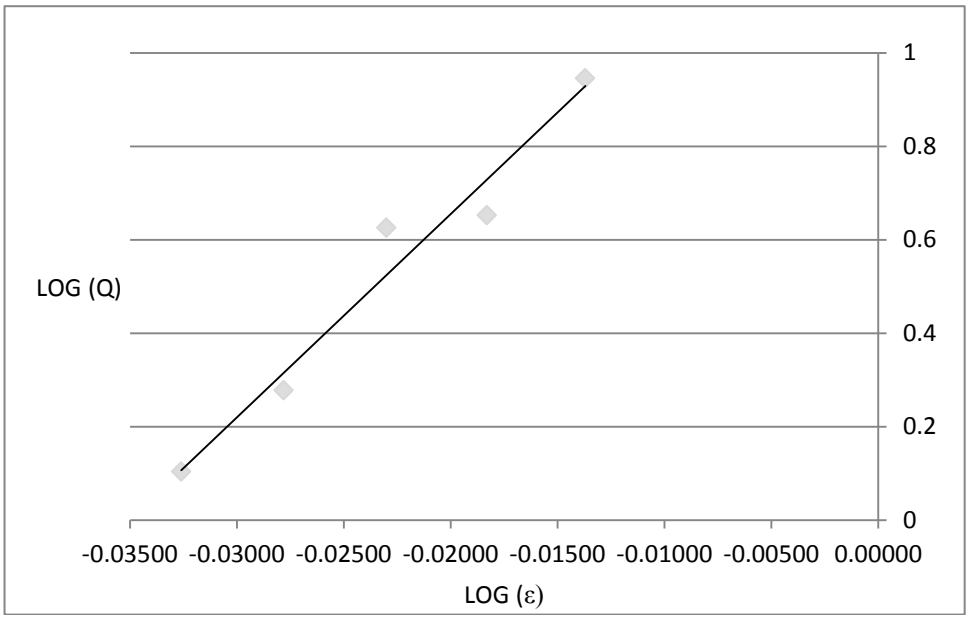

Figure 7-16: Richarson and Zaki equation plot for $Al(OH)_3$ suspensions in 0.05% PEG 1000 where the slope = 43.52, intercept = 1.5253, R^2=0.9596

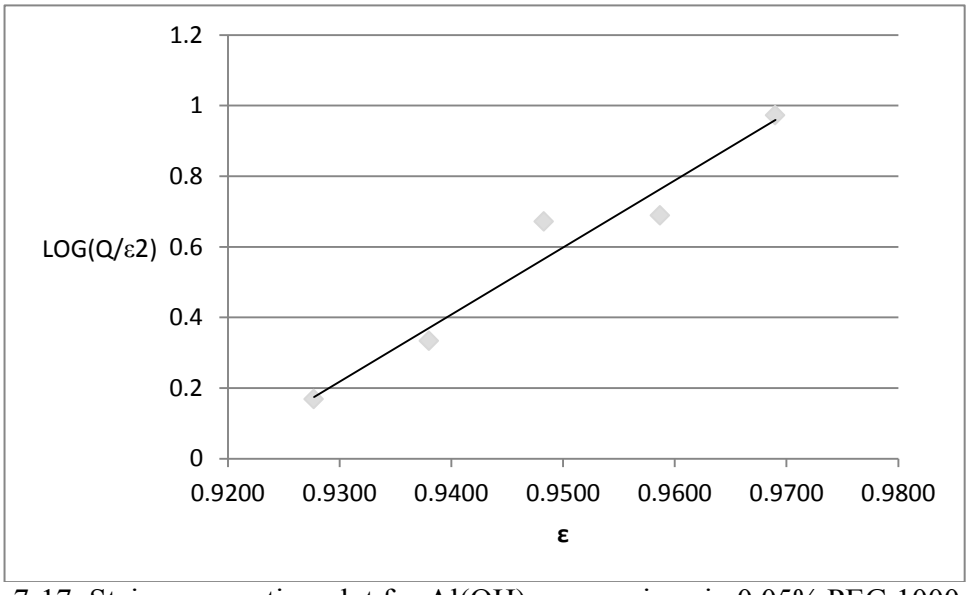

Figure 7-17: Steinour equation plot for $Al(OH)_3$ suspensions in 0.05% PEG 1000 where the slope = 18.998, intercept = -17.45, R^2=0.9546

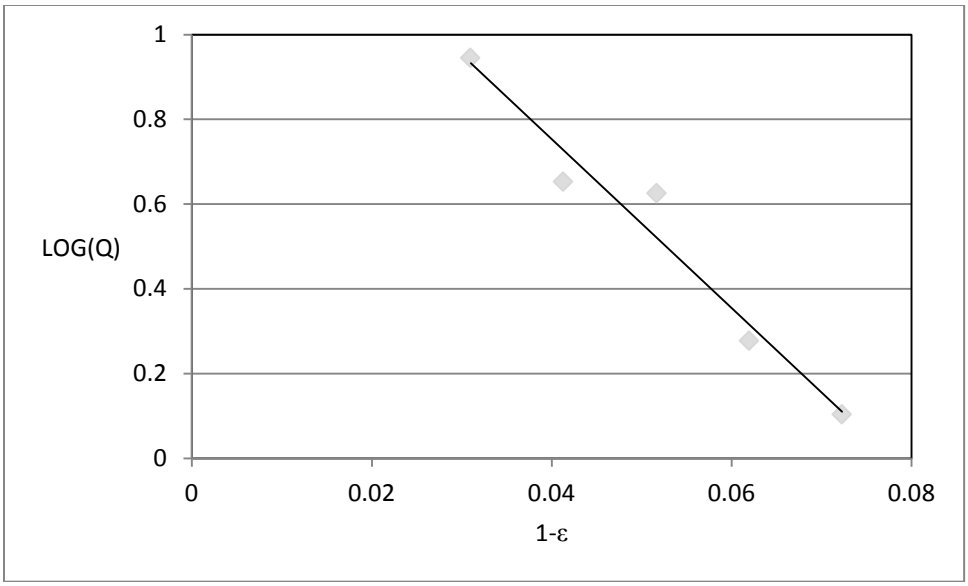

Figure 7-18: Dollimore and Mc Bride equation plot for $Al(OH)_3$ suspensions in 0.05% PEG 1000 where the slope = -19.916, intercept = 1.5497, R^2=0.9584

The slope and intercept values were used from the above plots to calculate the Vs values for Dried Aluminum hydroxide suspensions in various dispersion media. The particle size was calculated using the following formula.

$$r = \sqrt{\frac{(9\eta V_s)}{2g(\rho_m - \rho_f)}} \qquad (7.7)$$

Table 7.11: Data obtained from the Richarson and Zaki equation for $Al(OH)_3$ suspensions in various dispersion media

	Purified WaterUSP	0.01% PEG	0.03% PEG	0.05% PEG
Slope (n)	40.4880	43.205	46.234	43.5200
Intercept (LogVs)	1.2897	1.4243	1.5126	1.5253
R^2	0.9701	0.9887	0.9926	0.9596
Vs	19.4849	26.5644	32.5537	33.5197

Table 7.12: Data obtained from the Steinour equation for $Al(OH)_3$ suspensions in various dispersion media

	Purified WaterUSP	0.01% PEG	0.03% PEG	0.05% PEG
Slope (n)	17.631	18.88	20.26	17.212
Intercept (LogVs)	-16.319	-17.431	-18.722	-15.739
R^2	0.968	0.989	0.9924	0.9498
Log Vs	1.312	1.449	1.538	1.473
Vs	20.5116	28.11901	34.5144	29.7166

Table 7.13: Data obtained from the Dollimore and Mc Bride equation for $Al(OH)_3$ suspensions in various dispersion media

	Purified WaterUSP	0.01% PEG	0.03% PEG	0.05% PEG
Slope (n)	-18.549	-19.798	-21.176	-19.916
Intercept (LogVs)	1.3135	1.4499	1.5394	1.5497
R^2	0.9711	0.9901	0.9931	0.9584
Log Vs	20.5826	28.1773	34.62581	35.45683

Table 7.14: Calculation of V_s from the Richardson and Zaki equation

	η	Vs (mm/min)	Vs (cm/sec)	9*η*Vs
Purified Water USP	0.01000	19.48498	0.03225	0.00292
0.01% PEG 1000	0.01500	26.5644	0.04427	0.00598
0.03% PEG 1000	0.02006	32.55367	0.05425	0.00980
0.05% PEG 1000	0.02681	33.51969	0.05567	0.01348

Table 7.15: Calculation of particle size based on the Richardson and Zaki equation

	ρs-ρl	2*980* (ρs-ρl)	r(cm)	r(μm)
Purified Water USP	1.43242	2807.543	0.00102	10.20311
0.01% PEG 1000	1.43199	2806.7	0.001459	14.59295
0.03% PEG 1000	1.42776	2798.41	0.001871	18.70921
0.05% PEG 1000	1.42385	2790.746	0.002198	21.97778

Table 7.16: Calculation of V_s from the Steinour equation

	η	Vs (mm/min)	Vs (cm/sec)	9*η*Vs
Purified Water USP	0.01	20.51162	0.034186	0.003077
0.01% PEG 1000	0.015	28.11901	0.046865	0.006327
0.03% PEG 1000	0.02006	34.51437	0.057524	0.010385
0.05% PEG 1000	0.02681	29.7166	0.049528	0.011951

Table 7.17: Calculation of particle size based on the Steinour equation

	ρs-ρl	2*980* (ρs-ρl)	r(cm)	r(μm)
Purified Water USP	1.43242	2807.543	0.001047	10.46845
0.01% PEG 1000	1.43199	2806.7	0.001501	15.01389
0.03% PEG 1000	1.42776	2798.41	0.001926	19.2644
0.05% PEG 1000	1.42385	2790.746	0.002069	20.69348

Table 7.18: Calculation of V_s from the Dollimore and Mc Bride equation

	η	Vs (mm/min)	Vs (cm/sec)	9*η*Vs
Purified Water USP	0.01	20.58259	0.034304	0.003087
0.01% PEG 1000	0.015	28.17734	0.046962	0.00634
0.03% PEG 1000	0.02006	34.62581	0.05771	0.010419
0.05% PEG 1000	0.02681	35.45683	0.059095	0.014259

Table 7.19: Calculation of the particle size based on the Dollimore and Mc Bride equation

	ρs-ρl	2*980* (ρs-ρl)	r(cm)	r(μm)
Purified Water USP	1.43242	2807.543	0.001049	10.48654
0.01% PEG 1000	1.43199	2806.7	0.001503	15.02945
0.03% PEG 1000	1.42776	2798.41	0.00193	19.29547
0.05% PEG 1000	1.42385	2790.746	0.00226	22.60392

The data obtained from the the hindered settling theory has been summarized in Table 7.20. It was found that the particle size for the suspension of dried aluminum hydroxide gel in water was found to have the smallest particle size of 10.386 μm. The particle size was found to increase with the addition of a flocculating agent and also with the increase in the concentration of the polymeric solution. The particle size for dried aluminum hydroxide gel in 0.05% PEG 1000 solution was found to be the highest at

21.7584 μm. This increase in the particle size can be attributed to the increase in the flocculating effeciency with an increase in the polymer concentration.

Table 7.20: Summary of the particle size data (μm)

	Purified Water USP	0.01% PEG 1000	0.03% PEG 1000	0.05% PEG 1000
Steinour	10.47	15.01	19.26	20.69
Richardson Zaki	10.20	14.59	18.71	21.98
Dollimore and Mc Bride	10.49	15.03	19.30	22.60
Average Radius	10.39	14.88	19.09	21.76

The polymer solubilized in water is adsorbed onto the surface of the aluminum hydroxide particles, forming bridges between them. This leads to the formation of loose fluffy aggregates or flocs. The results from the hindered settling theory are not consistent with the rsults obtained from the sieve analysis. The mean particle size obatined from sieving is approximately five times greater than hindered settling results. The probable reason for this could be the fact that dry powder aluminum hydroxide gel exists as clusters. The force exerted by the mechanical motion is not sufficient to break these clusters thus leading to the determination of the cluster size instead of the size of the individual particles or due to maually shaking the sieves instead of using a mechanical shaker.

7.4 Laser Diffraction

The particle size was also determined by another analytical technique, laser diffraction. Malvern 2000[e] was used for this study. This technique is used for non-destructive analysis for both dry and wet samples. The results are summarized in Table 7.21. This technique is highly sensitive compared to sieve analysis. It was found that the particle size distribution was normal. There was an increase in the surface weighted mean (D[3,2]) particle size upon the incorporation of the flocculating agent, PEG 1000. There was also an increase with an increase in the concentration of PEG 1000. The results for this study are very close to the data obtained from hindered settling data, thus confirming the particle size. The data is given in Figures 7-19 to 7-22. However the results from the sieve analysis are not consistent with the data obtained from the Laser diffraction studies.

Table 7.21: Laser Diffraction data

Dispersion Medium	Surface Weighted Mean (μm)	Volume Weighted Mean (μm)
Water USP	17.134	55.091
0.01% PEG 1000	18.048	60.272
0.03% PEG 1000	18.688	59.033
0.05% PEG 1000	19.281	61.526

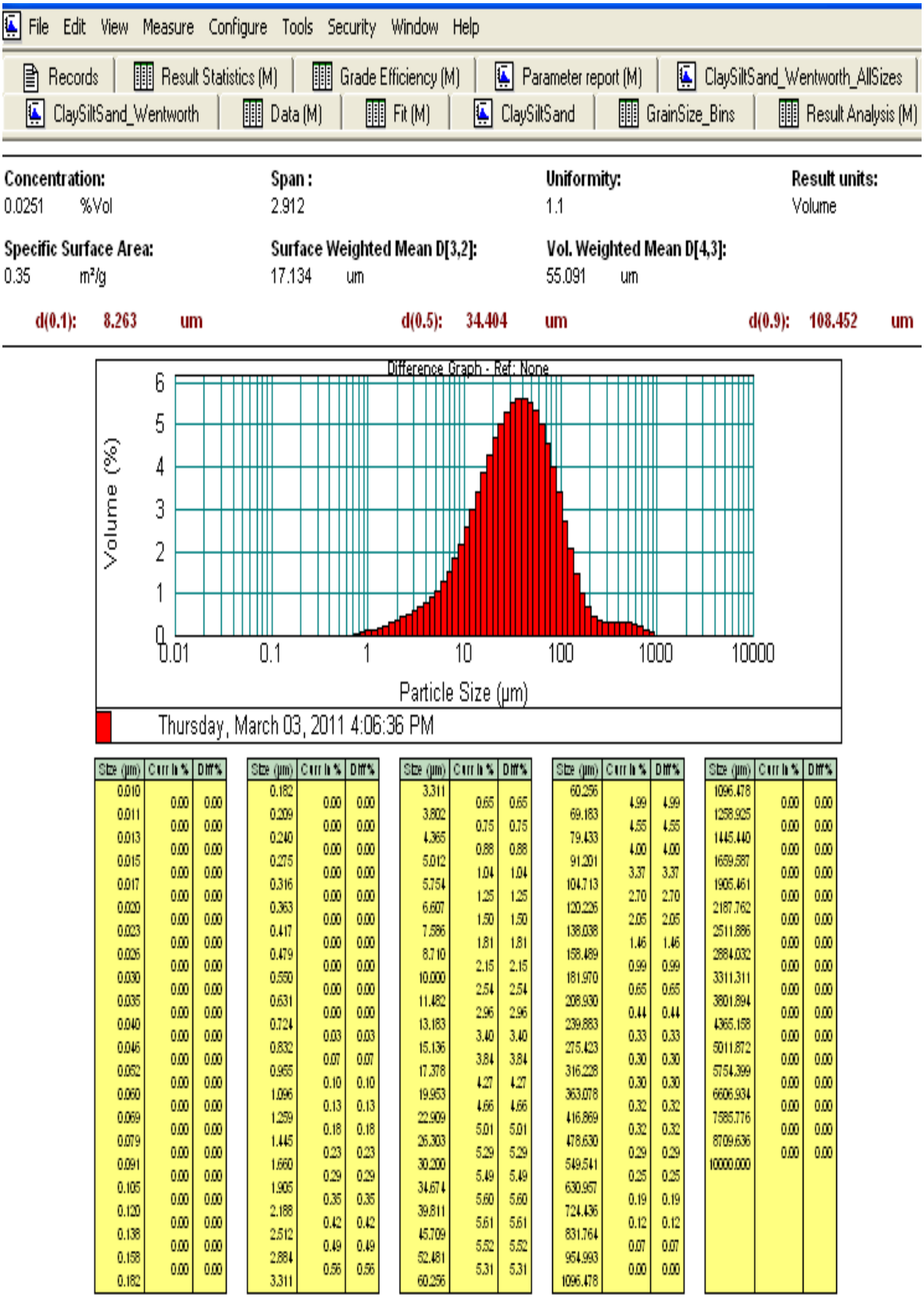

Figure7-19: Laser diffraction data for Dried Aluminum Hydroxide in Purified Water USP obtained using the Malvern Metasizer 2000[e]

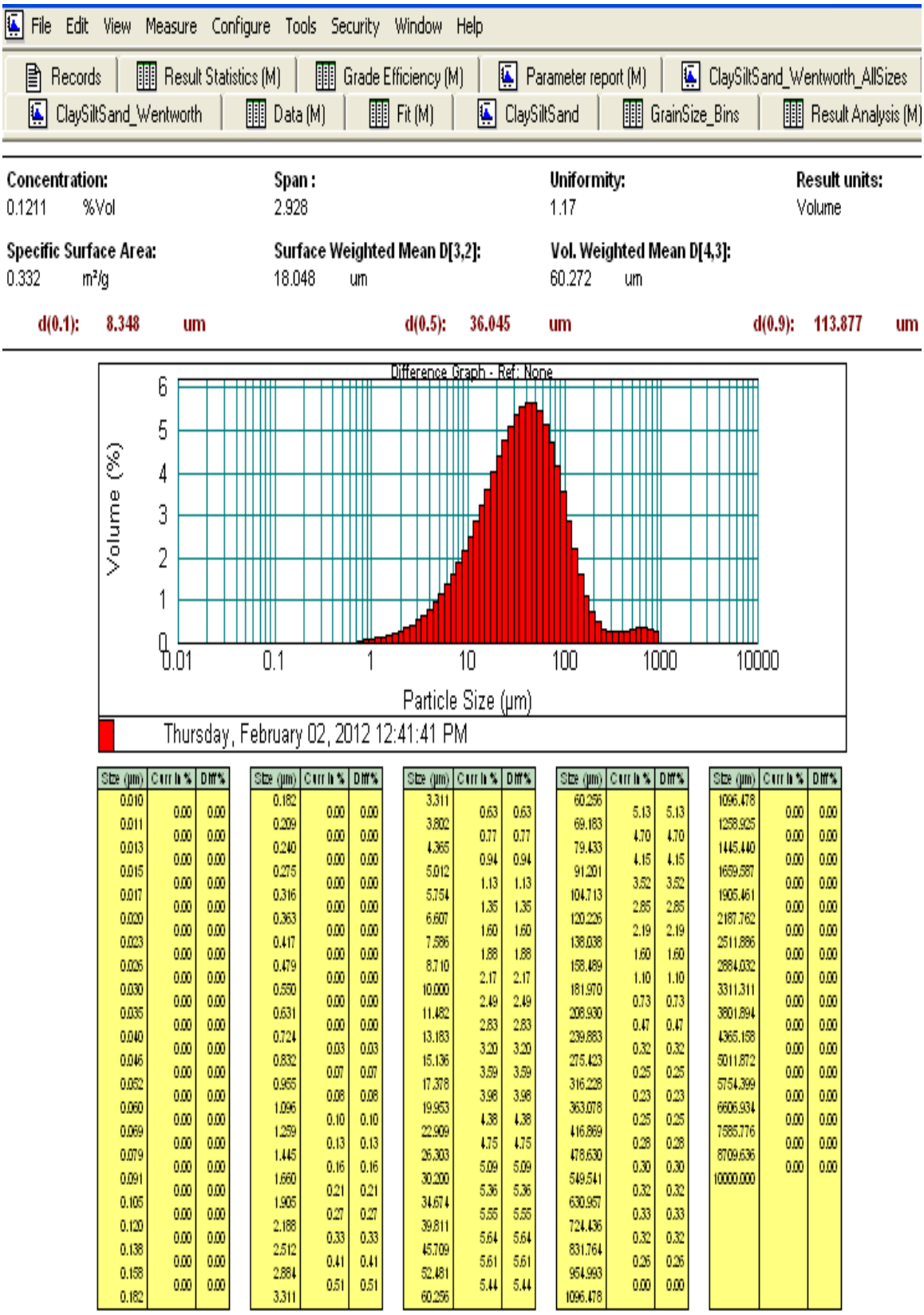

Figure 7-20: Laser diffraction data for Dried Aluminum Hydroxide in 0.01% PEG 1000 obtained using the Malvern Metasizer 2000[e]

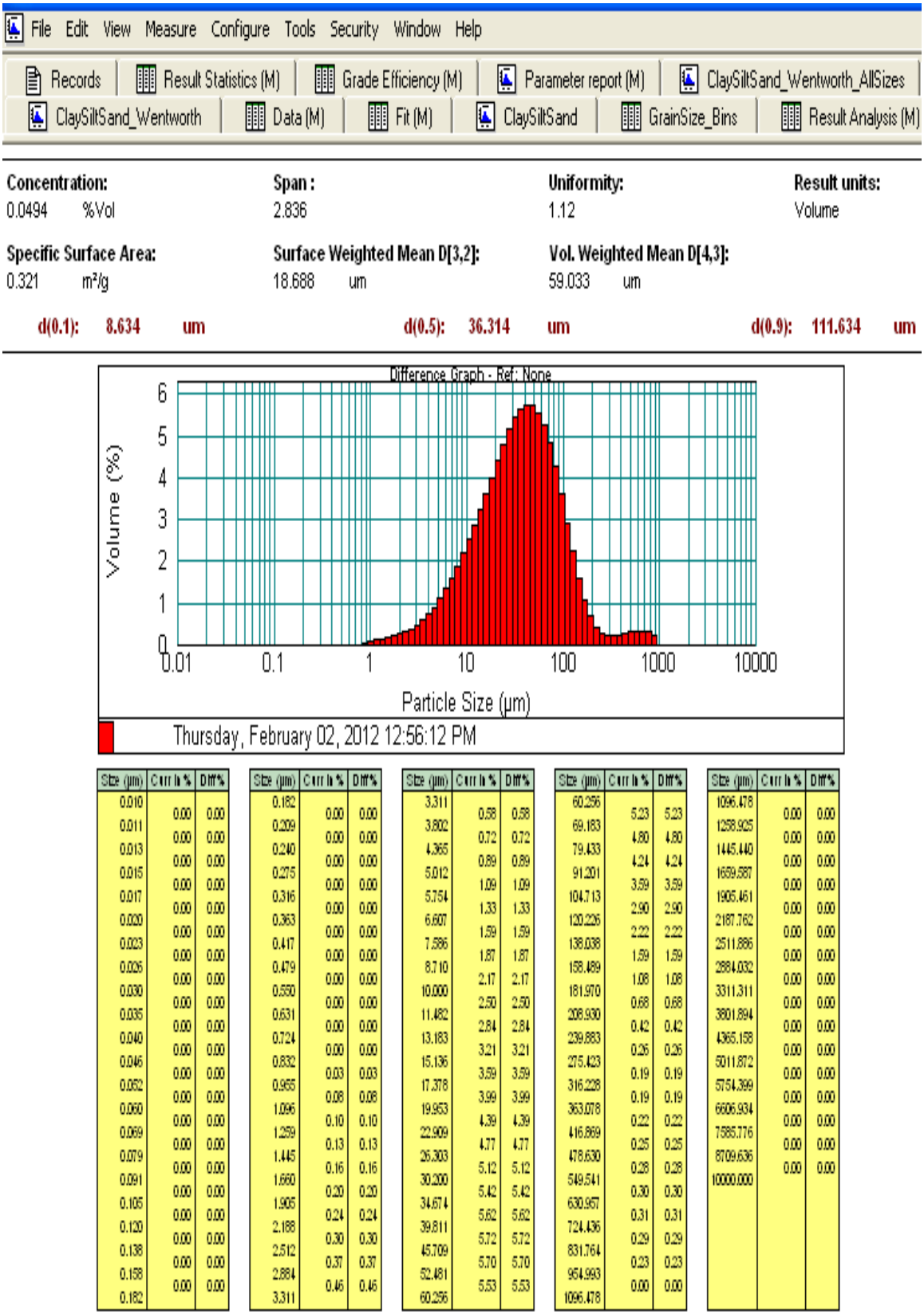

Figure 7-21: Laser diffraction data for Dried Aluminum Hydroxide in 0.03% PEG 1000 obtained using the Malvern Metasizer 2000[e]

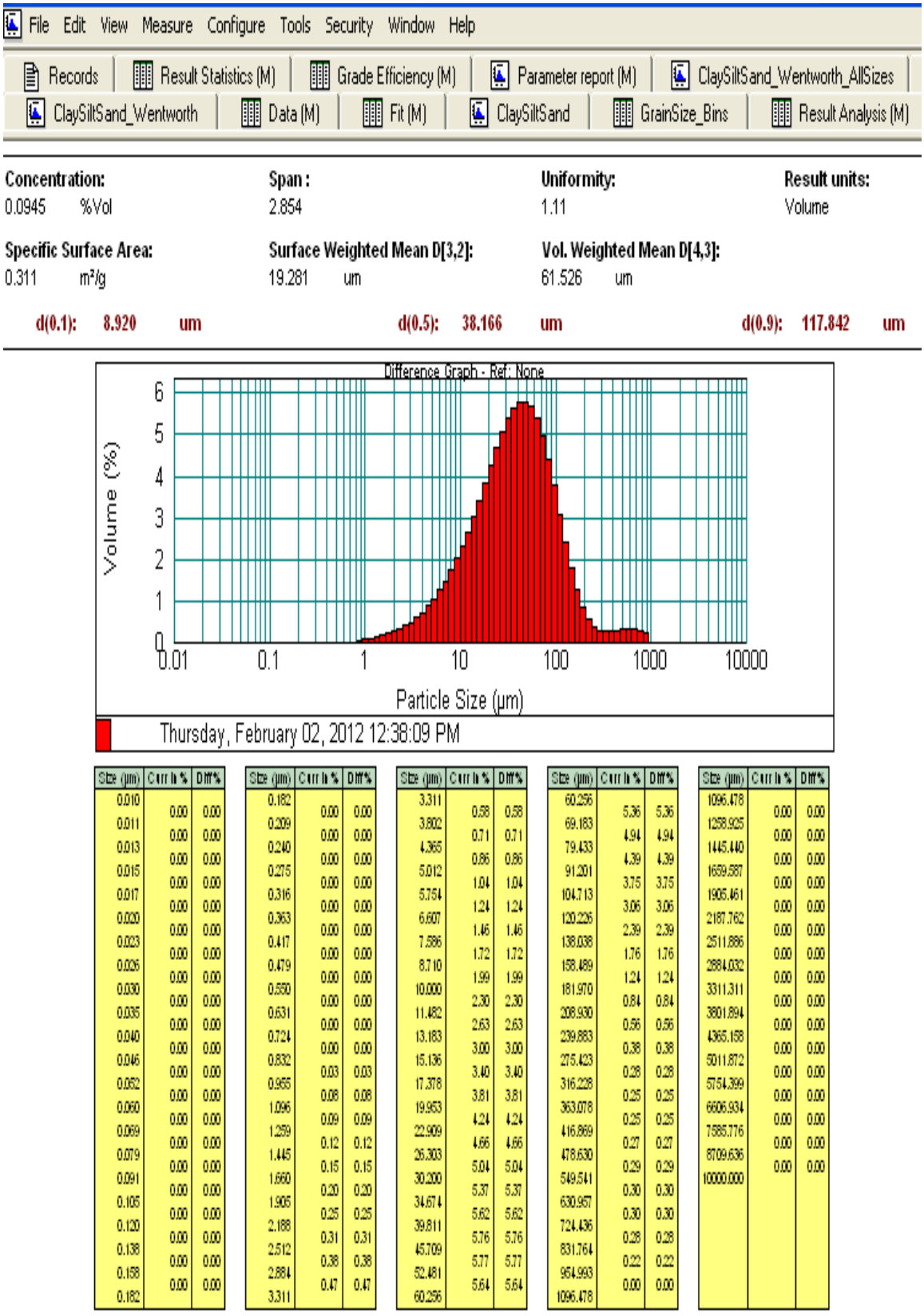

Figure 7-22: Laser diffraction data for Dried Aluminum Hydroxide in 0.05% PEG 1000 obtained using the Malvern Metasizer 2000[e]

7.5 Scanning Electron Microscopy

Scanning electron microscopy (SEM) was used to visualize how the particles would exist independently and in clusters after undergoing flocculation. The experimental procedure has been discussed in Section 6.2.7. It is difficult to determine the effect of various concentrations of PEG 1000 on the particle size distribution of the suspension from SEM. This is because a very small sample size is used, which might not represent the particle size distribution of the entire suspension. Figure 7-23 shows the independent existing of particles. It can be seen that particles are spherical in shape and most of the particles are around 15 to 20 μm.

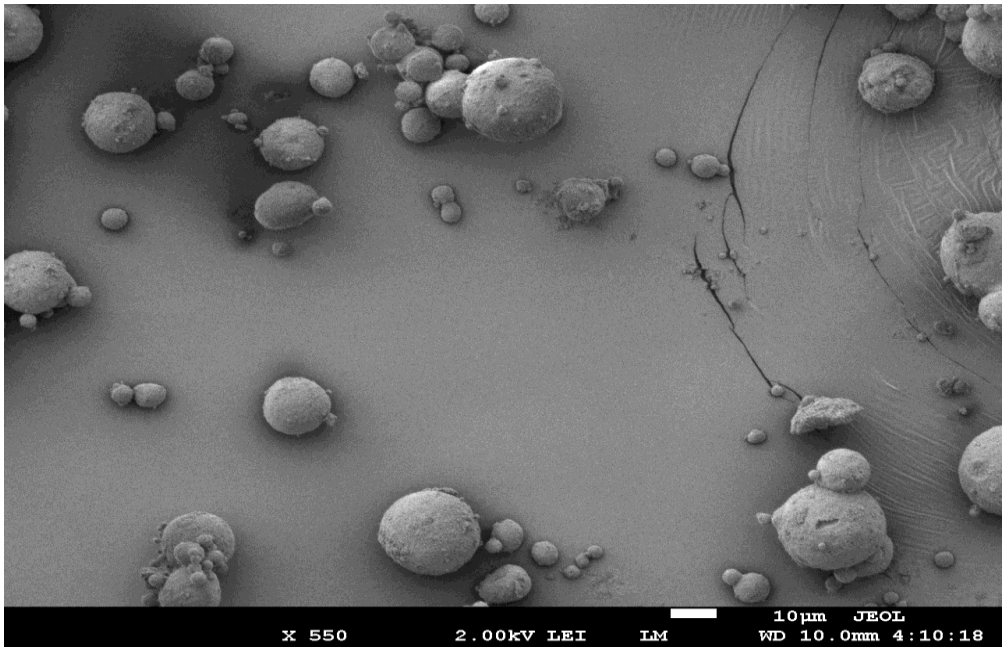

Figure 7-23: SEM image of particles in a suspension.

Figure 7-23 shows a group of particles in which a number of independent particles come together to form a fluffy floccule. Figure 7-24 is a closer image of the floccule.

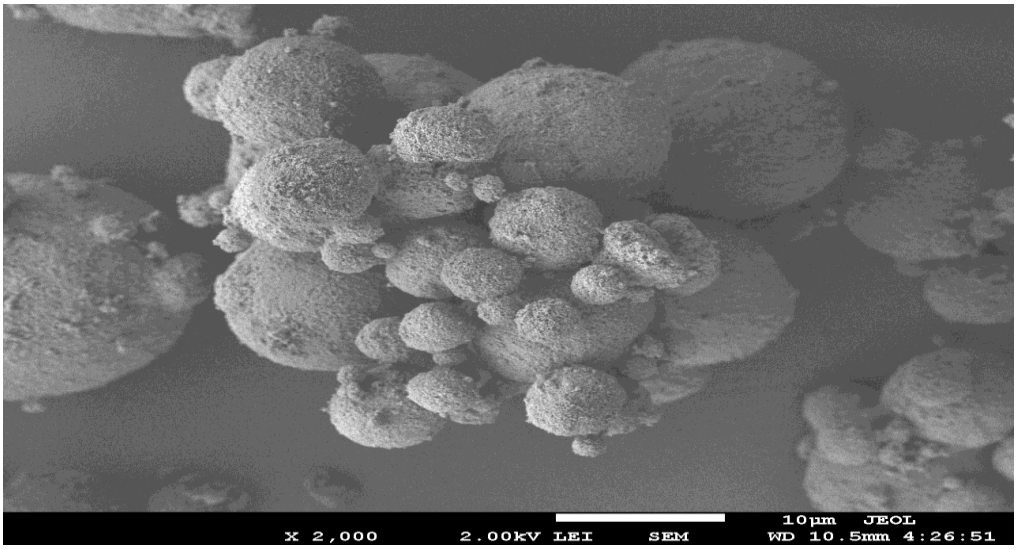

Figure 7-24: SEM image of a floccules in 0.03% PEG 1000 solution

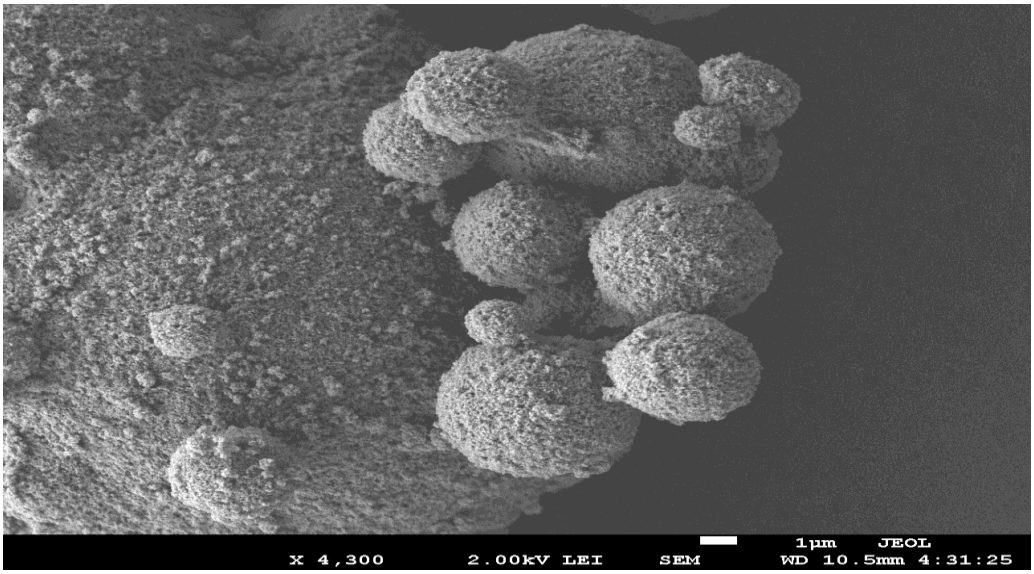

Figure 7-25: A closer SEM image of floccules in 0.03% PEG 1000 solution.

In a flocculated suspension, a clear interface is seen since even the small particles present in the suspension become a part of the flocs. This is clearly seen in Figures 7-24 and 7-25 where smaller particles are attached to larger particles.

All the SEM images show that the particles are spherical in shape therefore they fit well into the hindered settling theory.

7.6 Differential Scanning Calorimetry

DSC experiments were performed as discussed in Section 6.2.8. The DSC data is given in Figures 7-26 to 7-33. The free water content was calculated based on the heating and cooling cycles. The heat of crystallization (ΔH_c), the heat of fusion (ΔH_f) and (ΔH_v) were calculated for dried aluminum hydroxide gel suspension sediment in various dispersion media and the various dispersion media were used as references. Aluminum hydroxide starts degrading at 150-200^{0}C. [4] The degradation continues to up to a temperature of 550^{0}C. [5]The degradation is given as:

$$Al(OH)_3 \longrightarrow Al_2O_3 + 3H_2O \quad (7.7)$$

The heat of crystallization, heat of fusion and heat of vaporization for suspension sediments and various dispersion media are summarized in Table 7.22. The heat of crystallization, the heat of fusion and the heat of vaporization are used to determine the amount of the free water or unbound water. Table 7.10 summarizes the calculations for unbound water. The relative heats of crystallization, fusion and vaporization were calculated for various suspension sediments with respect to the reference dispersion media in order to calculate the amount of unbound water.

Table 7.22: Summary of DSC Data

	Heat of Crystallization (ΔH_c)	Heat of Fusion (ΔH_f)	Heat of Vaporization (ΔH_v)
$Al(OH)_3$ Suspension in Purified water USP	187.23	-225.16	-1140.06
Purified water USP as reference	339.38	-390.17	-2072.57
$Al(OH)_3$ Suspension in 0.01% PEG 1000	196.83	-203.21	-1527.77
0.01% PEG 1000 as reference	323.51	-390.14	2056.38
$Al(OH)_3$ Suspension in 0.03% PEG 1000	253.66	-274.57	-1575.48
0.03% PEG 1000 as reference	328.07	-370.97	-2188.45
$Al(OH)_3$ Suspension in 0.05% PEG 1000	273.54	-278.54	-1887.63
0.05% PEG 1000 as reference	324.44	-405.75	-2167.71

Table 7.23: Calculation of Relative ΔH_c % and Relative ΔH_f %

	Relative ΔH_c %	Relative ΔH_f %	Relative ΔH_v %	Average of ΔH_c, ΔH_f and ΔH_v
$Al(OH)_3$ Suspension in Purified water USP	55.1	57.77	55.01	55.96
$(OH)_3$ Suspension in 0.01% PEG 1000	60.84	52.08	74.29	62.40
$Al(OH)_3$ Suspension in 0.03% PEG 1000	77.31	74.01	71.99	74.44
$Al(OH)_3$ Suspension in 0.05% PEG 1000	84.31	68.62	87.07	80.0

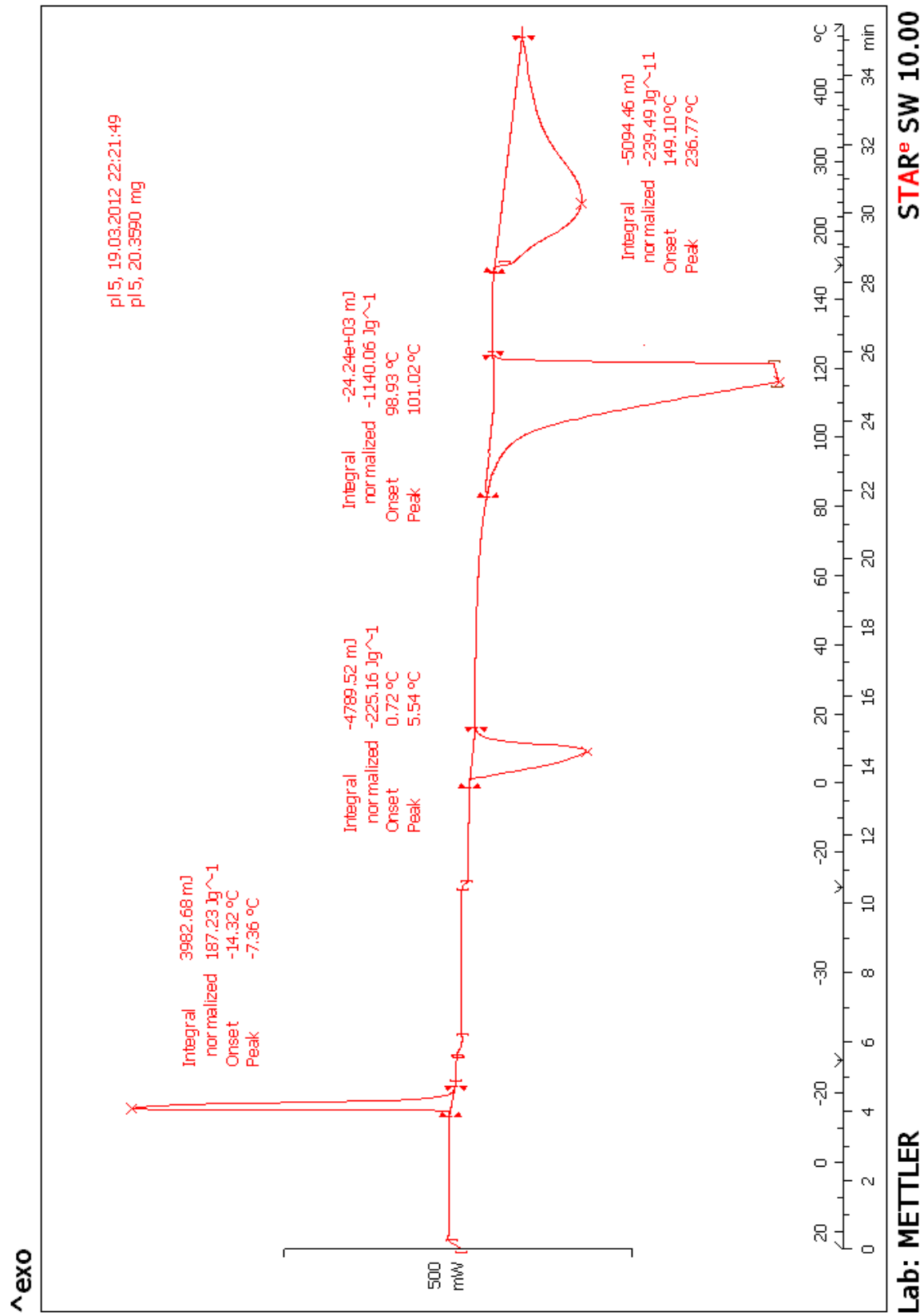

Figure 7-26: DSC data for $Al(OH)_3$ in Purified Water USP

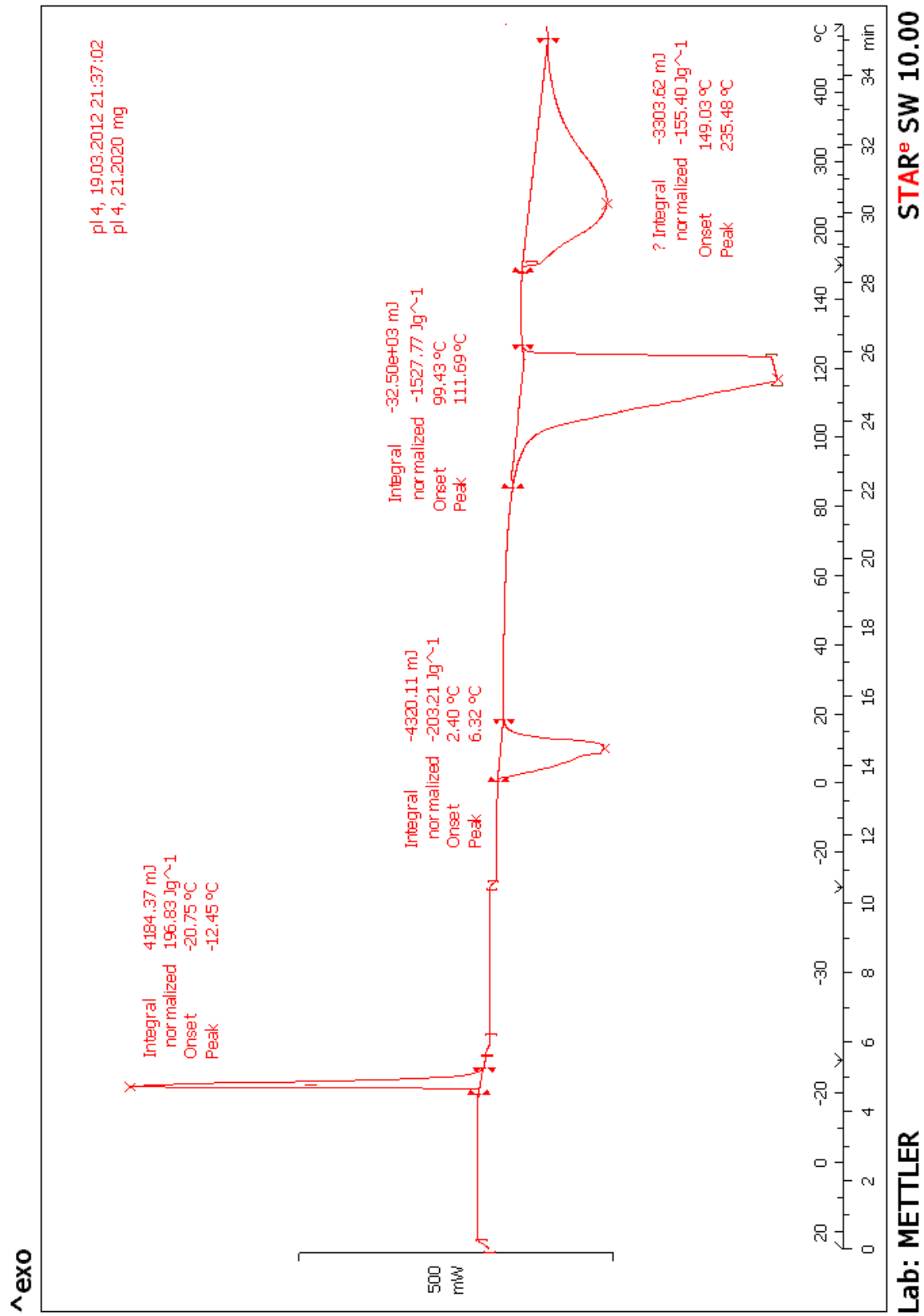

Figure 7-27: DSC data for $Al(OH)_3$ in 0.01% PEG 1000

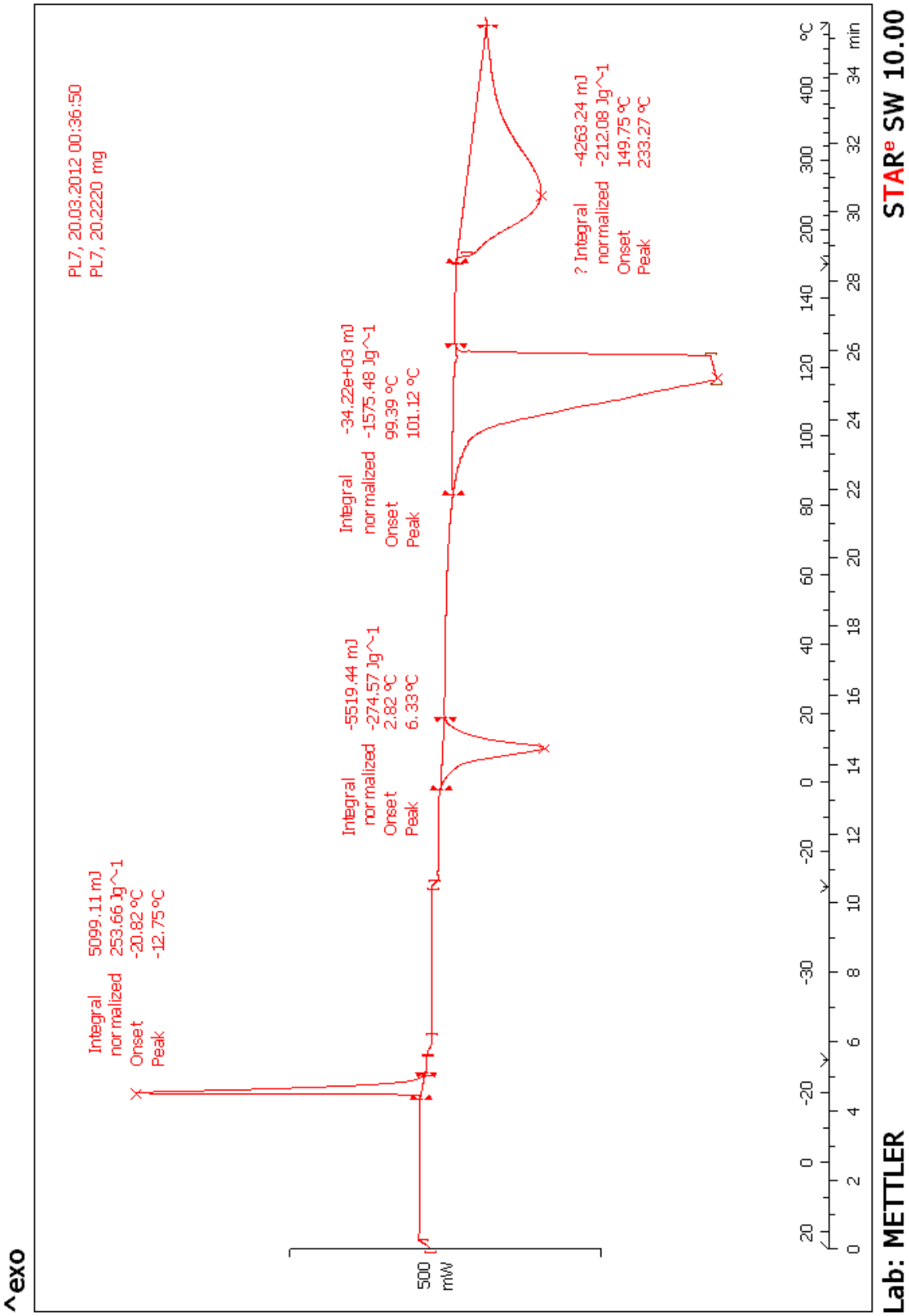

Figure 7-28: DSC data for $Al(OH)_3$ in 0.03% PEG 1000

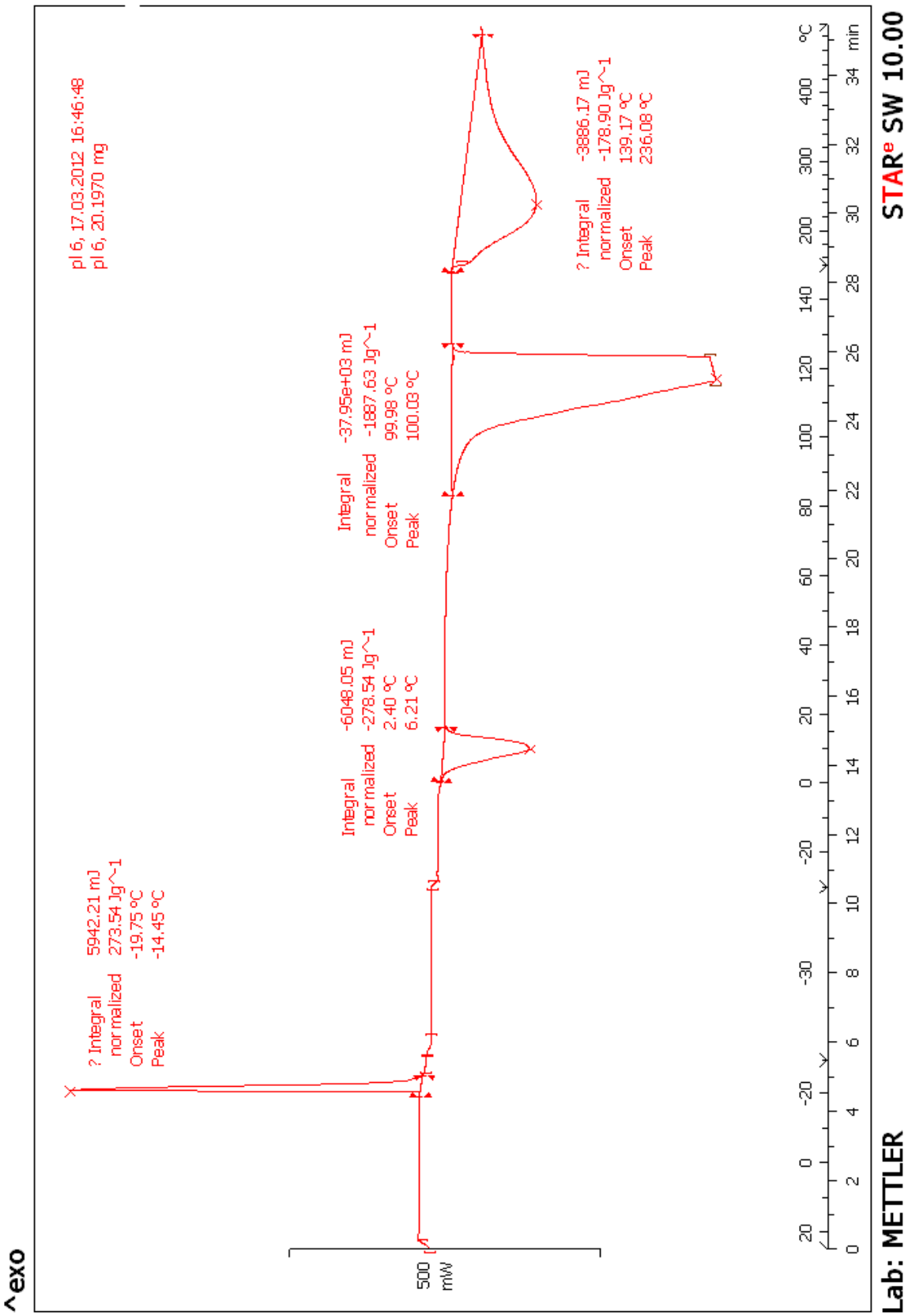

Figure 7-29: DSC data of $Al(OH)_3$ in 0.05% PEG 1000

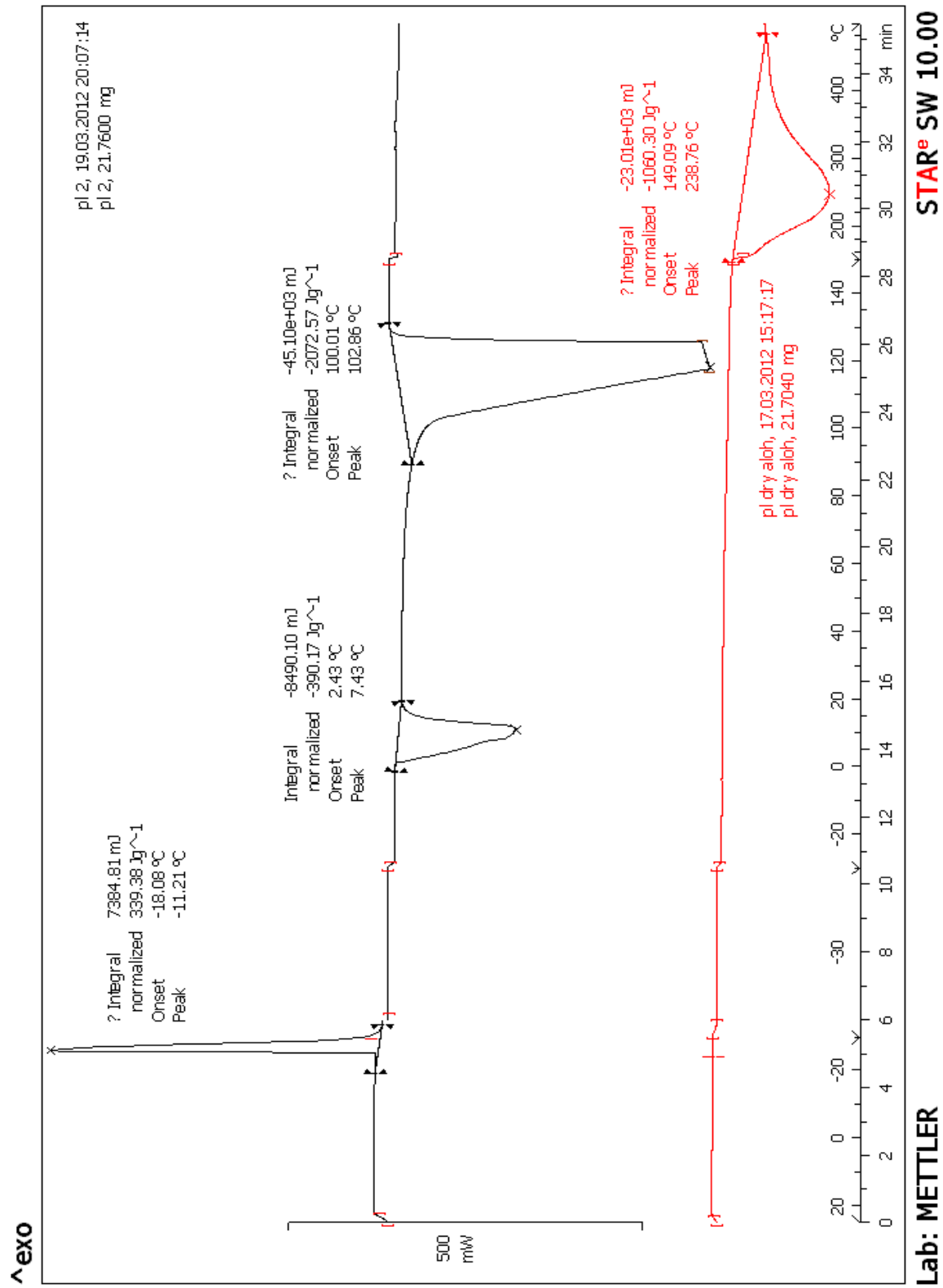

Figure 7-30: DSC data of Purified Water USP as the reference and $Al(OH)_3$ in Purified Water USP which has been dried overnight in oven.

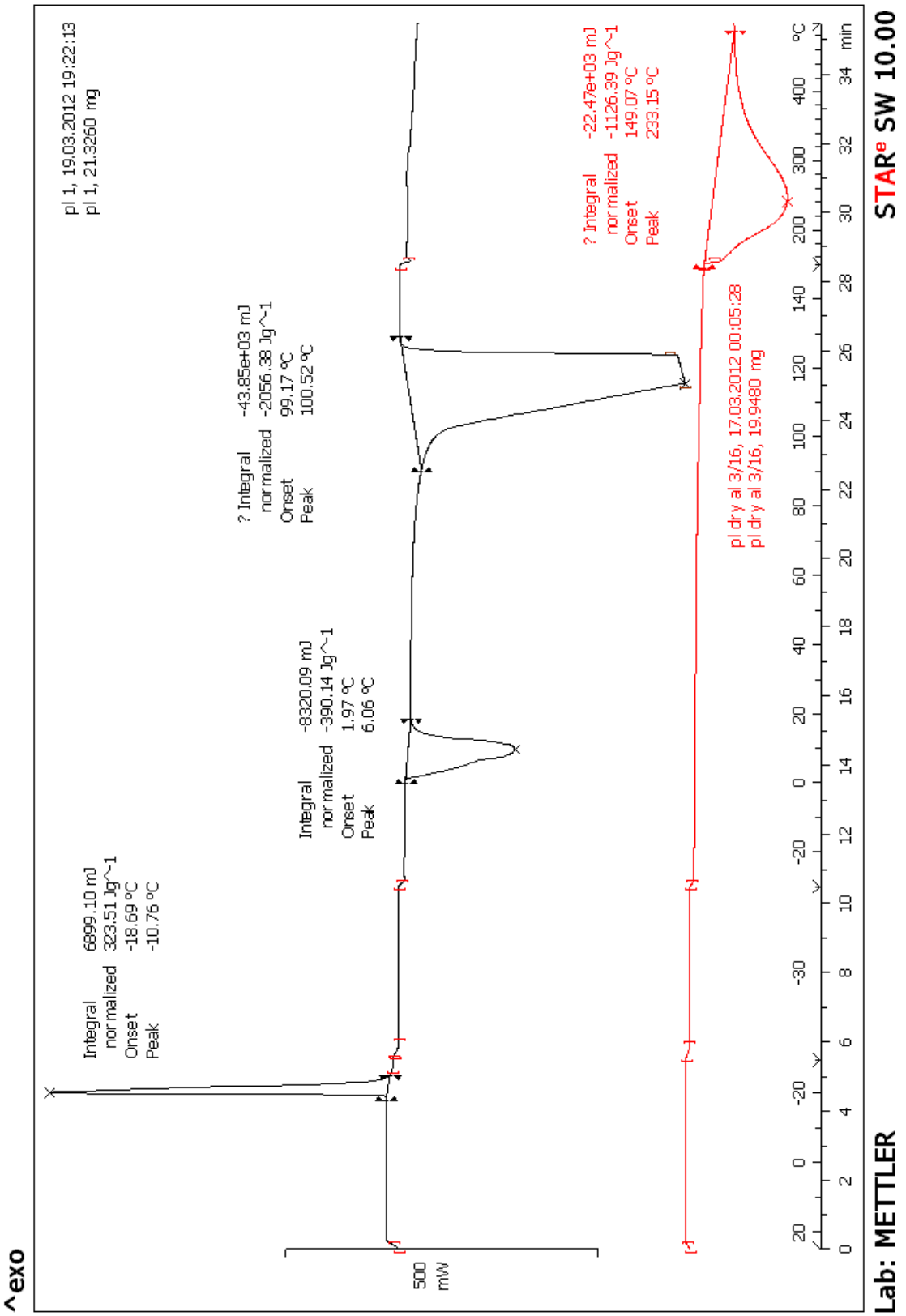

Figure 7-31: DSC data of 0.01% PEG 1000 as the reference and $Al(OH)_3$ in 0.01% PEG 1000 which has been dried overnight in oven.

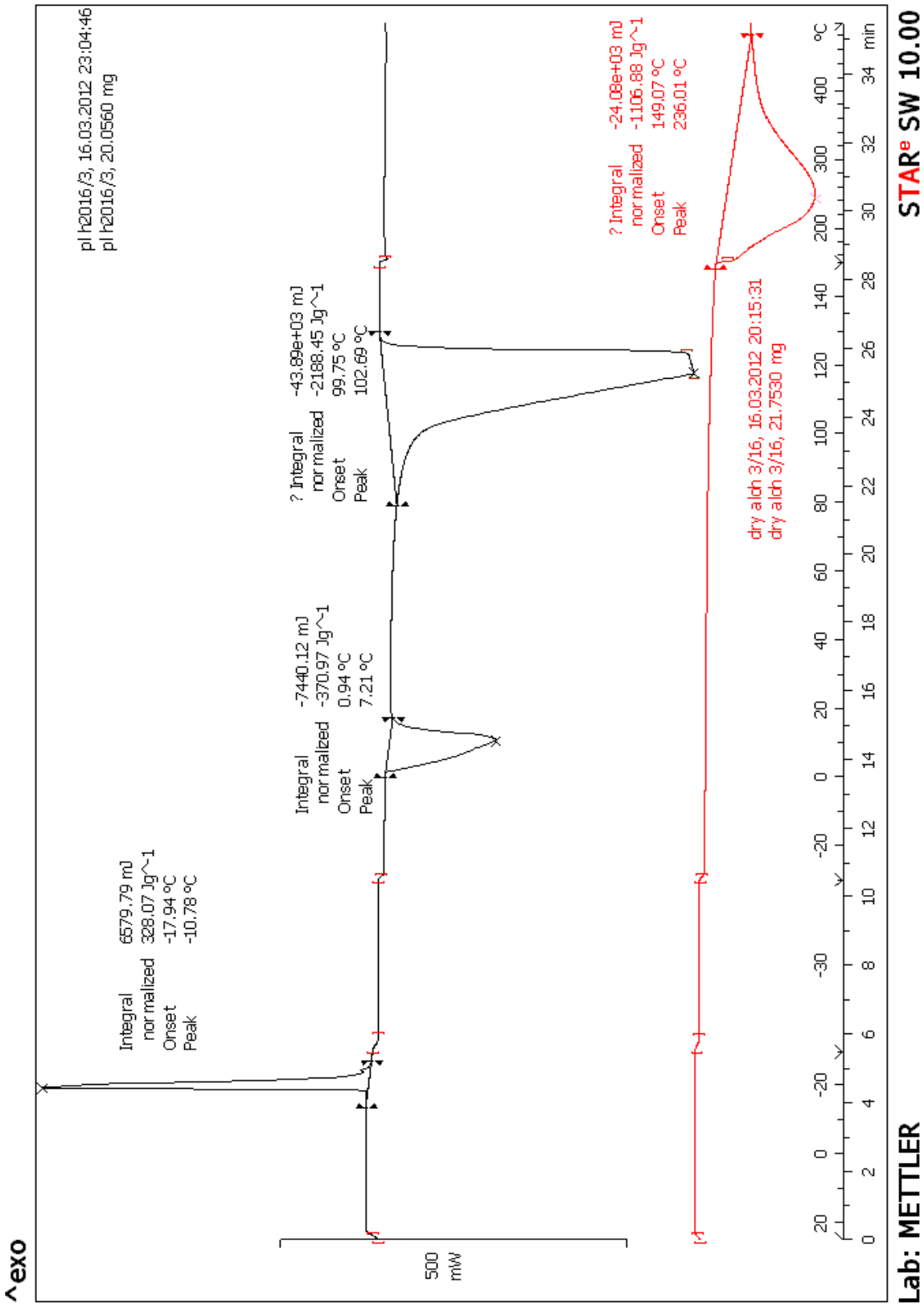

Figure 7-32: DSC data of 0.03% PEG 1000 as the reference and $Al(OH)_3$ in 0.03% PEG 1000 which has been dried overnight in oven.

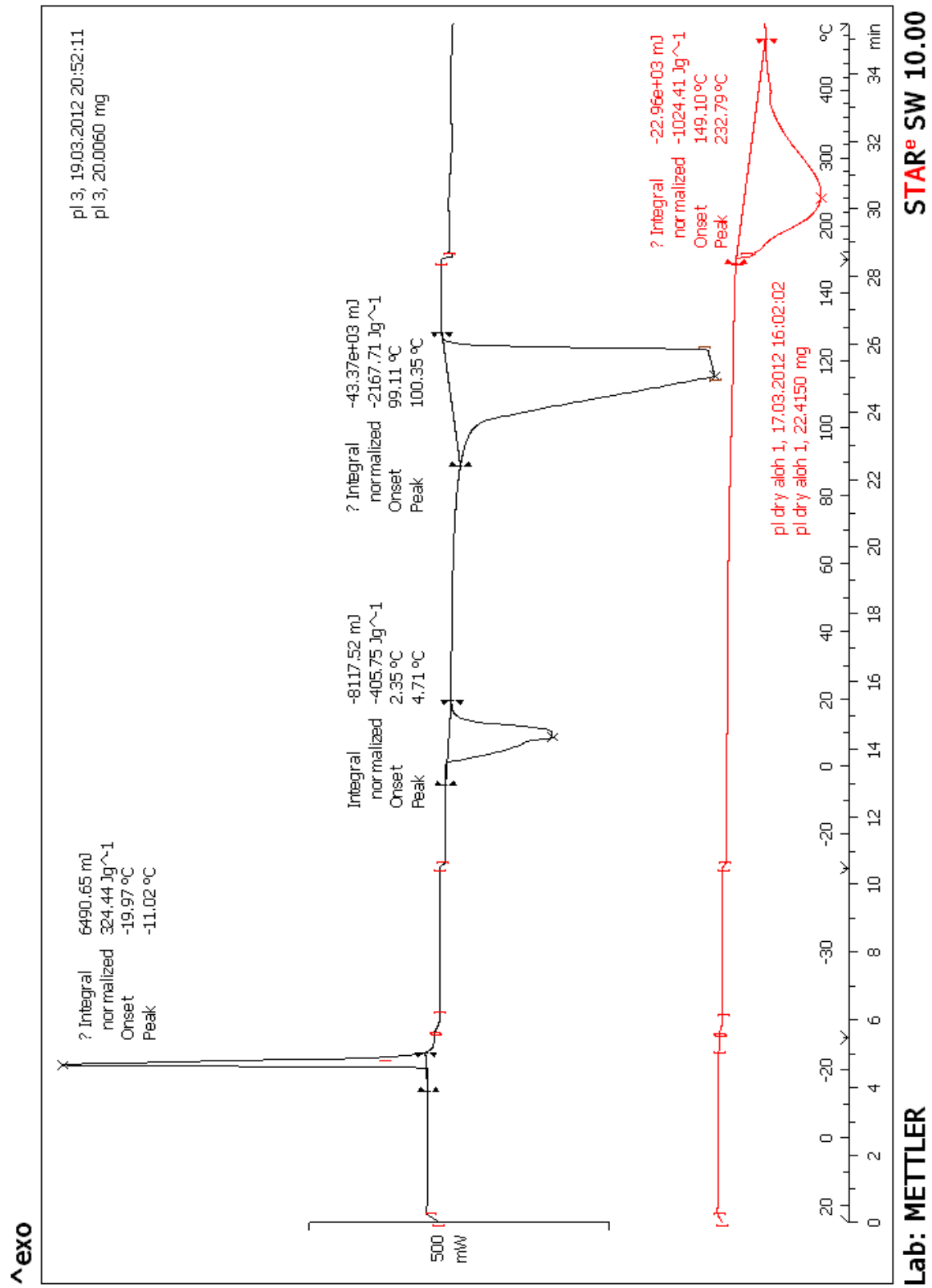

Figure 7-33: DSC data of 0.05% PEG 1000 as the reference and $Al(OH)_3$ in 0.05% PEG 1000

The unbound water content in the suspensions is summarized in Table 7.23. It was found that as the concentration of the polymer increased, the amount of unbound water associated with the suspension also increased. However, the amount of loosely bound water could not be determined due to the instrument limitations.

7.7 Thermogravimetry Analysis

The thermogravimetry analysis (TGA) was performed using the temperature program discussed in Section 6.2.7. TGA studies were performed for pure water, pure dried aluminum hydroxide gel as well as the suspensions of dried aluminum hydroxide gel in various dispersion media. The data obtained is shown in Figures 7-25 to 7-50 and summarized in Table 7.9.

Table 7.24: TGA data

Sample	Onset Temperature	Endset temperature	% Mass Loss
Pure water	73.09	107.93	96.4346
Pure Dried $Al(OH)_3$	132.05	474.31	36.5162
$Al(OH)_3$ in water	42.33	451.66	73.5152
$Al(OH)_3$ in 0.01% PEG 1000	48.65	449.17	75.2126
$Al(OH)_3$ in0.03% PEG 1000	48.64	452.79	75.3036
$Al(OH)_3$ in0.05% PEG 1000	51.60	450.49	77.6650

When pure water was analyzed, there was a 96% loss in the mass showing that the all the water had been lost upon heating. Aluminum hydroxide starts degrading at 150-200^{0}C[4]. It was found that the aluminum hydroxide thermally decomposes up to a temperature of 550^{0}C.[5] When pure aluminum hydroxide was heated to 500^{0}C, there

was about 36% loss in mass, which is correct stoichiometrically. This proved that aluminum hydroxide has decomposed to aluminum oxide.

When the suspensions of dried aluminum hydroxide gel in various media were studied, it was found that those containing water as the dispersion media has the lowest mass loss when compared to increasing concentrations of PEG 1000 solutions as the dispersion media. This data is supported by the data obtained from the DSC. Assuming that the same amount of aluminum hydroxide is degrading in all the suspensions, we can say that the increase in the mass loss could be due to the increase in the amount of water associated with the suspension. However, it is difficult to calculate the amount of bound and unbound water since the temperature of vaporization of water and the degradation temperature of aluminum hydroxide are close and the peaks overlap as it can be seen in the TGA data.

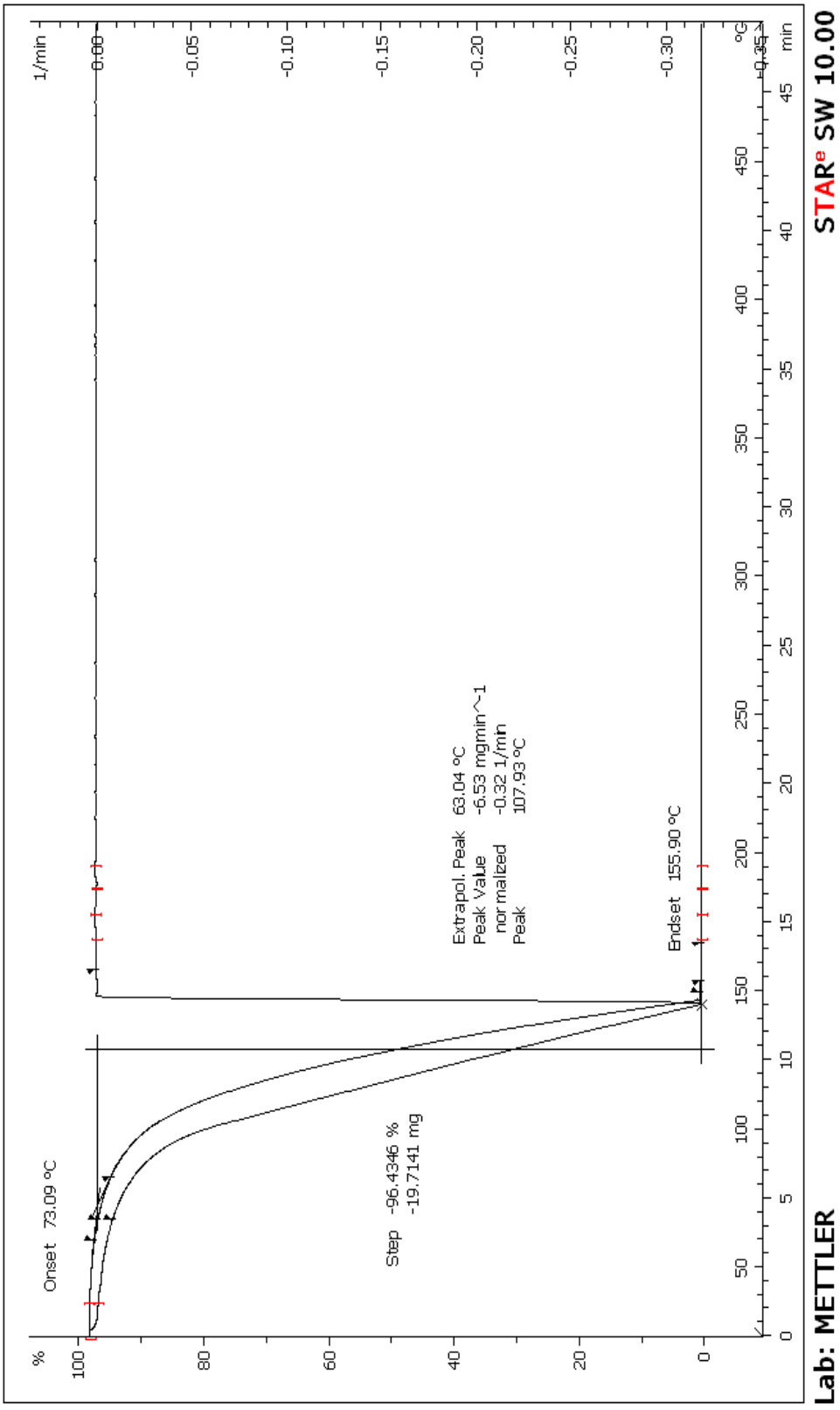

Figure 7-34: TGA data for Purified Water USP

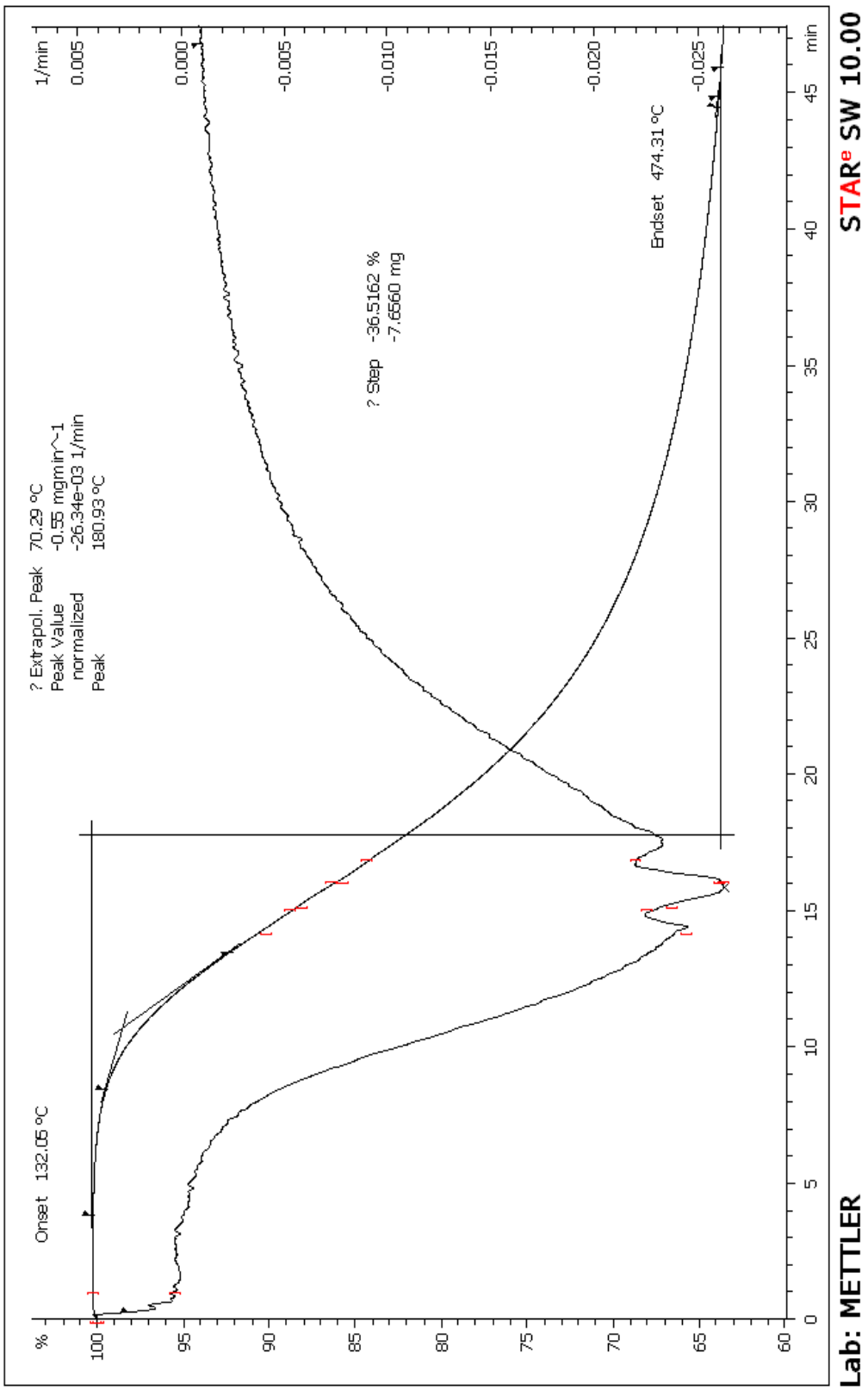

Figure 7-35: TGA data for Pure Dried Aluminum Hydroxide Gel

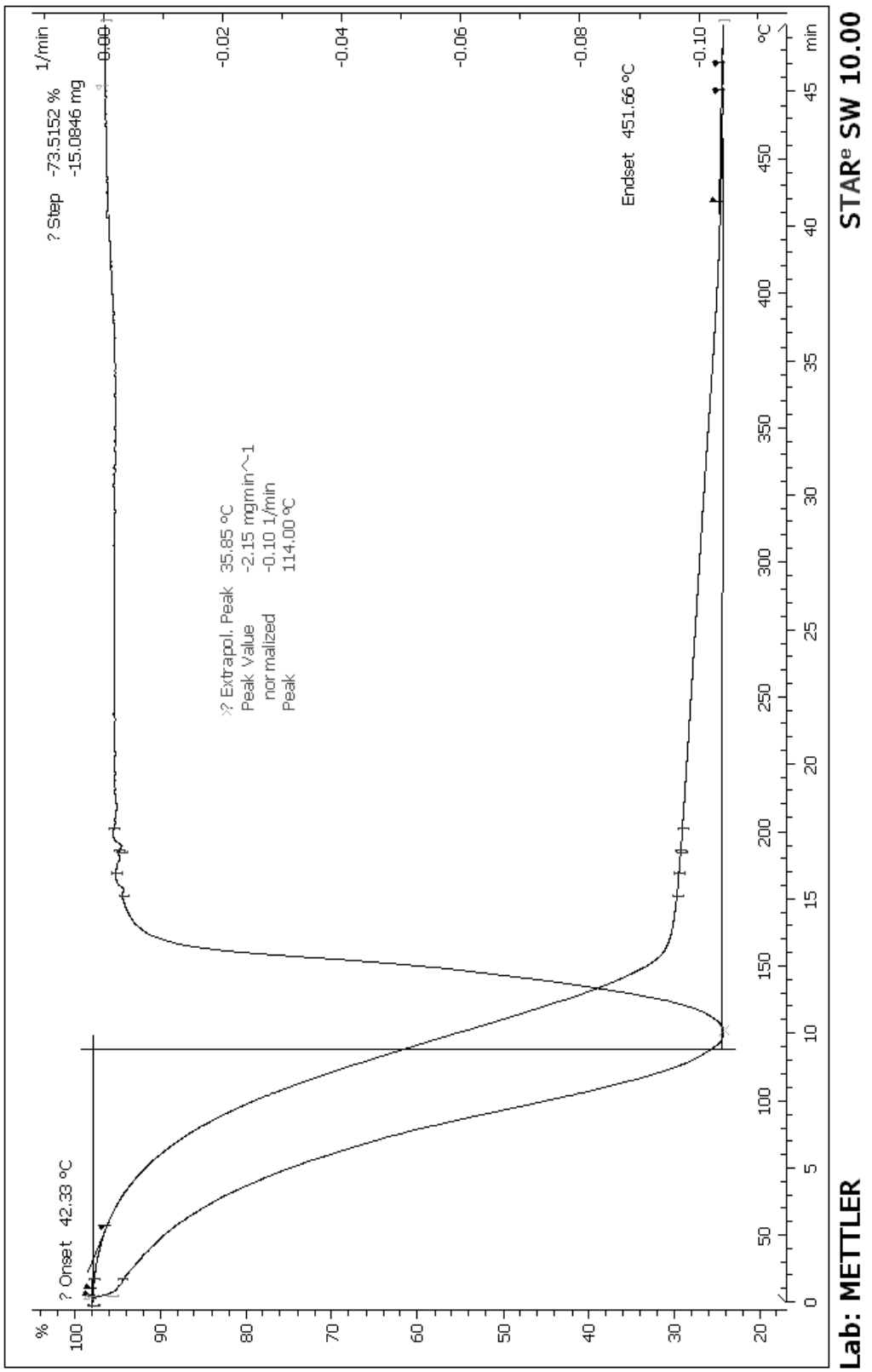

Figure 7-36: TGA data Dried Aluminum Hydroxide Gel in Purified Water USP

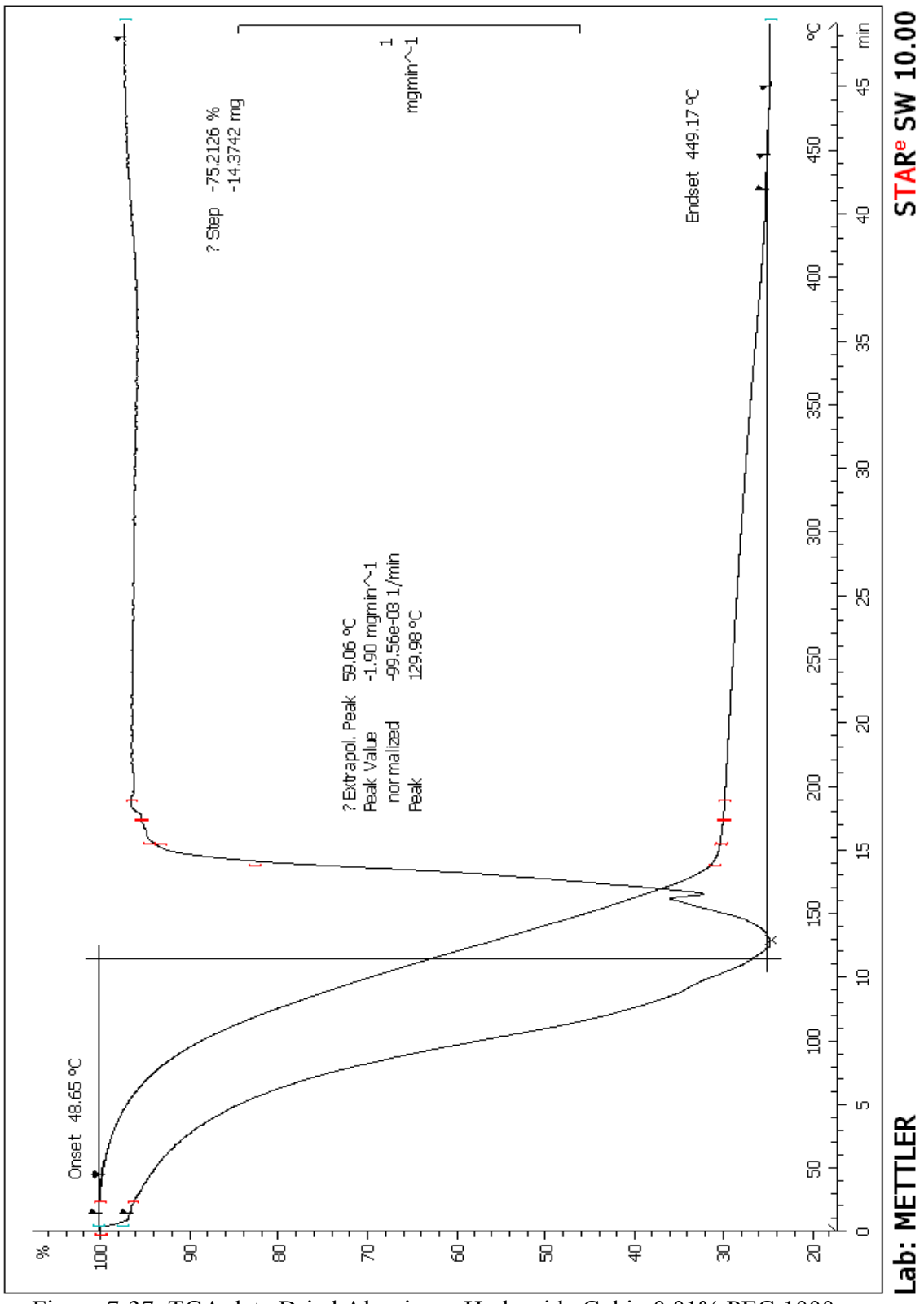

Figure 7-37: TGA data Dried Aluminum Hydroxide Gel in 0.01% PEG 1000

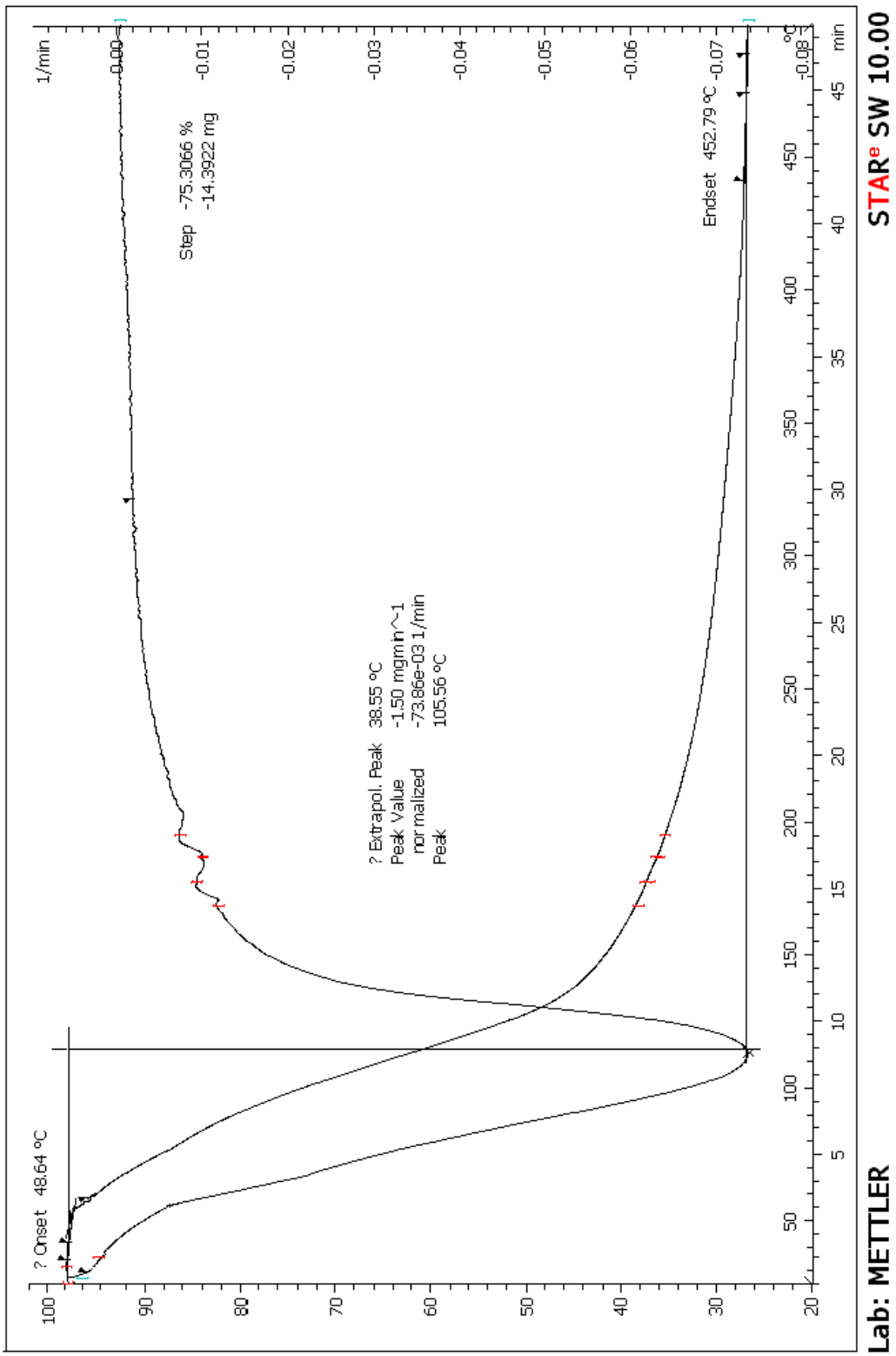

Figure 7-38: TGA data Dried Aluminum Hydroxide Gel in 0.03% PEG 1000

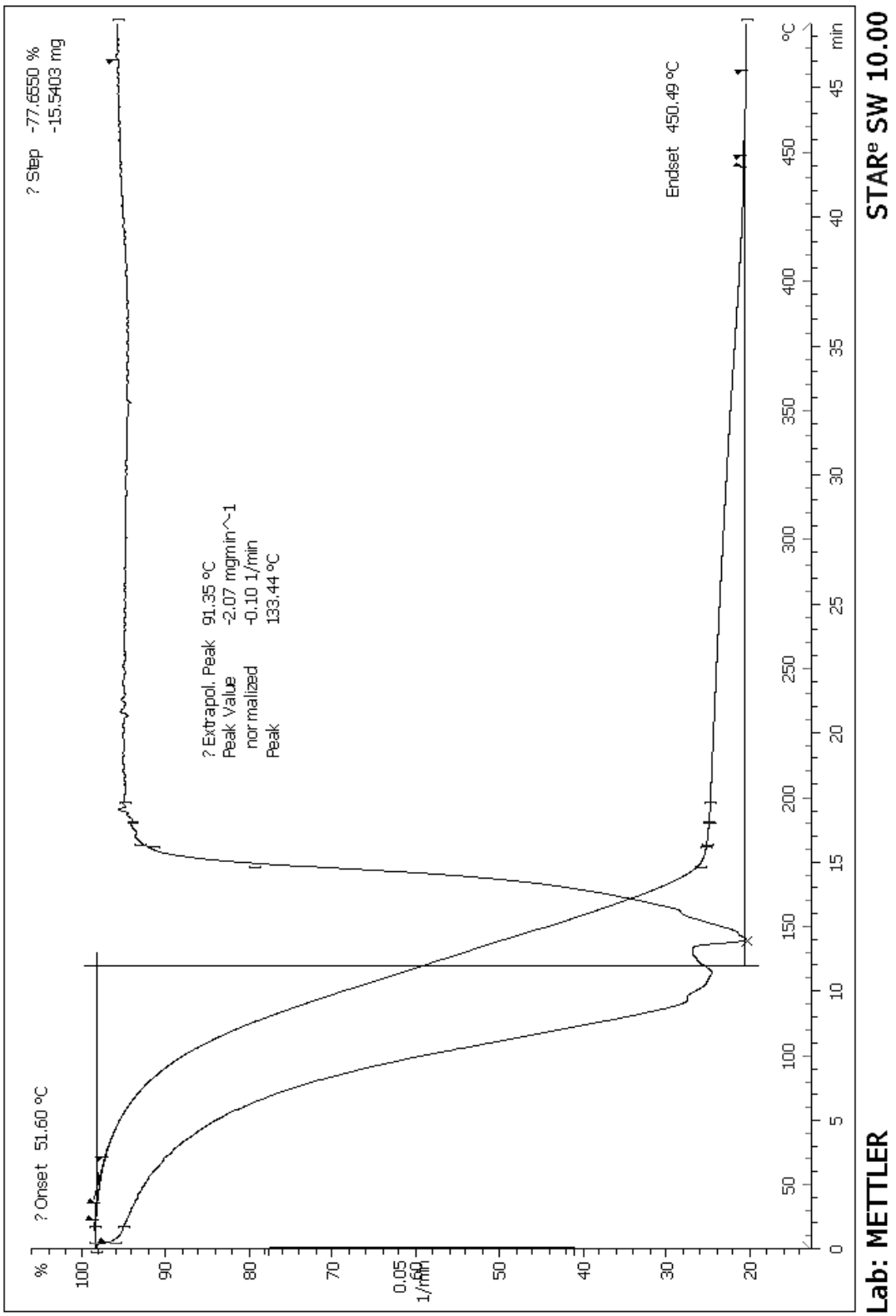

Figure 7-39: TGA data Dried Aluminum Hydroxide Gel in 0.05% PEG 1000

Chapter-8

Conclusions and Future Recommendations

8.1 Conclusions drawn from the Particle Size Analysis

The particle size of Dried Aluminum Hydroxide Gel USP dispersed in dispersion media such as Purified water USP and various concentrations of PEG 1000 have been determined using hindered settling theory, laser diffraction and sieving. From the hindered settling data, it was found that the particle size increased with an increase in concentration of the PEG 1000. It was found that a 0.05% concentration PEG 1000 solution brought about the maximum flocculation and the particle size was found to be 21.76 μm. The data obtained from the hindered settling theory was comparable to the results obtained from laser diffraction studies. The laser diffraction results showed that the highest amount of flocculation was seen for the suspension containing dried aluminum hydroxide suspensions in 0.05% PEG 1000 and the maximum particle size was found to be 19.281 μm. It can be concluded that the increase in the particle size could be due to the increase in flocculation. This means that more particles are connected to each other through a process of polymer bridging thereby bringing about an increase in the particle size. Scanning electron microscopy was used to determine the morphology and appearance of the floccules. SEM showed images of the floccules, where a number of particles came together to form loose aggregates, confirming flocculation of the

suspension. Sieving was used to determine the particle size distribution of the dry powder aluminum hydroxide. However, the data from sieving did not give comparable results. The particle size was almost five times greater than the results obtained from the hindered settling and laser diffraction results. This could be attributed to the fact that the sieves were shaken manually instead of using a mechanical shaker which could have changed the anticipated results. The other reason could be the fact that the force exerted by the mechanical motion was not enough to break the clusters thus unable to determine the size of the individual particles.

8.2 Conclusions drawn from Thermal Analysis

Differential Scanning Calorimetry and Thermogravimetry studies were performed on suspensions of dried aluminum hydroxide gel. The flocs in a suspension tend to preserve their structure in the sediment and contain entrapped water. Hence it is important to determine the amount of water associated with suspensions. The total amount of water associated with the suspensions was determined from the DSC data. It was found that the amount of water associated with the suspensions increased with increasing concentrations of PEG 1000. However, due to instrument limitations, the amount of bound and unbound water could not be determined. TGA data also could not determine the amount of bound and unbound water since the temperature of vaporization of water and degradation temperature of aluminum hydroxide, are very close and the peaks overlap. It was found that the percentage mass loss increased as the concentration of the polymer solution increased. It can be assumed that this increase in the mass loss could be due to the increase in the amount of water associated with the suspensions. The reason behind the increasing amount of water associated with increasing concentration of

the flocculating agent in suspension could be due to the increase in flocculation, as discussed under particle size analysis. The more the flocculation, the more that polymer bridging occurs leading to an increase in the floccule size. This leads to a greater entrapment of the liquid between the individual particles, hence there is an increase in water associated with the particles.

8.3 Future Recommendations

- More mathematical models could be developed in order to study the flocculated system, which can give a better understanding to the trends for the curves obtained.

- From the TGA results, the bound and unbound water associated with suspension could not be determined. Therefore, analytical studies should be done to calculate the exact amount of bound and water in order to provide definite conclusions for the system.

- PXRD could not be used to confirm the conversion of aluminum hydroxide to aluminum oxide because the samples were amorphous in nature. Further studies could confirm these changes and should be performed.

- Studies can be performed on the effects of other types of adjuvants such as colors and preservatives with respect to the extent these ingredients can have on the flocculation of suspensions.

References

Chapter 1

1. Mahato, R.I. and A.S. Narang, *Pharmaceutical dosage forms and drug delivery*. Vol. 27. 2011: CRC Press.
2. http://www.pharmainfo.net/free-books/pharmaceutical-suspensionsa-review.
3. Martin, A., *Martin's Physical Pharmacy*. 1993, Williams and Wilkins, Maryland. p. 477.
4. Remington, J.P., *Remington's pharmaceutical sciences*. 1980: Mack.

Chapter 2

1. Martin, A., *Physical Pharmacy*. 4th ed. 1993: Lippincott Williams and Wilkins.
2. *Aerosol Science and Technology*. 2nd ed. 1993, Mc-Graw Hill: New York. 59.
3. Maude, A. and R. Whitmore, *A generalized theory of sedimentation.* British Journal of Applied Physics, 1958. **9**: p. 477.
4. van Oss, C., *Interfacial Forces in Aqueous Media. 1994.* New York: Marceli Dekker.
5. Bhatti, A.S., et al., *The application of interface settling rates in hindered settling to the determination of the mean particle radii.* Surface technology, 1985. **26**(3): p. 287-293.
6. Washington, C., *Particle size analysis in pharmaceutics and other industries: theory and practice*. 1992: Taylor & Francis.

7. http://metallurguy.wordpress.com/2011/10/01/settling-of-particles-in-fluids/.
8. Newton, S.I., *Mathematical Principles of Natural Philosophy. By Sir Isaac Newton,.... Translated Into English, and Illustrated with a Commentary, by Robert Thorp,... Volume the First*. 1777: printed for W. Strahan; and T. Cadell.
9. Conference, S.o.P.E.T., *Antec 2001 Dallas, Texas May 6-10 Conference Proceedings*. Vol. 1. 2001: Technomic Pub Co.
10. Theodore, L., *Air pollution control equipment calculations*. 2008: Wiley-Interscience.
11. Carter, C.B. and M.G. Norton, *Ceramic materials: science and engineering*. 2007: Springer Verlag.
12. Allen, T., *particle size measurement*. 4th ed, ed. B.Scarlett. 1990, New York: Chapman and Hall.

Chapter 3

1. Davies, L., D. Dollimore, and J. Sharp, *Sedimentation of supsensions: implications of theories of hindered settling.* Powder Technology, 1975. **13**(1): p. 123-132.
2. Mirza, S. and J. Richardson, *Sedimentation of suspensions of particles of two or more sizes.* Chemical Engineering Science, 1979. **34**(4): p. 447-454.
3. Martin, A., *Physical Pharmacy*. 2nd ed. 1993 Lea & Febiger.
4. Stechemesser, H. and B. Dobiáš, *Coagulation and flocculation*. Vol. 126. 2005: CRC.

5. Bhatty, J., et al., *The use of hindered settling data to evaluate particle size or floc size, and the effect of particle-liquid association on such sizes.* Surface Technology, 1982. **15**(4): p. 323-344.

6. Rathi, S., *An investigation into the hindered settling of Pumice using various Surfactants*, in *Department of Industrial Pharmacy*. 2010, University of Toledo: Toledo.

7. McKay, R.B., *Hindered settling of organic pigment dispersions in hydrocarbon liquids.* Journal of Applied Chemistry and Biotechnology, 1976. **26**(1): p. 55-66.

8. Michaels, A.S. and J.C. Bolger, *Settling rates and sediment volumes of flocculated kaolin suspensions.* Industrial & Engineering Chemistry Fundamentals, 1962. **1**(1): p. 24-33.

9. Kissa, E., *Dispersions: characterization, testing, and measurement*. Vol. 84. 1999: CRC.

10. Richardson, J., *Sedimentation and fluidisation: Part I.* Trans. Inst. Chem. Eng., 1954. **32**: p. 35-53.

11. Davies, L., D. Dollimore, and G. McBride, *Sedimentation of suspensions: simple methods of calculating sedimentation parameters.* Powder Technology, 1977. **16**(1): p. 45-49.

12. Wang, Y., *The Investigation of Concentrated Suspensions of Magnesium Trisilicate*, in *The University of Toledo*. 2001.

13. Steinour, H.H., *Rate of sedimentation. Nonflocculated suspensions of uniform spheres.* Industrial & Engineering Chemistry, 1944. **36**(7): p. 618-624.

14. Steinour, H.H., *Rate of sedimentation.* Industrial & Engineering Chemistry, 1944. **36**(9): p. 840-847.

15. Steinour, H.H., *Rate of sedimentation. Concentrated flocculated suspensions of powders.* Industrial & Engineering Chemistry, 1944. **36**(10): p. 901-907.

16. Steinour, H., *Rate of sedimentation; Non-flocculated suspensions of uniform spheres Ind.* Eng. Chem, 1944. **36**(7).

17. Dollimore, D. and R. Karimian, *Sedimentation of suspensions: Factors affecting the hindered settling of alumina in a variety of liquids.* Surface Technology, 1982. **17**(3): p. 239-250.

Chapter 4

1. Hardee, G.E. and J.D. Baggot, *Development and formulation of veterinary dosage forms*. 1998: Marcel Dekker.

2. Florence, A.T. and D. Attwood, *Physicochemical Principles of Pharmacy*. 2011: Pharmaceutical Press.

3. Banker, G.S. and C.T. Rhodes, *Modern pharmaceutics*. 2002: Marcel Dekker.

4. Nash, R.A., *Pharmaceutical suspensions.* Pharmaceutical dosage forms: disperse systems, 1988. **1**: p. 151-198.

5. Ghosh, T.K. and B.R. Jasti, *Theory and practice of contemporary pharmaceutics*. 2005: CRC Press.

6. Martin, A.N. and P. Bustamante, *Physical pharmacy: physical chemical principles in the pharmaceutical sciences*. 1993: Lea & Febiger.

7. Tadros, T.F., *Applied surfactants: principles and applications*. 2005: Wiley-VCH.

8. Li, L.C. and Y. Tian, *Zeta potential.* Encyclopedia of pharmaceutical technology, 2002. **2**: p. 429–458.

9. Boch, P. and J.C. Nièpce, *Ceramic materials: processes, properties and applications*. 2007: ISTE.

10. http://www.groundwaterresearch.com.au/reference/Hydrology%20and%20the %20Clay% 20Minerals/Properties.htm.

11. Tadros, T.F., *Colloids in agrochemicals: colloids and interface science*. 2009: Wiley-VCH.

12. Remington, J.P. and A.R. Gennaro, *Remington's pharmaceutical sciences*. 1990: Mack Pub. Co.

13. Kulshreshtha, A.K., O.N. Singh, and G.M. Wall, *Pharmaceutical suspensions: from formulation development to manufacturing*. 2009: Springer Verlag.

14. Pelton, R. and L. Allen, *The effects of some electrolytes on flocculation with a cationic polyacrylamide.* Colloid & Polymer Science, 1983. **261**(6): p. 485-492.

15. Somasundaran, P., X. Yu, and S. Krishnakumar, *Role of conformation and orientation of surfactants and polymers in controlling flocculation and dispersion of aqueous and non-aqueous suspensions.* Colloids and Surfaces A: Physicochemical and Engineering Aspects, 1998. **133**(1-2): p. 125-133.

16. Gregory, J. and S. Barany, *Adsorption and flocculation by polymers and polymer mixtures.* Advances in Colloid and Interface Science, 2011.

17. Gregory, J., *Polymer adsorption and flocculation in sheared suspensions.* Colloids and Surfaces, 1988. **31**: p. 231-253.

18. Kissa, E., *Dispersions: characterization, testing, and measurement*. Vol. 84. 1999: CRC.

19. Somasundaran, P., *Encyclopedia of surface and colloid science*. 2006: Taylor & Francis.

20. Chibowski, S., J. Patkowski, and E. Grzadka, *Adsorption of polyethyleneimine and polymethacrylic acid onto synthesized hematite.* Journal of Colloid and Interface Science, 2009. **329**(1): p. 1-10.

21. Morrison, I.D. and S. Ross, *Colloidal dispersions: suspensions, emulsions, and foams*. 2002: Wiley-Interscience.

22. Zhulina, E.B., O.V. Borisov, and V.A. Priamitsyn, *Theory of steric stabilization of colloid dispersions by grafted polymers.* Journal of Colloid and Interface Science, 1990. **137**(2): p. 495-511.

23. Birdi, K.S., *Handbook of Surface and Colloid Chemistry*. 2008: CRC Press/Taylor & Francis.

24. Tadros, T.F., *Colloids in Agrochemicals: Volume 5: Colloids and Interface Science*. 2011: John Wiley & Sons.

25. Schramm, L.L., *Emulsions, foams, and suspensions: fundamentals and applications*. 2005: Wiley-VCH.

Chapter 5

1. Pommerville, J.C., *Alcamo's fundamentals of microbiology*. 2010: Jones & Bartlett Learning.

2. Angelo, P. and R. Subramanian, *Powder metallurgy: science, technology and applications*. 2008: Prentice-Hall of India.

3. Carlton, R.A., *Pharmaceutical Microscopy*. 2011: Springer Verlag.

4. Buseck, P., J.M. Cowley, and L.R. Eyring, *High-resolution transmission electron microscopy and associated techniques*. 1988: Oxford University Press, USA.

5. McMahon, G., *Analytical instrumentation: a guide to laboratory, portable and miniaturized instruments*. 2007: Wiley-Interscience.

6. Leng, Y., *Materials characterization: introduction to microscopic and spectroscopic methods*. 2008: Wiley. 121.

7. Egerton, R.F., *Physical principles of electron microscopy: an introduction to TEM, SEM, and AEM*. 2005: Springer.

8. Lawes, G., A.M. James, and ACOL, *Scanning electron microscopy and x-ray microanalysis*. 1987: Published on behalf of ACOL, Thames Polytecnic, London, by Wiley.

9. Zhou, W. and Z.L. Wang, *Scanning microscopy for nanotechnology: techniques and applications*. 2007: Springer Verlag.

10. Cao, G., *Nanostructures & nanomaterials: synthesis, properties & applications*. 2004: Imperial College Pr.

11. http://www4.nau.edu/microanalysis/Microprobe-SEM/Signals.html.

12. Khursheed, A., *Scanning electron microscope optics and spectrometers*. 2010: World Scientific.

13. Lee, R.E., *Scanning electron microscopy and x-ray microanalysis*. 1993: Prentice Hall. 444-49.

14. Goldstein, J., *Scanning electron microscopy and X-ray microanalysis*. Vol. 1. 2003: Springer Us.

15. Paszkowski, B., *Electron optics*. 1968: Iliffe.

16. Oatley, C.W., *The Scanning electron microscope*. 1972: Cambridge University Press.

17. Webb, C.E. and J.D.C. Jones, *Handbook of Laser Technology and Applications: Applications*. Vol. 3. 2004: Philadelphia.

18. McGlinchey, D., *Characterisation of bulk solids*. 2005: Blackwell.

19. Crompton, T.R., *Polymer reference book*. 2006: Smithers Rapra Technology.

20. Sample, M.A., *Characterization of the epikarst over the Hunton anticline, Arbuckle-Simpson aquifer, Oklahoma*. 2008, Oklahoma State University.

21. Myerson, A.S., *Handbook of industrial crystallization*. 2002: Butterworth-Heinemann.

22. Barth, H.G., *Modern methods of particle size analysis*. 1984: Wiley.

23. http://new.americanlaboratory.com/913-Technical-Articles/19522-Laser-Diffraction-A-Firm-Foundation-for-Particle-Characterization/

24. http://www.chemeurope.com/en/whitepapers/61205/measuring-particle-size-using-modern-laser-diffraction-techniques.html

25. Nollet, L.M.L., *Handbook of food analysis: Methods and instruments in applied food analysis*. 2004: Marcel Dekker.

26. Qiu, Y., et al., *Developing solid oral dosage forms: pharmaceutical theory and practice*. 2009: Academic Press.

27. Irudayaraj, J. and C. Reh, *Nondestructive testing of food quality*. 2008: Blackwell Pub./IFT Press.

28. Washington, C., *Particle size analysis in pharmaceutics and other industries: theory and practice*. 1992: Ellis Horwood.

29. McCave, I., et al., *Evaluation of a Laser-Diffraction-Size Analyzer for Use with Natural Sediments: RESEARCH METHOD PAPER.*

30. Storey, R.A. and I. Ym?n, *Solid State Characterization of Pharmaceuticals*. 2011: John Wiley & Sons.

31. Merkus, H.G., *Particle Size Measurements: Fundamentals, Practice, Quality*. 2008: Springer.

32. Dodge, L.G., D.J. Rhodes, and R.D. Reitz, *Drop-size measurement techniques for sprays: comparison of Malvern laser-diffraction and Aerometrics phase/Doppler.* Applied optics, 1987. **26**(11): p. 2144-2154.

33. Lee, D. and M. Webb, *Pharmaceutical analysis*. Vol. 8. 2003: Wiley-Blackwell.

34. W.Hemminger, *Reccommendations of the ICTAC Nomenclature committee.* ICTAC NEWS, 1998: p. 106-122.

35. Wendlandt, W.W., *Thermal Analysis*, ed. P.J. Elving. Vol. 19. 1974: John Wiley and Sons.

36. Brown, M.E., *Introduction to thermal analysis: techniques and applications*. Vol. 1. 2001: Springer Netherlands.9.

37. Groenewoud, W.M., *Characterisation of polymers by thermal analysis*. 2001: Elsevier Science.

38. Haines, P.J., *Thermal methods of analysis: principles, applications and problems*. 1995: Chapman & Hall. 65-69.

39. Lobo, H. and J.V. Bonilla, *Handbook of plastics analysis*. Vol. 68. 2003: CRC.

40. Fifield, F.W. and P.J. Haines, *Environmental analytical chemistry*. 2000: Wiley-Blackwell.

41. Kessler, M.R., *Advanced Topics in Characterization of Composites*. 2004: Trafford on Demand Pub.

42. Menczel, J.D. and R.B. Prime, *Thermal analysis of polymers*. 2009: Wiley Online Library.

43. Zuru, A., et al., *Adoption of thermogravimetric kinetic models for kinetic analysis of biogas production.* Renewable energy, 2004. **29**(1): p. 97-107.

44. Dollimore, D., *Catalysts-Thermal Analysis Applications.* SPECIAL PUBLICATION-ROYAL SOCIETY OF CHEMISTRY, 1992. **117**: p. 238-238.

45. Earnest, C.M., *Compositional analysis by thermogravimetry*. 1988: ASTM International. 1-3.

46. Earnest, C.M., *Compositional analysis by thermogravimetry*. 1988: ASTM International.5-8.

47. Haines, P., *Thermal methods of analysis*. Environmental analytical chemistry. 2000. 253.

48. Peraro, J.S., *Limitations of test methods for plastics*. 2000: ASTM International.

49. Haines, P.J., *Principles of thermal analysis and calorimetry*. 2002: Royal society of chemistry. 12.

50. Sepe, M.P., *Thermal analysis of polymers*. Vol. 95. 1997: Rapra Technology.

51. Storey, R.A., *Solid State Characterization of Pharmaceuticals*. 2011: Wiley-Blackwell.

52. Turi, E.A., *Thermal characterization of polymeric materials(Book).* New York, Academic Press, 1981. 985 p, 1981: p. 827-829.

53. Brown, M.E., *Introduction to thermal analysis: techniques and applications*. Vol. 1. 2001: Springer Netherlands. 44-45.

54. In, C.D., *Inorganic Thermogravimetric Analysis*. 1963, Elsevier, Amsterdam.

Chapter 6

1. Gennaro, A.R., *Remington: the science and practice of pharmacy*. Vol. 20. 2000: Lippincott Williams & Wilkins Philadelphia.

2. http://www.factsandcomparisons.com/.

3. https://www.spectrumchemical.com/MSDS/A3605.pdf.

4. Martindale, W.H., J.E.F. Reynolds, and A. Wade, *The extra pharmacopoeia: incorporating Squire's companion*. 1977: Pharmaceutical Press.

5. Prodromou, K. and A. Pavlatou-Ve, *Formation of aluminum hydroxides as influenced by aluminum salts and bases.* Clays and clay minerals, 1995. **43**(1): p. 111-115.

6. Ellms, J.W., *Water purification*. 1917: McGraw-Hill book company, inc.

7. Hessler, J.C. and A.L. Smith, *Essentials of chemistry*. 1912: B.J. Sanborn & co.

8. Philadelphia, U.S., *Remington: The Science & Practice of Pharmacy 21E, India Edition*. 2006: Lippincott Williams & Wilkins.

Chapter 7

1. Slater, R. and J. Kitchener, *Characteristics of flocculation of mineral suspensions by polymers.* Discuss. Faraday Soc., 1966. **42**(0): p. 267-275.
2. Purchas, D., *Flocculation and Coagulation.* Process Biochem, 1968. **3**: p. 10-17.
3. Walles, W.E., *Role of flocculant molecular weight in the coagulation of suspensions.* Journal of Colloid and Interface Science, 1968. **27**(4): p. 797-803.
4. Brown, N. and N. Putz, *Process for the production of aluminum hydroxide*, 2003, Google Patents.
5. Chen, I., S.K. Hwang, and S. Chen, *Chemical kinetics and reaction mechanism of thermal decomposition of aluminum hydroxide and magnesium hydroxide at high temperature (973-1123 K).* Industrial & engineering chemistry research, 1989. **28**(6): p. 738-742.